Scholars' Mine

Doctoral Dissertations   Student Theses and Dissertations

Fall 2015

Development of ionic liquid multi-mode spacecraft micropropulsion systems

Steven Paul Berg

Follow this and additional works at: https://scholarsmine.mst.edu/doctoral_dissertations

Part of the Aerospace Engineering Commons

Department: Mechanical and Aerospace Engineering

Recommended Citation

DEVELOPMENT OF IONIC LIQUID MULTI-MODE

SPACECRAFT MICROPROPULSION SYSTEMS

by

STEVEN PAUL BERG

A Dissertation

Presented to the Faculty of the Graduate School of the

MISSOURI UNIVERSITY OF SCIENCE AND TECHNOLOGY

In Partial Fulfillment of the Requirements for the Degree

DOCTOR OF PHILOSOPHY IN AEROSPACE ENGINEERING

2015

Approved by

Dr. Joshua Rovey, Advisor
Dr. Umit Koylu
Dr. Henry Pernicka
Dr. Benjamin Prince
Dr. David Riggins

PUBLICATION DISSERTATION OPTION

This dissertation consists of the following articles that have been submitted for publication or are being held for submission pending patent applications:

Pages 7-56 have been submitted to the AIAA <u>Journal of Propulsion and Power</u>. Submitted 5/15/2011, revision submitted 9/20/2012, accepted 9/12/2012, published 2/13/2013.

Pages 57-87 will be submitted to the AIAA <u>Journal of Spacecraft and Rockets</u>. In preparation.

Pages 88-107 will be submitted to the AIAA <u>Journal of Propulsion and Power.</u> In preparation.

Pages 108-133 will be submitted to the AIAA <u>Journal of Propulsion and Power.</u> In preparation.

ABSTRACT

This dissertation presents work on development of multi-mode specific spacecraft propulsion systems. Specifically, this work attempts to realize a single propellant capable of both chemical monopropellant and electric electrospray rocket propulsion, develop methods to characterize multi-mode propulsion system performance, and realize a system capable of both monopropellant and electrospray propulsion for a small spacecraft. Selection criteria for ionic liquid propellants capable of both monopropellant and electrospray propulsion are developed. These are based on desired physical properties and performance considering use in both propulsive modes. From these insights, a monopropellant mixture of 1-ethyl-3-methylimidazolium ethyl sulfate and hydroxylammonium nitrate is selected and synthesized. Multi-mode spacecraft micropropulsion systems which include a high-thrust chemical mode and high-specific impulse electric mode are assessed. Due to the combination of a common propellant for both propulsive modes, low inert mass, and high electric thrust, the monopropellant/electrospray system has the highest mission capability in terms of delta-V for missions lasting shorter than 150 days. The ionic liquid monopropellant mixture is tested for decomposition on heated platinum, rhenium, and titanium surfaces. It was found that the propellant decomposes at 165 $^{\circ}$C on titanium, which is the decomposition temperature of HAN, and 85 $^{\circ}$C on platinum. Arrhenius-type reaction rate parameters were calculated from the results and used to develop thruster models. The [Emim][EtSO4]-HAN propellant mixture is tested in a capillary electrospray emitter and exhibits stable electrospray emission at a nominal extraction voltage of 3400 V. The highest specific impulse attained in these experiments was 412 seconds; however, this could be improved with a more robust feed system design. This data, along with data from the monopropellant decomposition experiment is used to design a multi-mode micropropulsion system using a common propellant and common thruster geometry. This system is capable of ~20-40% greater delta-V capability at a given mission duration compared to a system utilizing separate, state-of-the-art monopropellant and electrospray thrusters.

ACKNOWLEDGMENTS

First and foremost, I would like to thank my advisor, Dr. Joshua Rovey, for his support, advice, motivation, and trust in my abilities over the last five years. I am also extremely grateful that he thinks enough of me to give me a postdoctoral position to continue this research and pursue my dream of being an entrepreneur in the space industry.

I would like to thank my faculty committee members Drs. Umit Koylu, Henry Pernicka, and David Riggins. Their advice on this thesis has been extremely valuable and their instruction through classes helped develop my passion and convinced me to pursue graduate school in the first place. I am also grateful to off campus committee member, Dr. Ben Prince, for not only serving on my committee and providing valuable insights and expertise in electrospray physics, but also allowing me to visit AFRL Kirtland and conduct my electrospray work.

Over the course of my graduate education, I have had the unique opportunity to spend summers away from Rolla (valuable in its own right) and develop my skills through various internships. In the summer of 2012 I had the opportunity to work in the Space Chemistry II Lab at AFRL under the guidance of Dr. Jaime Stearns and Dr. Russ Cooper. I am grateful to them not only for the opportunity, but for teaching me how to think scientifically as well as engineeringly (not a word, but I'm publishing it anyway because I can). In the summers of 2013 and 2014 I had the unique opportunity to work in the propulsion systems development team at SpaceX. Special thanks to Jon Edwards, Mike Rossoni, and Darin Van Pelt for giving me the opportunity and providing a prime example of how to lead an engineering team. I would also like to thank Michael Clive in particular, who has basically taught me everything I know about valves, fittings, and McMaster. It was truly a pleasure to work with him.

Members of the APLab are also to be thanked for providing a source of discussion, or just a source to vent frustrations onto. To Warner Meeks and Ryan Pahl: MEEEHHHH. To Timothy Nichols and Mark Emanuel: Mo Money Less Problems. To

my undergraduate students Tim Collard, Matt Glascock, Brynne Coleman, and Alex Mundahl: thanks for your diligent efforts even though sometimes, purposefully or not, I asked impossible tasks of you. And yes, Matt, you're still to be referred to as my undergrad (or at least ex-undergrad).

I should call special attention to what is now being referred to as my 'accidental co-op'. Thanks to the Stage 2 team at SpaceX. It has been a pleasure working with you, though for a shorter duration than initially planned. Special thanks to Greg Krauland for not only understanding my decision, but for actually being excited that I am pursuing my passions.

I would like to thank all of my friends that have made grad school somewhat more tolerable. Thanks to Jacob Darling and the AREUS Lab gang even though the word 'covariance' does not appear at any point in this dissertation hereafter. Thanks to the crew comprising the infamous late March 2013 trip out west because 'Oh s*** that's you guys!?!' Thanks to Timothy and Mark for the bi-weekly bushmaster classic. Thanks to Alex Dunn for being Alex Dunn. I have, undoubtedly, left off many folks whose company I have had the pleasure of encountering over these past five years. Thanks to all for helping to blow off steam after the many frustrating days that, by definition, comprises grad school.

As far as inanimate objects, I would like to thank, as per tradition, Kapton Tape, but also JB Weld for their magical properties of adhesion combined with high temperature resistance and low electrical conductivity.

Thanks to my family for their love and support over these years, even though with the time commitment of graduate school it made it difficult to spend time with you. Even though I hear stories about October Sky and pooping at fancy restaurants just about every time I visit home, I am truly thankful for your love.

Finally, I would like to thank Katelyn because without your reassurance every night over the final stages of this dissertation, I may very well have not ever finished this.

TABLE OF CONTENTS

LIST OF ILLUSTRATIONS

LIST OF TABLES

NOMENCLATURE

C_A	=	Concentration of reactant A, [mol/m^3]
C_{PA}	=	Specific heat of reactant A, [J/mol-K]
F	=	Thrust, [N]
F_{A0}	=	Initial molar flow rate of reactant A, [mol/s]
F_i	=	Molar flow rate, [mol/s]
g_0	=	Acceleration of gravity, [m/s^2]
H_i	=	Enthalpy of species i, [J/mol]
I	=	Current, [A]
I_{sp}	=	Specific impulse, [s]
MW_A	=	Molecular weight of reactant A, [g/mol]
$\dot{m}$	=	Mass flow rate, [g/s]
Q	=	Volumetric flow rate, [m^3/s]
$\dot{Q}$	=	Heat transfer rate, [W]
r_A	=	Reaction rate of reactant A, [mol/s-m^3]
T	=	Temperature, [K]
V	=	Volume, [m^3]
$\dot{W}_s$	=	Shaft work, [W]
X	=	Conversion, [mol reacted/mol initial]
ΔH_{RX}	=	Heat of reaction, [J/mol]

1. INTRODUCTION

This thesis presents work on development of multi-mode specific spacecraft propulsion systems. Specifically, this work attempts to realize a single propellant capable of both chemical monopropellant and electric electrospray rocket propulsion, develop methods to characterize multi-mode propulsion system performance, and realize a system capable of both monopropellant and electrospray propulsion for a small spacecraft. Previous attempts at realizing a dual-mode propulsion system have focused on utilizing available monopropellants in some electrical propulsion mode, results of which have thus far been mixed as the monopropellants tend to be unsuitable for use, or have very low performance in electric propulsion devices. The approach taken in the first part of this study is to quantify traits of the propellant necessary to achieve functionality and high performance in both chemical and electric modes. Thus, a novel multi-mode specific propellant can be selected, synthesized, and tested. This is not intended to develop an 'optimal' propellant, since as will be described given current ionic liquid knowledge that task is not possible. Rather, selection criteria are developed such that known ionic liquids can be selected for study.

From a propulsion system perspective, proposed multi-mode propulsion systems analysis has left a lot to be desired. Specifically, focus has been on simply outlining concepts with focus on individual thruster specific impulse and thrust and comparison of multi-mode systems, which by nature rely on component integration, has been lacking. Analysis methods for multi-mode spacecraft propulsion systems are developed in the second portion of this dissertation with particular focus on small satellite spacecraft systems, which are not well described by specific impulse alone due to their high inert mass fractions.

The final three sections of this dissertation focus on chemical monopropellant and electrospray capability of the propellant developed in Part I and application to multi-mode propulsion system design. Monopropellant decomposition characteristics are obtained through the use of a batch reactor, and electrospray performance is obtained

through a capillary type emitter experiment. Results from these experiments are then used to design a conceptual multi-mode propulsion systems using insights from Part II.

In this thesis, four papers intended for publication are presented which describe the methods and results of research on multi-mode spacecraft propulsion. Paper I provides a roadmap to dual-mode propellant design by describing the physical properties and performance that can be attained within the class of ionic liquids selected for study. Paper II presents multi-mode micro propulsion systems analysis methods. Paper III presents experimental work on the synthesis and catalytic decomposition of a novel propellant selected from the results of Paper I. Evidence of catalytic decomposition provides initial proof-of-concept for use in monopropellant systems, and represents the first step on the development path. Paper IV describes results of the electrospray emission of the same propellant. These papers are preceded by an introduction which describes the motivation for pursuing the research and the basic concepts of both multi-mode spacecraft propulsion and ionic liquids. The final section uses results from all sections to present a conceptual design of a multi-mode spacecraft propulsion system. That section is not intended as an optimal or final design, but rather an example of the overall methodology and design considerations developed in the previous sections.

1.1. MULTI-MODE SPACECRAFT PROPULSION

The main benefit of a multi-mode system is increased mission flexibility through the use of both a high-thrust chemical thruster and a high-specific impulse electric thruster. By utilizing both thrust modes, the mission design space is much larger [1]. Missions not normally accessible by a single type of thruster are possible since both are available. The result is the capability to launch a satellite with a flexible mission plan that allows for changes to the mission as needs arise. Since a variety of high specific impulse and high thrust maneuvers are available in this type of system, this may also be viewed as a technology enabling launch of a satellite without necessarily determining its thrust history beforehand. Research has shown that a dual mode system utilizing a single ionic liquid propellant in a chemical bipropellant or monopropellant and electrical electrospray mode has the potential to achieve the goal of improved spacecraft mission flexibility [2-

4]. Furthermore, utilizing a single ionic liquid propellant for both modes would save system mass and volume to the point where it becomes beneficial when compared to the performance of a system utilizing a state-of-the-art chemical and electric thruster with separate propellants, despite the performance of the ionic liquid being less than that of each thruster separately. While a bipropellant thruster would provide higher chemical performance, a monopropellant thruster provides the most benefit because the utilization of a bipropellant thruster in this type of system could inherently lead to unused mass of oxidizer since some of the fuel is used for the electrical mode [3].

1.1.1. Monopropellant Propulsion. Monopropellant propulsion is a combustion-based propulsive method that consists of a single propellant being ignited through some external stimulus in order to produce an energy release, and therefore a temperature and pressure increase in a combustion chamber. The pressurized gas is then expanded through a nozzle to produce thrust. High thrust can be attained with monopropellant devices, but specific impulse is limited due to energy being lost to random thermal collisions which reduces the exhaust velocity. A schematic of a typical monopropellant thruster is shown in Figure 1.1.
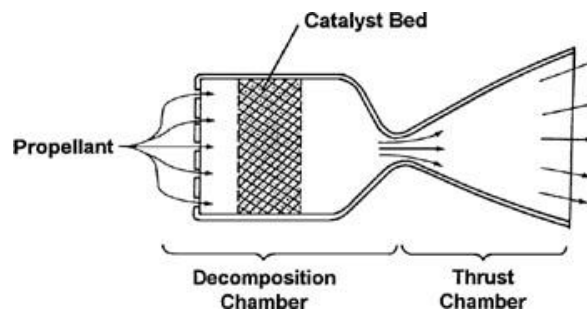
Figure 1.1. Simplified Schematic of Monopropellant Thruster.

A monopropellant must be thermally stable under storage conditions, but also readily ignitable. Typically, hydrazine has been employed as a spacecraft monopropellant because it is storable and easily decomposed to give good propulsion performance [5].

Because it is also highly toxic, recent efforts have focused on finding an alternative "green" monopropellant. Binary or ternary mixtures including the energetic salts hydroxyl ammonium nitrate (HAN), ammonium dinitramide (ADN), or hydrazinium nitroformate (HNF) have been proposed as potential replacements [6-10]. These are not true monopropellants in the traditional sense, but rather essentially premixed bipropellants with separate oxidizer and fuel components in the mixture. Since all of these have melting points above room temperature, they are typically stored as an aqueous solution. A compatible fuel component such as methanol, glycerol, or triethanolammonium nitrate (TEAN) is typically also added to provide increased performance.

Nonspontaneously ignitable propellants, such as monopropellants, must be decomposed by some external means before ignition can begin. Ignition is a transient process in which reactants are rapidly transitioned to self-sustained combustion via some external stimulus. For practical applications, the amount of energy needed to provide ignition must be minimal, and the ignition delay time should be small [5]. The most reliable methods of monopropellant ignition on spacecraft include thermal and catalytic ignition, in which the monopropellant is sprayed onto a heated surface or catalyst. Other ignition methods include spark or electrolyte ignition [11, 12]. These have been investigated, but are less practical for spacecraft application as they require a high-voltage power source, further increasing the weight and cost of the spacecraft. Hydrazine monopropellant is typically ignited via decomposition by the commercially manufactured iridium-based catalyst Shell 405. For optimum performance, the catalyst bed is typically heated up to $200^{o}C$, but can be 'cold-started' with no preheat in emergency situations [5]. The Swedish ADN-based monopropellant blends require a catalyst bed preheat of $200^{o}C$. They cannot be cold-started, which is a major limitation presently [10].

1.1.2. Electrospray Propulsion. Electrospray, or colloid, propulsion utilizes and electrostatic-type device to extract ions or charged droplets from a liquid meniscus, which in turn are accelerated through an intense electric field to produce a high exhaust velocity. As with most electric propulsion devices, the mass flow rates that can be attained in this type of device are low. Electrospray devices are therefore high-specific impulse, low-thrust type devices. A typical electrospray thruster consists of an emitter,

which is essentially a needle, an extraction grid, and a power supply. The propellant may be either externally wetted or injected through a capillary tube. A potential is applied between the extraction grid and the needle, which causes the formation of a Taylor cone on the surface of the propellant meniscus. If the electric field on the meniscus is sufficiently high, ions or charged droplets are extracted and accelerated by the grid. A typical electrospray thruster is shown in Figure 1.2.
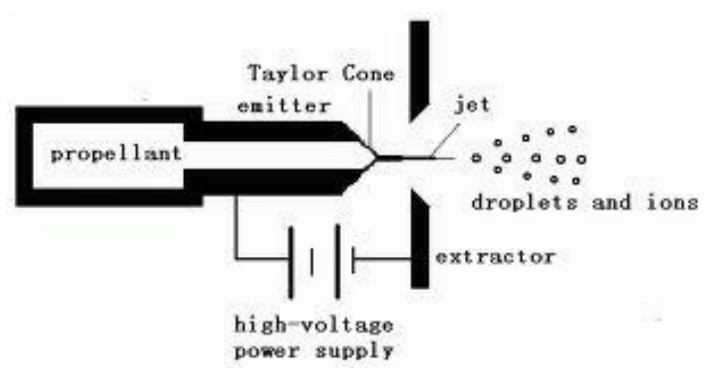
Figure 1.2. Simplified Schematic of Electrospray Thruster.

1.2. IONIC LIQUIDS

An ionic liquid is essentially a molten, or liquid, salt. All salts obtain this state when heated to high enough temperature; however, a special class of ionic liquids is known as room temperature ionic liquids (RTIL's) that remain liquid well below room temperature. These differ from traditional aqueous ionic solutions, such as salt water, in that a solute is not required to dissolve the ionic portion, but rather the ionic substance is liquid in and of itself. Ionic liquids have been known since the early 20th century; research in the field, however, has only currently begun to increase, with the number of papers published annually increasing from around 120 to over 2000 in just the last decade [13]. As a result, many of the ionic liquids that have been synthesized are still being researched, and data on their properties is not yet available. Current research has aimed at

synthesizing and investigating energetic ionic liquids for propellants and explosives, and current work has highlighted the combustibility of certain ionic liquids as they approach decomposition temperature [14, 15]. This leads to the possibility of using an ionic liquid as a storable spacecraft propellant.

Ionic liquids have been investigated as electrospray propellants. Electrospray liquids with relatively high vapor pressure boil off the emitter and produce an uncontrolled, low performance emission. Ionic liquids are candidates for electrospray propulsion due to their negligible vapor pressure and high electrical conductivity [16]. Ionic liquid emissions can range from charged droplets to a purely ionic regime (PIR) similar to that of field emission electric propulsion with specific impulses in the range of 200-3000 seconds for current propellants [17]. The ionic liquid 1-ethyl-3-methylimidazolium bis(trifluoromethylsulfonyl)imide ([Emim][Im]) was selected as the propellant for the ST7 Disturbance Reduction System mission, and represents the only application of electrospray, or colloid, thrusters to date [18]. Several other imidazole-based ionic liquids have been suggested for research in electrospray propulsion due to their favorable physical properties [19].

PAPER

I. Assessment of Imidazole-Based Ionic Liquids as Dual-Mode Spacecraft Propellants

Steven P. Berg and Joshua L. Rovey
Missouri University of Science and Technology, Rolla, Missouri, 65409

ABSTRACT

Imidazole-based ionic liquids are investigated in terms of dual-mode chemical monopropellant and electrospray rocket propulsion capability. A literature review of ionic liquid physical properties is conducted to determine an initial, representative set of ionic liquids that show favorable physical properties for both modes, followed by numerical and analytical performance simulations. Ionic liquids [Bmim][dca], [Bmim][NO$_3$], and [Emim][EtSO$_4$] meet or exceed the storability properties of hydrazine and their electrochemical properties indicate that they may be capable of electrospray emission in the purely ionic regime. These liquids are projected to have 13-23% reduced monopropellant propulsion performance in comparison to hydrazine due to the prediction of solid carbon formation in the exhaust. The use of these ionic liquids as a fuel component in a binary monopropellant mixture with hydroxylammonium nitrate shows 1-4% improved specific impulse over some 'green' monopropellants. Also, this avoids volatility issues and reduces the number of electrospray emitters by 18-27% and power required by 9-16%, with oxidizing ionic liquid fuels providing the greatest savings. A fully oxygen balanced ionic liquid will exceed the state-of-the-art performance in both modes, but will require advances in hardware technology in both modes to achieve minimum functionality.

NOMENCLATURE

E_{max}	=	Maximum electric field, [V/m]
e	=	Fundamental charge, [C]
F	=	Thrust, [N]
g_0	=	Acceleration of gravity, [m/s^2]
I_d	=	Density specific impulse, [kg-s/m^3]
I_{emit}	=	Current flow per emitter, [A]
I_i	=	Output current associated with charged particle i, [A]
I_{sp}	=	Specific impulse, [s]
K	=	Electrical conductivity, [S/m]
MW	=	Molecular weight, [g/mol]
m	=	Mass of emitted species, [kg]
m_i	=	Mass of particle i, [kg]
$\dot{m}_{emit}$	=	Mass flow rate per emitter, [kg/s]
$\dot{m}_{tot}$	=	Total mass flow rate, [kg/s]
N_{emit}	=	Number of emitters
P_c	=	Chamber pressure, [psi]
P_e	=	Nozzle exit pressure, [psi]
P_{sys}	=	Power of electric propulsion system, [W]
Q	=	Volume flow rate, [L/s]
q	=	Particle charge, [C]
R	=	Gas constant, [J/kg-K]
R_A	=	Ion fraction
T_c	=	Combustion temperature, [K]
T_m	=	Melting temperature, [K]

V_{acc}	=	Electrostatic acceleration potential, [V]
V_e	=	Exit velocity, [m/s]
$V_{e,N=0}$	=	Exit velocity of pure ions, [m/s]
$V_{e,N=1}$	=	Exit velocity of ions in $N=1$ solvated state, [m/s]
x_i	=	Mass fraction of species i
ΔH_f^0	=	Heat of formation, [J/mol]
$\Delta\phi$	=	Net accelerating potential, [V]
δ_{av}	=	Average specific gravity
ε	=	Dielectric constant, or nozzle expansion ratio
ε_0	=	Permittivity of free space, [F/m]
η	=	Viscosity, [cP]
η_{sys}	=	Efficiency of power conditioning system
γ	=	Specific heat ratio, or surface tension, [dyne/cm]
$\varphi(\varepsilon)$	=	Proportionality coefficient
ρ	=	Density, [g/cm^3]
ρ_i	=	Density of species i, [g/cm^3]
ρ_n	=	Density of mixture n, [g/cm^3]

1. INTRODUCTION

In a true dual-mode spacecraft propulsion system, the same propellant is used for both high thrust, low specific impulse (chemical propulsion) and low thrust, high specific impulse thrusters (electric propulsion). This has many advantages, most importantly higher mission flexibility in terms of the ability to dictate maneuvers as mission needs arise on orbit rather than before launch. At the same time, utilizing a single propellant provides maximum flexibility and significantly reduces system mass and volume over a

spacecraft utilizing separate propellants for each thrust mode. Ionic liquids have potential to be utilized in either a chemical thruster or an electric thruster. The goal of this paper is to examine typical ionic liquids in terms of their capability for use as propellants in a dual-mode propulsion system. Since the list of available ionic liquids is enormous, and most liquids are not yet well characterized, this study will also attempt to identify trends favorable toward dual-mode propulsion in order to provide guidelines for the selection of ionic liquids for future use in dual-mode propellant research. This paper describes and examines requirements on the physical properties of various ionic liquids to assess their potential for use as propellants in a potential dual-mode system. Projected chemical and electrical propulsion performance of sample ionic liquids that have shown favorable properties toward feasible operation in both modes is then computed and compared to the current state-of-the-art in both chemical monopropellant and electrospray propulsion.

As stated, the main benefit of a dual-mode system is increased mission flexibility through the use of both a high-thrust chemical thruster and a high-specific impulse electric thruster utilizing the same fuel. By utilizing both thrust modes, the mission design space is much larger [1]. Missions not normally accessible by a single type of thruster are possible since both are available. Furthermore, this enables mission designers to develop with a flexible mission plan that allows for changes to the mission as needs arise. Since a single propellant is utilized for both modes, this may also be viewed as a technology enabling launch of a satellite without necessarily even determining any thrust history beforehand because both types of maneuvers are available, while still resulting in 100% propellant utilization regardless of the specific type, frequency, or order of desired maneuvers . Research has shown that a particular dual mode system concept utilizing a single ionic liquid propellant in a chemical monopropellant and electric electrospray mode has the potential to achieve mission flexibility gains and mass savings over a system utilizing separate propellants for each mode even if the common propellant performs below state-of-the-art in either mode [2-4].

An ionic liquid is essentially a molten, or liquid, salt. All salts obtain this state when heated to high enough temperature; however, an ionic liquid is typically defined as attaining liquid state below $100^{o}C$. There exists a special class of ionic liquids known as room temperature ionic liquids (RTIL's) that remain liquid well below room temperature.

Ionic liquids have been known since the early 20th century; research in the field, however, has only currently begun to increase, with the number of papers published annually increasing from around 120 to over 2000 in just the last decade [5]. As a result, many of the ionic liquids that have been synthesized are still being researched, and data on their properties is not yet available. Additionally, the number of ionic liquids theorized, but not yet synthesized has been estimated in the millions [6] and the estimated number of possible ionic liquids is on the order of $\sim 10^{18}$ [7]. Current research has aimed at synthesizing and investigating energetic ionic liquids for propellants and explosives, and current work has highlighted the combustibility of certain ionic liquids as they approach decomposition temperature [8, 9]. This leads to the possibility of using an ionic liquid as a storable spacecraft monopropellant.

Hydrazine has been the monopropellant of choice for spacecraft and gas generators because it is storable and easily decomposed to give good combustion properties [10]. However, hydrazine is also highly toxic and recent efforts have been aimed at replacing hydrazine with a high-performance, non-toxic monopropellant. The energetic salts hydroxylammonium nitrate (HAN), ammonium dinitramide (ADN), and hydrazinium nitroformate (HNF) have received attention as potential replacements [10-14]. All of these salts have melting points above room temperature, and it is therefore necessary to use them in an aqueous solution to create a storable liquid propellant. Typically, these are also mixed with a compatible fuel component to provide improved performance. The main limitation to the development of these as monopropellants has been excessive combustion temperatures [14, 15]. Engineers in Sweden, however, have recently flight tested an ADN-based thruster capable of handling combustion temperatures exceeding 1900 K [14].

Electrospray is a propulsion technology in which charged liquid droplets or ions are extracted from an emitter via an applied electric field [16]. Electrospray liquids with relatively high vapor pressure boil off the propellant and produce an uncontrolled, low performance emission. Ionic liquids are candidates for electrospray propulsion due to their negligible vapor pressure and high electrical conductivity [17]. Ionic liquid emissions can range from charged droplets to a purely ionic regime (PIR) similar to that of field emission electric propulsion with specific impulses in the range of 200-3000

seconds for current propellants [16]. The ionic liquid 1-ethyl-3-methylimidazolium bis(trifluoromethylsulfonyl)imide ([Emim][Im], or [Emim][Tf$_2$N]) was selected as the propellant for the ST7 Disturbance Reduction System mission, and represents the only planned flight application of electrospray, or colloid, thrusters to date [18]. Several other imidazole-based ionic liquids have been suggested for research in electrospray propulsion due to their favorable physical properties [19].

The following sections analyze the potential of ionic liquids to be used as spacecraft propellants in a dual-mode system and develops criterion for selection or design of true dual-mode propellants. Section II identifies the physical properties required for acceptable performance in both modes. Sample ionic liquids are then selected for performance analysis. Section III investigates the projected chemical performance of these ionic liquids as monopropellants. Section IV examines the projected electrospray performance of the ionic liquid propellants. The results of the preceding sections are discussed, and criteria for future dual-mode propellant selection and developments are presented in Section V. Section VI presents conclusions based on the entirety of analyses.

2. IONIC LIQUID PHYSICAL PROPERTIES

Fundamental physical properties required of ionic liquids to perform as both monopropellants and electrospray propellants in a spacecraft environment are identified. These properties are compared to those of the current state-of-the-art propellants to develop tools and criterion to assess the feasibility of using these and other ionic liquids for the intended application.

2.1. THERMOCHEMICAL PROPERTIES

The fundamental thermochemical properties required to initially analyze the ability of ionic liquids to perform as spacecraft propellants include the following: melting temperature, density, viscosity, and heat of formation [10]. High density, low melting

temperature, and low viscosity are desired traits common to both propulsive modes in the dual-mode system because they do not have a significant effect on the operation of each thruster, but represent the storability of propellants only. A low viscosity aids in transporting the propellant from the tank and its subsequent injection into either type of thruster. A low melting temperature is desired so that the power required to keep the propellant in liquid form is minimal. Monopropellant grade hydrazine has a melting temperature of 2° C, so it is reasonable to assume that new propellants must fall near or below this value. Density is an additional storability consideration. A high density is desired to accommodate a large amount of propellant in a given volume on a spacecraft. The chemical propellant must also be easily ignitable and give good combustion properties. The heat of formation of the compound is required to estimate the equilibrium composition, and subsequently compute the estimated chemical performance, namely specific impulse. A high heat of formation results in a greater energy release upon combustion, therefore a higher combustion temperature, and subsequently a higher specific impulse for a given species and number of combustion products.

2.2. ELECTROCHEMICAL PROPERTIES

The electrochemical properties important for electrospray propulsion include both surface tension and electrical conductivity. The highest performance in terms of specific impulse is attained for emissions in the purely ionic regime (PIR). Emission of charged droplets, rather than clusters of ions, greatly reduces the specific impulse and efficiency of the emitter. [Emim][Im], for example, operates in the purely ionic regime with a specific impulse of around 3500 seconds [20], but in the droplet regime, this drops to lower than 200 seconds [21]. Droplet emission, however, does produce a larger amount of thrust due to emission of heavier species, and this may be desirable in some instances, but ultimately the most flexible ionic liquids for electrospray propulsion will attain emission in the PIR. Liquids with sufficiently high surface tension and electrical conductivity have been shown to be capable of operating in the PIR. This has been shown both theoretically and experimentally [19, 22, 23], and is related to the maximum electric field on the meniscus of the liquid on the emitter [18, 19]

$$E_{max} = \varphi(\varepsilon)\gamma^{1/2}\varepsilon_0^{-2/3}(K/Q)^{1/6} \qquad (1)$$

Additionally, De La Mora [19, 23] has shown that the smallest flow rate that can form a stable Taylor cone scales as γ/K, hence [19]

$$E_{max} \sim (\gamma K)^{1/3} \qquad (2)$$

Experimental results indicate that the PIR is achieved at a meniscus electric field of roughly 1 V/nm [16]. It should be noted that Eqs. (1) and (2) do not accurately predict the meniscus electric field for PIR emissions. Instead, because experimental results indicate a similar trend for liquids that have attained PIR emission, Eq. (2) will be used as a comparison tool. This relation is a measure of the ability of an ionic liquid to form a Taylor cone with emission in the purely ionic regime, and does not necessarily translate to thruster performance. The thrust and specific impulse for an electric propulsion system by an individual particle are calculated as [10, 16]

$$F = I_i\sqrt{2V_{acc}(m_i/q)} \qquad (3)$$

$$I_{sp} = (1/g_0)\sqrt{2V_{acc}(q/m_i)} \qquad (4)$$

A high charge per mass is desired for high specific impulse, but is inversely proportional to thrust. As a result, practical specific impulse is limited by power available, since an excessively high specific impulse requires large amounts of power to process enough current to produce even small amounts of thrust. Higher molecular weight propellants are desirable due to the higher thrust produced by emission of heavier ions. Therefore, ionic liquids with electrical conductivity and surface tension close to the current state-of-the-art electrospray propellants that have achieved PIR operation and high molecular weight are of greatest benefit.

2.3. PHYSICAL PROPERTIES OF IONIC LIQUIDS USED IN THIS STUDY

The number of ionic liquids available for study is numerous; therefore, this study has initially been restricted to only imidazole-based ionic liquids. The main reason for selecting imidazole-based ionic liquids is their capability as electrospray propellants, particularly those based on the [Emim]$^+$ cation [19]. A recent patent on this particular type of dual-mode system lists several potential ionic liquid propellants, most of which are imidazole-based [24]. These are used in the initial screening for chemicals of interest; however, many ionic liquids do not have enough published physical property data to make definite estimates of initial system feasibility. In particular, heat of formation is not available for many of the ionic liquids considered initially. It is therefore necessary and useful to consider trends in the physical properties of ionic liquids. This will be discussed in further detail in a later section, but in the interest of providing examples in this study and to discern performance trends, three ionic liquids are selected for further study based on availability of property data: 1-butyl-3-methylimidazolium nitrate ([Bmim][NO$_3$]), 1-butyl-3-methylimidazolium dicyanamide [Bmim][dca], and 1-ethyl-3-methylimidazolium ethyl sulfate ([Emim][EtSO$_4$]). Representative physical property data for these ionic liquids are shown in Table 1. The properties of hydrazine and [Emim][Im] are shown for comparison of thermochemical and electrochemical properties, respectively. The density, viscosity, electrical conductivity, and surface tension reported in the table are at a temperature of 298 K for all liquids listed, except for the electrical conductivity of [Bmim][NO$_3$], where the only data point given in literature is at a temperature of 379 K. The properties found in the literature vary slightly due to differences in experimental technique and purity of the ionic liquid sample, but in general the results agree within less than 1% [46-56]. The values shown in Table 1 are the most conservative values in reference to the discussions in this paper.

Table 1. Physical Properties of Ionic Liquids Selected for Further Study.

Propellant	Formula	ρ [g/cm^3]	T_m [^{o}C]	ΔH_f^o [kJ/mol]	K [S/m]	γ [dyn/cm]	η [cP]
[Bmim][NO$_3$]	C$_8$H$_{15}$N$_3$O$_3$	1.157 [25]	<10 [25]	-261.4 [26]	0.820 [27]		165 [28]
[Bmim][dca]	C$_{10}$H$_{15}$N$_5$	1.058 [29]	-10 [29]	206.2 [30]	1.052 [31]	46.6 [32]	32 [33]
[Emim][EtSO$_4$]	C$_8$H$_{16}$N$_2$O$_4$S$_1$	1.236 [34]	-37 [35]	-579.1 [36]	0.382 [37]	45.4 [38]	100 [39]
[Emim][Im]	C$_8$H$_{11}$F$_6$N$_3$O$_4$S$_2$	1.519 [40]	-18 [41]		0.910 [42]	36.9 [43]	32 [40]
Hydrazine	N$_2$H$_4$	1.005 [10]	2 [10]	109.3 [44]	0.016 [45]	66.4 [45]	0.9 [45]

All of the ionic liquids have density greater than that of hydrazine. The melting temperature of [Bmim][dca] and [Emim][EtSO$_4$] is less than that of hydrazine. [Bmim][NO$_3$] has a slightly higher melting temperature, but the exact melting temperature is not reported. The value shown in Table 1 represents the fact that liquid viscosity measurements are reported for as low as 10 ^{o}C in literature [26, 28]. The final consideration is the viscosity of the ionic liquids, which is much higher than typical chemical propellants, such as hydrazine, and is even still an order of magnitude higher than ADN-based monopropellant blends [57]. This could lead to difficulties in engine calibration and injector performance, but likely can be mitigated through clever design. In terms of electrospray considerations, the viscosity of [Bmim][dca] is roughly the same as [Emim][Im], which has been successfully sprayed through a capillary emitter [58]. The viscosity of the other two ionic liquids is higher than [Emim][Im], but not unlike some higher molecular weight propellants that have been electrosprayed successfully, but only by heating the emitter [58]. Similarly, heating [Bmim][NO$_3$] to 60°C [28] and [Emim][EtSO$_4$] to 50°C [39] lowers the viscosity to levels equal to [Emim][Im].

The electrochemical properties should be assessed in terms of the likelihood of the candidate ionic liquid to attain PIR emission since, as mentioned, operation in the mixed, or droplet, regime causes the efficiency of the thruster and specific impulse to drop drastically. Therefore, this assessment should be one of the first considerations when considering new candidate propellants for dual-mode systems. Since electrical conductivity of ionic liquids increases greatly with temperature, the emitter can be heated

to attain PIR emission. Using Eq. (2) as an estimate and comparison tool to assess the combined effects of surface tension and electric field, the estimated maximum electric field parameter in Eq. (2) was computed and shown as a function of temperature in Fig. 1. The surface tension and electrical conductivity of [Emim][Im], [Bmim][dca], and [Emim][EtSO$_4$] as a function of temperature were obtained from literature [31, 40, 46]. [Emim][Im] has been shown experimentally to achieve PIR emission at an emitter preheat temperature of 80°C [58]. From Fig. 1, the electric field on the surface of the meniscus for [Bmim][dca] and [Emim][EtSO$_4$] is comparable at temperatures of 45°C and 80°C, respectively. This is not surprising as these liquids were selected specifically due to their electrospray potential. The same data for [Bmim][NO$_3$] is not available, and it can therefore not be fully assessed in the same manner. As stated, the electrical conductivity reported for [Bmim][NO$_3$] is at a temperature of 379 K, making it slightly less feasible to use as an electrospray propellant since it will have to be heated to well over 100°C to achieve an electrical conductivity nearly equal to that of [Emim][Im] at 80°C. Surface tension for [Bmim][NO$_3$] is not reported; however, it can be reasonably inferred based on trends reported in literature. A longer alkyl chain in imidazole-based ionic liquids has been reported to result in decreased surface tension [47]. [Emim][NO$_3$], the lower alkyl chain derivative of [Bmim][NO$_3$] has a surface tension of 82.7 [dyne/cm] [48]. The value reported for the lower alkyl chain derivative of [Bmim][dca] is 1-ethyl-3-methylimidazolium dicyanamide, [Emim][dca] is 64 [dyne/cm] [49]. Following these trends, the surface tension for [Bmim][NO$_3$] should fall below that of [Emim][NO$_3$], but above that of [Bmim][dca]; therefore, the surface tension of [Bmim][NO$_3$] should be higher than that of [Emim][Im], and may allow for a slightly lower electrical conductivity.
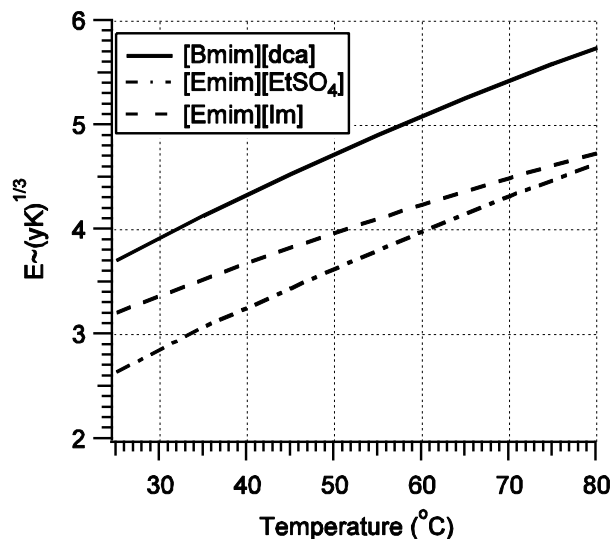
Figure 1. Electric Field on Meniscus Parameter, Eq. (2), as a Function of Temperature.

It should also be noted that the numbers computed in Fig. 1 provide an estimate only and are predictions based on the minimal number of ionic liquids that have experimentally exhibited PIR emission. Of the PIR capable ionic liquids listed in Garoz et. al. [58], only the ionic liquid 1-butyl-3-methylimidazolium bis(perfluoroethylsulfonyl)imide, [Bmim][Beti], had the requisite physical property data available to test the validity of the use of Eq. (2) as a predictor for PIR capability [40]. In comparison to [Emim][Im], Eq. (2) predicts that this ionic liquid will achieve PIR near a $180^{\circ}C$ preheat temperature. This ionic liquid has been observed to emit in the PIR regime with a preheat of $204^{\circ}C$ [58]. So, while the type of data presented in Fig. 1 should be used with heed, it can be used to screen out obviously poor candidates and provide a reasonable means of comparison to ionic liquids that have attained PIR emission.

3. CHEMICAL PERFORMANCE ANALYSIS

The three aforementioned liquids are feasible candidates for both chemical and electrical propulsion purely based on their reported physical properties. Although initially selected mainly because of electrospray considerations, a chemical rocket performance analysis is conducted to determine if they have potential as chemical monopropellants with the understanding that they may perform below state-of-the-art, but have dual-mode capability. Equilibrium combustion analysis is conducted using the NASA Chemical Equilibrium with Applications (CEA) computer code [44]. In each case, the temperature of the reactants is assumed to be 298 K. Where applicable, specific impulse is calculated by assuming frozen flow at the throat [10]

$$I_{sp} = \sqrt{\left(\frac{2\gamma}{\gamma-1}\right)\left(\frac{RT_c}{MW}\right)\left(1-\left(\frac{P_e}{P_c}\right)^{\frac{(\gamma-1)}{\gamma}}\right)} \qquad (5)$$

$$\frac{1}{\varepsilon} = \left(\frac{\gamma+1}{2}\right)^{\frac{1}{\gamma-1}}\left(\frac{P_e}{P_c}\right)^{\frac{1}{\gamma}}\sqrt{\frac{\gamma+1}{\gamma-1}\left(1-\frac{P_e}{P_c}\right)^{\frac{\gamma-1}{\gamma}}} \qquad (6)$$

Given a combustion pressure and nozzle expansion ratio, Eqs. (5) and (6) are then only functions of the combustion gas temperature and products, which are given in the CEA output. When condensed species are found to be present in the equilibrium combustion products, a shifting equilibrium assumption through the nozzle must be applied instead to account for the multi-phase flow. For each simulation hereafter a chamber pressure of 300 psi and nozzle expansion ratio of 50 are assumed. These represent typical values for on-orbit engines [59]. The ambient pressure is taken as vacuum, therefore the specific impulse computed is the absolute maximum for the given design conditions. As an additional measure of chemical performance, the density specific impulse, is computed simply from [10]

$$I_d = \delta_{av} I_{sp} \qquad (7)$$

3.1. MONOPROPELLANT PERFORMANCE

The CEA computer code is utilized to determine the expected performance of the ionic liquids as monopropellants with the assumptions and conditions described above. The reaction is then decomposition of the ionic liquid into gaseous products. The computed specific impulse and density impulse values are shown in Table 2. CEA predicts condensed carbon in the exhaust species for the ionic liquids; therefore, the specific impulse shown in the table is for shifting equilibrium. For comparison, the performance of ADN-based monopropellant FLP-103 (63.4% ADN, 25.4% water, 11.2% methanol) is also computed. The specific impulse computed in this analysis for FLP-103 agrees precisely with the theoretical calculations performed by Wingborg, et.al. [57] at the same design conditions and a frozen flow assumption, as CEA was also utilized in that study for performance prediction. The maximum specific impulse for hydrazine is 257 sec [45] and is where the catalyst bed has been designed to allow for no ammonia to dissociate. Typically, however, hydrazine monopropellant thrusters operate around 243 sec since the catalyst bed cannot handle the high combustion temperature [10]. None of the ionic liquids show performance comparable to that of hydrazine, with [Bmim][NO$_3$] coming closest at a value of 13.2% lower specific impulse. The performance of the ionic liquids is slightly more promising in terms of density specific impulse. [Bmim][dca], and [Emim][EtSO$_4$] fall 18% and 5.3%, respectively, below that of hydrazine, while [Bmim][NO$_3$] has a density specific impulse equal to that of hydrazine. None of the ionic liquids compete with the theoretical density specific impulse of advanced monopropellant FLP-103, which is predicted to be 35% higher than hydrazine.

Table 2. Chemical Performance of Ionic Liquids

Propellant	I_{sp} [s]	I_d [kg-s/m^3]
[Bmim][NO$_3$]	211	244000
[Bmim][dca]	189	200000
[Emim][EtSO$_4$]	186	231000
FLP-103	254 (Equilibrum)	333000
	251 (Frozen)	329000
Hydrazine	243	244000

Analysis of the equilibrium combustion products, Table 3, indicates a large amount of solid carbon in the theoretical exhaust gases, indicating incomplete combustion, and leading to the poor performance of the ionic liquids. [Bmim][dca] has no oxidizing components in its anion and as expected it has the highest mole fraction of carbon of the three ionic liquids. The other two liquids have 15% less carbon in the exhaust due to the oxygen present in their anions, which tends to form the oxidized species CO, H_2O, and CO_2. Decomposition of [Emim][EtSO$_4$] shows a higher mole fraction of H_2O and CO_2 compared to that of [Bmim][NO$_3$] due to the additional oxygen atom in the anion with the same carbon content. Each of the ionic liquids is predicted to form roughly 10% CH_4, a product that could be combusted further with additional oxidizer. Additionally, some of the hydrogen is used to form H_2S due to the presence of the sulfur atom in the anion, another product that with additional oxidizer will combust further.

Table 3. Equilibrium Decomposition Products of Ionic Liquids

	Mole Fraction		
Product Species	[Bmim][NO_3]	[Bmim][dca]	[Emim][$EtSO_4$]
C	0.35	0.50	0.35
N_2	0.10	0.15	0.07
H_2	0.27	0.24	0.19
H_2O	0.07	0.00	0.11
CO	0.09	0.00	0.07
CO_2	0.02	0.00	0.05
CH_4	0.09	0.11	0.09
H_2S	0.00	0.00	0.07

3.2. IONIC LIQUIDS IN BINARY MIXTURES AS MONOPROPELLANTS

The possibility of using ionic liquids as fuel components in a binary monopropellant mixture is considered. This may, in fact, be possible due to the ionic liquids capability as solvents, particularly [Bmim][dca] and [Bmim][NO_3], as their anions have H-bond accepting functionality [53, 60]. Furthermore, many imidazole-based ionic liquids tend to have solubility properties close to those of methanol and ethanol [6]. HAN, also, is noted for its solubility in water and fuels such as methanol, which led to its initial application as a liquid gun propellant [61]. Additionally, these are the ingredients to FLP-103, and the solubility of ADN in both water and methanol was a key to the development of the monopropellant [12, 57]. [Bmim][dca] has been tested for hypergolicity with HAN oxidizer, and, notably, it showed no visible signs of reactivity at room temperature [62]. A monopropellant mixture of the ionic liquids with HAN, or another oxidizer salt, may be created which would be thermally stable at room temperature, and ignited thermally or catalytically.

CEA is again employed with the same conditions applied previously, and with shifting equilibrium assumption. Specific impulse is calculated as a function of percent HAN

oxidizer by weight in the binary mixture. This is shown in Fig. 2. The highest performance is seen at mixture ratios near the stoichiometric value, around 80%, and represents values nearer to bipropellant performance. However, this performance is not feasible when considering current monopropellant thruster technology. The main issue facing monopropellant development is the fabrication of catalyst material that can withstand the high combustion temperatures. A typical hydrazine thruster may operate at temperatures exceeding 1200 K [10]; however, after a painstaking trial and error process lasting more than a decade, engineers in Sweden have developed a monopropellant thruster capable of operation with ADN-based propellant at combustion temperatures exceeding 1900 K [14]. Considering 1900 K to be the current technology limit on monopropellant combustion temperature, the ionic liquids [Bmim][dca], [Bmim][NO$_3$], and [Emim][EtSO$_4$] exceed this value at roughly a 69%, 61%, and 59% binary mixture with HAN by weight, respectively, as shown in Fig. 3. From Fig. 2, these mixture ratios correspond to a specific impulse of 263, 263, and 255 seconds for [Bmim][dca], [Bmim][NO$_3$], and [Emim][EtSO$_4$], respectively. This is promising as the specific impulse of the binary mixtures is higher than the ADN-based FLP-103 (Table 2) at the same design conditions.
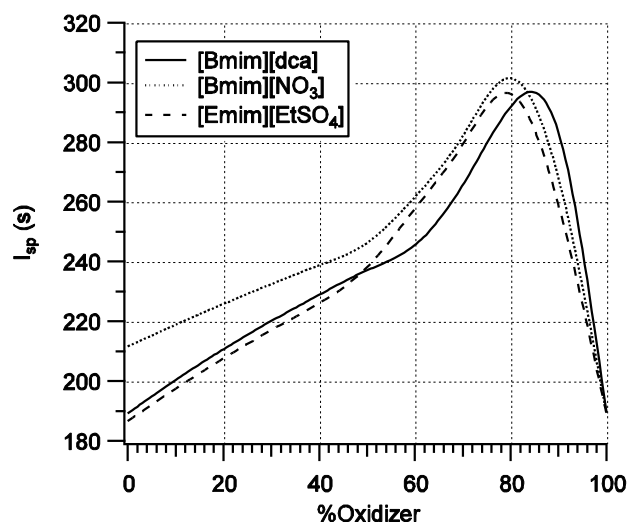
Figure 2. Specific Impulse of Binary Mixture of Ionic Liquid with HAN Oxidizer
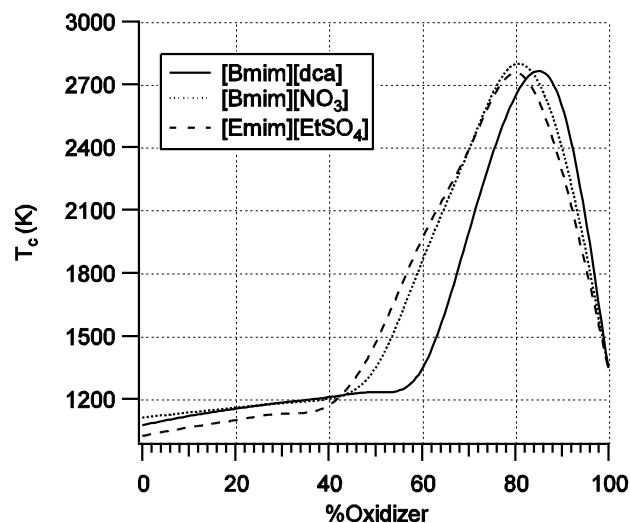
Figure 3. Combustion Temperature of Binary Mixture of Ionic Liquid with HAN Oxidizer.

Additional conclusions can be made by further consideration of the equilibrium combustion products associated with the ionic liquid binary mixtures in Fig. 4. For [Bmim][dca], as the percent by weight of HAN oxidizer is increased, the solid carbon species decreases as both CO and H_2 increase and reach a maximum at 58% oxidizer. Further HAN addition leads to formation of complete combustion products CO_2 and H_2O at the highest combustion temperatures. The same trend is observed in the other ionic liquids, with the exception of the solid carbon disappearing at 44% oxidizer for [Bmim][NO$_3$] and at 41% oxidizer for [Emim][EtSO$_4$]. The sulfur atom in the [Emim][EtSO$_4$] fuel functions to form oxidized sulfur species SO_2, which peaks at roughly 2% near the stoichiometric mixture ratio. From Fig. 2, at the 58% oxidizer mixture ratio, the specific impulse with [Bmim][dca] is 213 seconds, 15% below that of FLP-103. For [Bmim][NO$_3$], the specific impulse at a 44% mixture of HAN oxidizer is 212 seconds, and for [Emim][EtSO$_4$] at a 41% mixture of HAN the specific impulse is 200 seconds. So, at the minimum oxidizer amount required for conversion of the predicted solid carbon to gaseous combustion products, the specific impulse of a mixture with an ionic liquid fuel is 15-20% below that of advanced monopropellant FLP-103, but at a much lower combustion temperature of roughly 1300 K in each case.
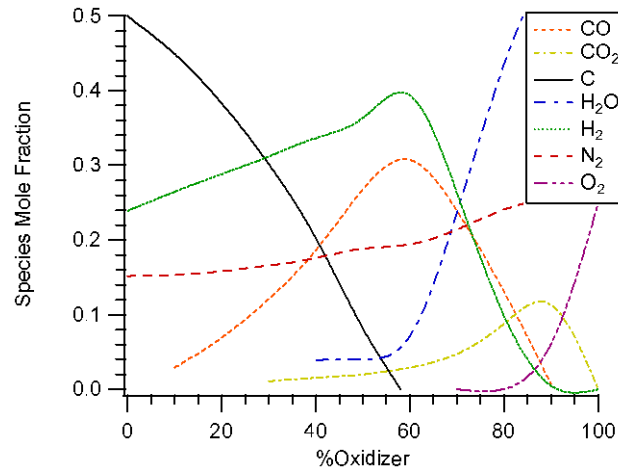
Figure 4. Major Combustion Products of Binary Mixture of [Bmim][dca] and HAN.

The greatest performance gain in the current generation of proposed 'green' monopropellants is their superior density to traditional hydrazine monopropellant. As mentioned, ADN-based propellant FLP-103 is predicted to have a density specific impulse 35% higher than that of hydrazine, as calculated by Eq. (7). The density of a mixture of liquids can be estimated by assuming volume is additive,

$$\frac{1}{\rho_n} = \sum \left(\frac{x_i}{\rho_i} \right) \tag{8}$$

Eq. (8) is a conservative estimate since it does not take into account intermolecular attraction between the constituent liquids. The density specific impulse can then be computed for a desired mixture ratio using Eq. (7). The results for each ionic liquid fuel as a function of percent HAN oxidizer are shown in Fig. 5. Again looking at the mixture ratio that produces a 1900 K combustion temperature, the density specific impulse is 358000, 362000, and 362000 [kg-s/m^3] for [Bmim][dca], [Bmim][dca], and [Emim][EtSO$_4$], respectively. This corresponds to an improvement in density specific

impulse of 8-9% over FLP-103 advanced monopropellant. Considering the minimum oxidizer amount required to form completely gaseous products, the density specific impulse for [Bmim][dca], [Bmim][NO$_3$], and [Emim][EtSO$_4$] binary mixtures is 287000, 284000, and 277000 [kg-s/m^3], a 13-18% improvement over hydrazine.
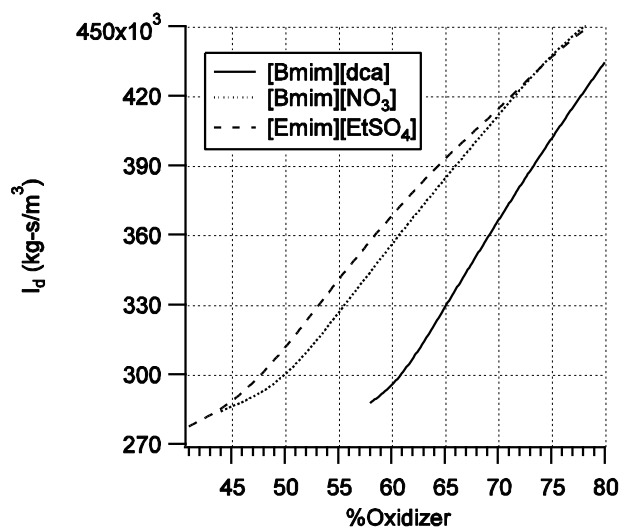
Figure 5. Density Specific Impulse of IL/HAN Binary Mixture.

4. ELECTROSPRAY PERFORMANCE ANALYSIS

The three candidate ionic liquids selected may exceed the performance of state-of-the-art monopropellants when considered as a fuel component in a binary mixture with HAN oxidizer. To fully assess the dual-mode capability of each ionic liquid, the electrospray performance must also be considered. Electrospray performance can be estimated by considering emission in the desired purely ionic regime (PIR) [2-4, 16]. For ionic liquids, PIR emission consists of both pure ions and clusters with ions attached to N

number of neutral pairs. Typically, ionic liquids that achieve PIR emit mostly ions ($N=0$) and ions attached to a single neutral pair ($N=1$), although small amounts of the third ion state ($N=2$) are also detected [16]. The actual ratio of $N=0$ to $N=1$ states in an electrospray emission is determined experimentally. Furthermore, experiments have shown that this ratio cannot be controlled, but rather for a stable emission a single ratio is preferred and may be related to the thermal stability of the ion clusters [63]. Of the few ionic liquids that have achieved emission in the PIR regime, the ratio of pure ions ($N=0$) to ions in the first solvated state ($N=1$) generally lies between 0.5 and 0.7 [20]. The number of $N=2$ states or greater is typically less than 5% of the total emission current. Additionally, for a single ionic liquid, this ratio may also vary depending on the polarity of the extractor, but again the ratio falls within the same bounds.

Electrospray performance in the PIR regime can be estimated by the following methods. First, since the number of $N=2$ states is typically small, it is ignored. The specific impulse for an emission consisting of the first two ion states is given by [2-4]

$$I_{sp} = \frac{V_{e,N=0}R_A + V_{e,N=1}(1-R_A)}{g_0} \tag{9}$$

where R_A is the fraction of the flow that is pure ions. For an electrostatic device, the following relations hold [10]. The velocity of a charged particle accelerated through a net potential is given by

$$V_e = \sqrt{\frac{2e\Delta\phi}{m}} \tag{10}$$

The power supplied to the system is related to thrust and specific impulse by

$$\eta_{sys}P_{sys} = \frac{1}{2}FI_{sp}g_0 \tag{11}$$

Thrust is therefore inversely proportional to specific impulse for an electrostatic thruster regardless of the ionization method. The total mass flow rate required to produce the given thrust is calculated by

$$F = \dot{m}_{tot} I_{sp} g_0 \tag{12}$$

where the total mass flow rate is the sum of the mass flow from all electrospray emitters

$$\dot{m}_{tot} = N_{emit} \dot{m}_{emit} \tag{13}$$

The mass flow produced by a single emitter is related to the current produced by a single emitter by

$$\dot{m}_{emit} = \frac{I_{emit} m}{e} \tag{14}$$

4.1. ELECTROSPRAY SYSTEM PARAMETERS

The relations described in Eqs. (9)-(14) are used to estimate the electrospray propulsion performance of the three ionic liquid fuels analyzed in the previous sections. In terms of electrospray operation, two parameters govern the performance of the thruster: current per emitter and extraction voltage. For this analysis, these parameters are held constant in order to discern the effect of the propellant on total system performance and mass. Improvements in the current electrospray technology level will affect all propellants the same [2-4], provided it is not the physical properties of the propellant that drive the technology improvement; therefore, for this analysis it is prudent to use constant system parameters with respect to estimated current technology levels. The possibility of the physical properties affecting the current and extraction voltage will be discussed in a later section. Emitters being investigated for PIR electrospray devices can emit a current on the order of 1 μA per emitter [20]. Also, typical extraction voltages range from 1.5 to 2.5 kV [16, 20]. Therefore, in this analysis, a current of 1 μA per emitter and an

extraction voltage of 2000 V will be used for all calculations. The final consideration made is with respect to the operation mode of the thruster. An alternating polarity (AC) mode has been selected because both positive and negative ions are extracted. This is most likely the mode in which future electrospray systems will operate because all of the propellant is extracted, it provides a net neutral beam, and it generally avoids the problem of electrochemical fouling. The result of AC operation is an averaged thrust and specific impulse of the emitted cations and anions. Finally, although the actual ratio of ions to clusters of ions is not constant with respect to polarity, for simplification and because these ratios are not known for new ionic liquids it is assumed to be the same for either cation or anion emission.

4.2. ELECTROSPRAY PERFORMANCE OF SINGLE IONIC LIQUIDS

The electrospray performance of the three ionic liquid fuels alone is computed through the aforementioned analysis techniques and conditions. Throughout the analysis, the ionic liquids [Emim][Im] and HAN have been shown for comparison. From Eqs. (9)-(14), it is seen that the electrospray performance when all system parameters are held constant is a function of the propellant mass alone. The cation and anion masses for each propellant used in this study are given in Table 4.

Table 4. Mass Data for Ionic Liquid Propellants

Propellant	Chemical Formula		MW [g/mol]	
	Cation	Anion	Cation	Anion
[Bmim][dca]	$C_8H_{15}N_2$	C_2N_3	139	66
[Bmim][NO$_3$]	$C_8H_{15}N_2$	NO_3	139	62
[Emim][EtSO$_4$]	$C_6H_{11}N_2$	$C_2H_5SO_4$	111	125
[Emim][Im]	$C_6H_{11}N_2$	$C_2NF_6S_2O_4$	111	280
HAN	NH_3OH	NO_3	34	62

The specific impulse of each propellant is calculated for a net accelerating voltage of 2000 V and for ion fractions of 0.5 and 0.7. The results are shown in Table 5. From the table, it is clear that the specific impulse increases as ion fraction increases because more massive clusters are emitted in the first solvated state at lower ion fraction. The thrust per unit power is inversely proportional to specific impulse and increases as the ionic liquid molecular weight increases. The variation in specific impulse and thrust calculated between ion fractions of 0.5 and 0.7 varies by roughly 10 percent for all propellants. The remainder of this analysis will be restricted to the 0.5 ion fraction case. Based on current knowledge of ionic liquid electrosprays in the PIR regime, all subsequent calculations could therefore overestimate thrust and underestimate specific impulse by roughly 10 percent. This becomes important when considering ionic liquid propellants of similar molecular weight and could be a difference maker when choosing between ionic liquids such as [Bmim][dca] and [Bmim][NO$_3$]. But, as seen in Table 5, with a modest 13% difference in molecular weight, even if [Emim][EtSO$_4$] were to emit only at an ion fraction of 0.7, it would still have more thrust per unit power than the 0.5 ion fraction case for [Bmim][dca].

Table 5. Specific Impulse and Thrust per Unit Power.

	I_{sp} (s)		F/P (μN/W)	
Ion Fraction	0.5	0.7	0.5	0.7
[Bmim][dca]	5100	5700	40.0	35.8
[Bmim][NO$_3$]	5200	5800	39.2	35.2
[Emim][EtSO$_4$]	4600	5000	44.3	40.8
[Emim][Im]	3800	4200	53.7	48.5
HAN	7400	8200	27.6	24.9

One of the major limitations on electrospray propulsion currently is the number of emitters required to produce thrust levels high enough to be useful in actual satellite operations. At a constant extraction voltage, and therefore a constant specific impulse, lighter ionic liquids will require a larger total current to produce thrust equal to that of heavier ionic liquids. Fig. 6 shows the number of emitters required to produce a given thrust level for each propellant. As expected, for a constant current per emitter, the heavier propellants require less emitters to produce a given thrust due to heavier species being extracted. At every thrust level, [Bmim][dca], [Bmim][NO$_3$], and [Emim][EtSO$_4$] require 40 %, 41%, and 35% more emitters, respectively, than [Emim][Im]; however, the number of emitters required is 33%, 32%, and 35% less than HAN, respectively. If the required thrust is 10 mN, the sheer number of emitters required is enormous: 140000 for HAN and roughly 90000 for [Bmim][dca]. Reduction in the number of emitters will require an increase in the current processed per emitter, or a reduction in the net accelerating voltage. How this may be achieved and how it relates to the overall goals of dual-mode propellant design will be discussed further in a later section.
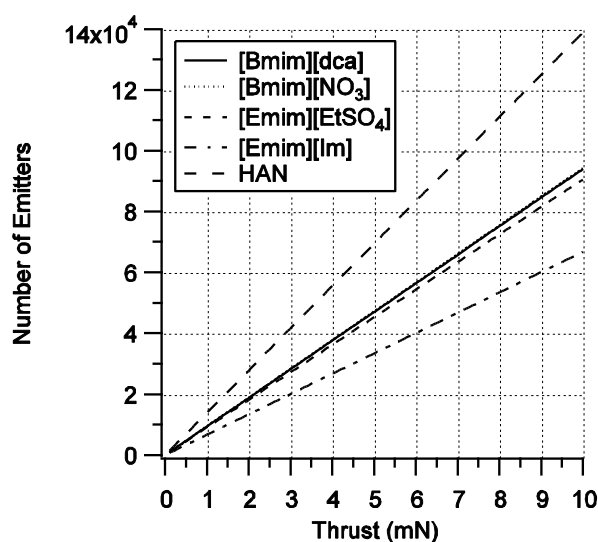
Figure 6. Number of Emitters as a Function of Thrust for IL Propellants for R_A=0.5.

Perhaps the most important drawback in any electric propulsion device is the mass of the power processing unit. The power required to produce a given thrust can be calculated from Eq. (11). Since an extraction voltage has been specified, and the corresponding specific impulse, Eqs. (9) and (10), is therefore constant across every thrust level, the power required is then not a function of current per emitter. In other words, the emitter design does not affect the requirements for the power system provided the required extraction voltage is not affected greatly by emitter design or propellant selection. The required power as a function of thrust for each propellant is shown in Fig. 7. Fig. 7 appears similar to that of Fig. 6. [Bmim][dca], [Bmim][NO_3], and [Emim][$EtSO_4$] require 36%, 38%, and 22% more power than [Emim][Im] at any given thrust level, respectively. In comparison to HAN, the same ILs require 31%, 30%, and 38% less power, respectively. The effect of utilizing higher molecular weight electrospray propellants is therefore twofold: higher molecular weight requires less emitters and lower power. It should also be noted that the required power in Fig. 7 is the power input required and does not take into account the efficiency of the power processing unit. The actual efficiency is likely to be less than 50%, which is the efficiency of hall thruster PPUs [64], and therefore the power required of the PPU will be at least double that of Fig. 7.
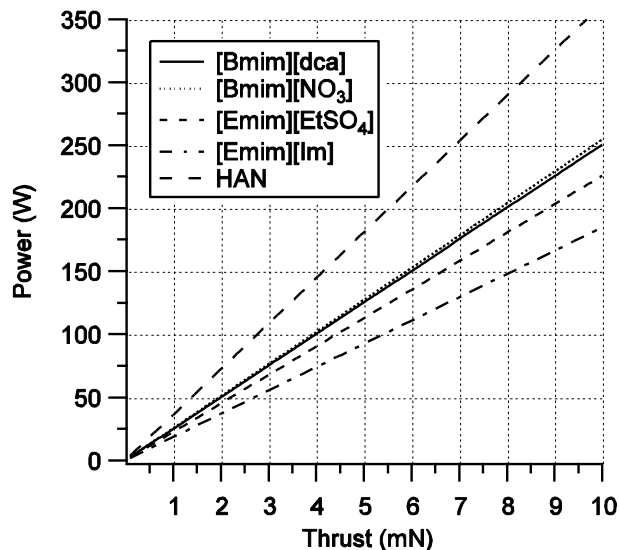
Figure 7. Power as a Function of Thrust for IL Propellants for R_A=0.5.

4.3. ELECTROSPRAY PERFORMANCE OF IONIC LIQUIDS IN BINARY MIXTURES

In the preceding sections, ionic liquid binary mixtures have been suggested as a potential route toward development of a true dual-mode propellant. It was shown that the chemical performance of these propellants may theoretically exceed that of some state-of-the-art monopropellants. The electrospray performance is more difficult to analyze because electrospray research on ionic liquids has focused on single ionic liquids. Mixtures of liquids have been studied as electrospray propellants, but most were simply solutions consisting of a salt and an electrically insulating solvent [16]. Garoz [58] studied a mixture of two ionic liquids, but did not study the composition of the droplets in the plume. A mixture of two ionic liquids may yield emissions more complicated than a single liquid since field emission of additional ion masses occurs. Extraction of pure ions would yield four possible emitted species: two cations and two anions. Extraction of higher solvated states may yield many more possible emitted species since the two salts essentially dissociate in solution and remain in chemical equilibrium, although the solution remains neutral. For example, the only N=1 solvated state of the cation of

[Bmim][dca] is [Bmim]$^+$-[Bmim][dca]; however, extraction of the [Bmim]$^+$ cation in an *N*=1 solvated state from a mixture of HAN and [Bmim][dca] could yield [Bmim]$^+$-[Bmim][dca], [Bmim]$^+$-HAN, or even [Bmim]$^+$-[Bmim]$^+$-[NO$_3$]$^-$. Although this poses an interesting research question, analysis of binary mixtures as electrospray propellants for this study is restricted to the extraction of pure ions only. As shown in the preceding section, the comparisons between various propellants should still hold somewhat, but the calculated thrust will be much lower than what will be attained in actuality; therefore power and number of emitters will be higher.

The number of emitters required and power required to produce an electrospray thrust level of 5 mN is computed as a function of percent oxidizer in the binary monopropellant mixture. The same conditions of 1μA current per emitter and 2000 V extraction voltage are also applied. The results are shown in Figs. 10 and 11. The same trends are shown as with the single ionic liquids: higher molecular weight mixtures require less emitters and less power to produce a given thrust. For emission of pure ions, [Emim][Im] requires 51000 emitters to produce 5 mN of thrust, and HAN requires 109000. From the chemical performance analysis, the binary mixture of fuels [Bmim][dca], [Bmim][NO$_3$], and [Emim][EtSO$_4$] with HAN oxidizer reached a combustion temperature, and thus performance, roughly equal to ADN-based monopropellant FLP-103 at 69%, 61%, and 59% oxidizer. From Fig. 8, this equates to 18%, 21%, and 27% less emitters than required for pure HAN, but pure [Emim][Im] requires 43%, 40%, and 36% less emitters than the ionic liquid fuels, respectively. From Fig. 9, the required power is 9.5%, 12%, and 16% lower than for pure HAN, but 75%, 70%, and 63% higher than [Emim][Im], respectively. From the chemical performance analysis, the minimum amount of oxidizer required for elimination of solid exhaust species is 58%, 44%, and 41% for each fuel respectively. At these mixture ratios, the required number of emitters is now 24%, 27%, and 31% less than required for pure HAN. The power required is 13%, 16%, and 23% lower than for pure HAN.
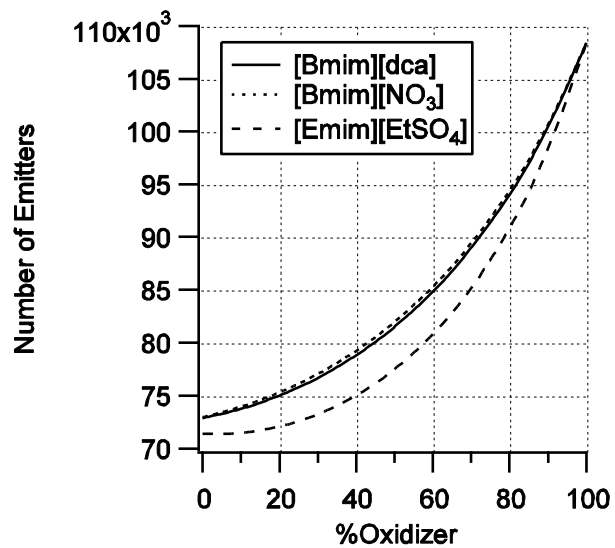
Figure 8. Number of Emitters Required to Produce 5 mN of Thrust as a Function of Percent HAN Oxidizer for IL Binary Mixtures.
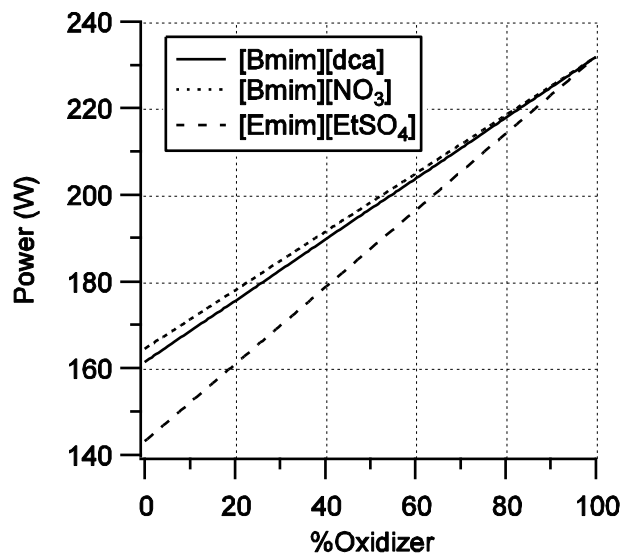
Figure 9. Required Power to Produce 5 mN of Thrust as a Function of Percent HAN Oxidizer for IL Binary Mixtures.

5. DISCUSSION

The results of the chemical performance analysis are promising for dual-mode propulsion since the performance of high-molecular weight ionic liquids as fuel components in a binary monopropellant mixture theoretically exceeds the performance of some state-of-the-art advanced monopropellants. The electrospray performance of these ionic liquids is promising and may yield higher performance than the current state of the art, but also may be limited by current technology levels. The results of the preceding sections are discussed and overall feasibility of imidazole-based ionic liquids as dual-mode propellants is assessed. Finally, using the results of this paper, trends are discussed and extrapolated into a selection guide for future dual-mode propellant development.

5.1. IMIDAZOLE BASED IONIC LIQUIDS AS MONOPROPELLANTS

Although these ionic liquids have favorable physical properties toward electrospray propulsion, considering solely a thermal decomposition of the ionic liquids as monopropellants shows poor performance in terms of specific impulse, but slightly more acceptable performance in terms of density specific impulse as all of the ionic liquids in the study have greater density than hydrazine. However, this must be re-examined considering the fact that a shifting equilibrium assumption was employed due to the solid carbon present in the exhaust. Typically, shifting equilibrium specific impulse is an over-estimate of actual specific impulse. Sutton [10] suggests that this is a 1-4% over-estimate. If this is taken as 4%, the highest performing ionic liquid, [Bmim][NO_3], now falls 9% below hydrazine in terms of density specific impulse and 22% below hydrazine in terms of specific impulse. The solid carbon formation in the exhaust gases leads to the poor performance directly. Furthermore, solid exhaust particles are also objectionable in many spacecraft applications because they degrade functional surfaces such as lenses and solar cells [10], and could cause a cloud of orbital debris. And, for monopropellant thrusters, solid particles may agglomerate on the catalyst bed, rendering it unusable. The solid carbon formation in decomposition of the ionic liquids is a direct

result of the lack of oxidizer present in the anion compared to the large organic alkyl substituted chains in the cation for the imidazole-based ionic liquids. While these high molecular weight organic chains are favorable for electrospray propulsion application, they are detrimental to the chemical aspect of a dual mode system. The highest performing ionic liquid is [Bmim][NO$_3$], which contains three oxygen atoms that form small amounts of water and carbon monoxide that lead to its higher performance. Despite having an additional oxygen atom, the large negative heat of formation of [Emim][EtSO$_4$] produces a lower overall energy release, and therefore leads to its poor performance. [Bmim][dca] performs slightly better than [Emim][EtSO$_4$] because it has a large, positive heat of formation despite containing zero oxidizing components. In order for a single imidazole-based ionic liquid to achieve even acceptable chemical performance, it must have enough oxygen to eliminate the solid carbon species in the exhaust. Ideally, in terms of just chemical performance, this type of ionic liquid will also contain a high number of nitrogen bonds, and therefore higher heat of formation [65].

5.2. BINARY MIXTURES OF IONIC LIQUIDS AS MONOPROPELLANTS

Imidazole-based ionic liquids as fuel components in a binary mixture with HAN oxidizer may be a viable option for dual-mode monopropellants. The specific impulse computed via the shifting equilibrium assumption at a combustion temperature of roughly 1900 K for the ionic liquid monopropellant blends is 1-4% higher than that of FLP-103, and roughly equal to that of FLP-103 with a frozen flow assumption. This is a feat considering the predicted combustion temperature for FLP-103 is actually 2000 K. The reason for the improved performance of the ionic liquid monopropellant blends is the combustion products that are formed. At the conditions producing a 1900 K chamber temperature, the binary ionic liquid mixtures form incompletely oxidized species CO, H$_2$, and N$_2$, as shown in Fig. 4. By contrast, the ADN-based monopropellants such as FLP-103 have been specifically designed to provide a complete combustion with major products CO$_2$, H$_2$O, and N$_2$ [12]. Examination of Eq. (5) shows that lower molecular weight exhaust products yield higher specific impulses. The lower molecular weight combustion products of the binary ionic liquid mixtures lead to higher specific impulse

despite slightly lower combustion temperature compared to FLP-103. In terms of density specific impulse, the binary mixtures of ionic liquids have 8-9% greater than that of FLP-103 for the frozen flow assumption, which yielded roughly equal specific impulse. The main consideration here is the ingredients in each mixture. The density of the fuel component, methanol, in FLP-103 is 0.79 [g/cc] [57]. The ionic liquid fuels have a much higher density, making their use as fuel components in a monopropellant mixture attractive. Additionally, FLP-103 contains a large amount of water, which also lowers the density of the mixture.

These types of binary mixtures have been shown to be advantageous in terms of performance, but practically they must be chemically compatible and also be thermally stable and readily ignitable. As mentioned previously, mixtures of [Bmim][dca] with HAN have notably shown no visible reactivity, leading to the possibility that they may indeed be thermally stable at room temperature. However, this represents somewhat of an unknown presently as this has not been measured quantitatively. Literature suggests that mixtures of ammonium salts with dicyanamide anions may not be compatible [66-69]. [Bmim][NO_3] or [Emim][$EtSO_4$] may be compatible with HAN, but HAN may not be miscible in either liquid, requiring a third liquid solvent which may be undesirable. Furthermore, it is also unknown whether these mixtures will ignite either thermally or catalytically at reasonable temperatures (typically $< 200^0$C). These ignition methods represent the most common and reliable means of igniting a monopropellant and verification of this is a major milestone in any monopropellant development effort.

5.3. IMIDAZOLE-BASED IONIC LIQUIDS AS ELECTROSPRAY PROPELLANTS

In terms of electrospray performance, the ionic liquid fuels investigated show potential to be higher performing than the current state-of-the-art in electrospray propellants; however, they may present a challenge in terms of the current technology levels, if high specific impulse emission is desired. The ionic liquid fuels investigated in this study have the potential to have higher performance, and also greater flexibility, than the current state-of-art electrospray propellant [Emim][Im]. This is a direct result from the lower molecular weight of the investigated ionic liquids compared to [Emim][Im].

However, low molecular weight may be a detriment to electrospray propulsion overall, as evidenced by the pure number of emitters and power required as shown in Figs. 6-9. Considering the number of emitters required to produce thrust levels typical of electric propulsion missions shows this effect. To produce 10 mN of thrust with emission of half $N=0$ ions and half $N=1$ ion clusters, [Emim][Im] requires 67000 emitters. If the current technology limit is taken as 13000 emitters per cm^2 [70], this equates to a total area of 5.2 cm^2 for [Emim][Im]. The 200 W SPT-35 Hall thruster has an area of 9.6 cm^2 and produces a comparable thrust of 11 mN [71]. By contrast, purely ionic emission of HAN at an ion fraction of 0.5 requires a total area of 10.8 cm^2 to produce 10 mN of thrust. While the number of emitters can be effectively reduced by a deceleration grid [72], this adds complexity to the system, and requires even more power. Even without a deceleration grid, considering a PPU of equal efficiency to a typical hall thruster (~50%) [Emim][Im] requires 370 W to produce 10 mN of thrust, while HAN requires 730 W. The trend is clear: irrespective of technological advances, higher molecular weight propellants are more advantageous in terms the hardware and power requirements on electrospray systems.

The large power requirements precluded by emission in the PIR may be detrimental overall to dual-mode if the molecular weight is lower than state-of-the-art propellants. This is a direct consequence of the required extraction voltage to produce a PIR emission, typically 1.5-2.5 kV, which without a deceleration grid produces a high specific impulse. However, designers have the option to operate the system in the droplet regime, which may ultimately be a viable option, especially on first generation dual-mode systems. As mentioned, operation in the droplet mode usually results in very low specific impulse compared to the PIR, but produces more thrust due to higher mass to charge ratio. Furthermore, the size of droplets, and therefore the specific impulse, can be controlled without the addition of a deceleration grid. For example, the ionic liquid [Emim][Beti] has experimentally reached a specific impulse from less than 200 seconds and 2.7 µN per emitter up to 1500 seconds and 0.79 µN per emitter have been attained in the droplet regime [73]. It should be noted, however, that the highest specific impulse in the droplet regime was obtained by increasing the backing pressure at an emitter temperature above which PIR was attained. Additionally, the lower efficiency in droplet

mode lowered the thrust per emitter to levels equal to the PIR attained by further heating of the emitter, but at much higher specific impulse (~2300 sec). Therefore, while the droplet mode may be easier to achieve, the most flexible and highest performing dual-mode propellants will be able to achieve the PIR.

One of the assumptions made in this analysis was that all propellants could emit at the same current per emitter. In reality, with current state-of-the-art emitter technology considered, this may not be entirely the case. In perhaps the most promising advancement in emitter technology for dual-mode purpose, Legge and Lozano [20] use a porous metal emitter geometry to produce PIR electrospray emission. What was most intriguing was that with this geometry, the same heavier, less electrically conductive ionic liquids that required a preheat of over $200^{o}C$ were able to emit in the purely ionic regime at room temperature. However, the current emitted was much less at the same extraction voltage in comparison to lighter molecular weight propellants such as [Emim][BF$_4$]. The higher molecular weight propellants will therefore require either higher extraction voltage or heating of the emitter to produce the same current per emitter as lighter, less viscous and more electrically conductive propellants. Each propellant, however, still required roughly 1.5 kV extraction voltage to begin emission. So, while the number of emitters could be reduced if the propellant is less viscous and also more electrically conductive, the power requirements should remain roughly the same even without heating the emitter. However, emitter technology, especially the novel porous metal emitter described here, is still very much in its infancy and these conclusions could eventually change.

5.4. BINARY MIXTURES OF IONIC LIQUIDS AS ELECTROSPRAY PROPELLANTS

The chemical performance of ionic liquids in binary mixtures is promising; however achieving high specific impulse with current technology in the electrospray mode may present more of a challenge than for a single ionic liquid. The reason is the same as discussed above: the low molecular weight of the propellants. This issue is compounded by adding ionic oxidizers, such as HAN or ADN, which have a much lower molecular weight than even the ionic liquid fuels investigated in this paper. To achieve chemical performance equal to ADN-based FLP-103, the number of emitters required to

produce 5 mN of thrust is 88000, 82000, and 79000 emitters when using [Bmim][dca], [Bmim][NO$_3$], and [Emim][EtSO$_4$] as fuels, respectively, but assuming only ions are emitted. Therefore, to achieve equal chemical and electrospray performance, [Emim][EtSO$_4$] requires 10% less emitters than [Bmim][dca], thereby saving roughly 10% mass in terms of the emitter hardware. Additionally, considering the minimum amount of oxidizer to achieve no solid carbon in the theoretical exhaust species, [Emim][EtSO$_4$] will require nearly 15% less emitters than [Bmim][dca]. In terms of power requirements, at the condition where chemical performance is greater than FLP-103, [Emim][EtSO$_4$] requires 7% less power than [Bmim][dca]. At the minimum oxidizer amount, [Emim][EtSO$_4$] requires 15% less power than [Bmim][dca]. It is therefore more ideal for dual-mode propellant blends to use fuels with high molecular weight, but that have a higher oxygen balance, as equal performance may be obtained in both modes, but with a reduction in electrospray hardware.

5.5. CONSIDERATIONS FOR DUAL-MODE PROPELLANT DESIGN

Based on the results presented in this paper there are two logical methods to achieving a workable dual-mode propellant: a single, oxygen-balanced, task specific ionic liquid or a mixture of two or more ionic liquids. While this may seem to not depart from conventional wisdom in energetic ionic liquid monopropellant design, when viewed as a dual-mode propellant the requirements will have to change somewhat. Based on the results described in the above paragraphs, expected properties and performance characteristics in terms of what can be reasonably expected at current technology levels for each method are shown in Table 6.

Table 6. Estimated Attainable Physical Properties and Performance Characteristics of Imidazole-based Dual-Mode Propellants.[a]

Physical Properties	Single Ionic Liquid	Binary Mixture
melting point	$< 2\,^{\circ}C$	$< 2\,^{\circ}C$
density	$< 1.4 \text{ g/cm}^3$	$> 1.4 \text{ g/cm}^3$
viscosity	< 100 cP	< 100 cP
surface tension	< 100 dyne/cm	< 100 dyne/cm
electrical conductivity	< 1 S/m	~ 1 S/m
thermal stability	$< T_{PIR}$[b]	$> T_{PIR}$
molecular weight	$> MW_{SOA}$	$< MW_{SOA}$
heat of formation	Negative $< \Delta H^o_{f,SOA}$	Negative $\sim \Delta H^o_{f,SOA}$
Performance Properties		
chemical I_{sp}	> 270 sec	> 250 sec
combustion temperature	> 2500 K	> 1900 K
electrical I_{sp}	200-1500 sec	200-5000 sec
power required	$< P_{SOA}$	$> P_{SOA}$
emitters required	$< N_{SOA}$	$> N_{SOA}$

[a]SOA=State-of-the-Art [b]Capillary emitter

In terms of pure performance, the ultimate in dual-mode propellants may be a single liquid which would provide enough oxidizer in the anion to combust to gaseous products CO, H_2, and N_2, while still retaining reasonable electrospray properties. This would not only provide good chemical performance, but inherently this would also be a high-molecular weight propellant assuming $[Emim]^+$ or higher molecular weight cations were used. This idea of an oxygen-balanced ionic liquid as a chemical monopropellant is not new, as attempts have been made to synthesize such a liquid for energetic use [74-76]. The ionic liquids in [74] were based on lanthanide nitrate complex anions and either triazole- or tetrazole-based cations. The ionic liquids in [75] were imidazole-based. Many of the liquids in these efforts were not thermally stable, but a few of these ionic liquids

were reportedly stable at room temperature, for example 1-ethyl-3-methylimidazolium tetranitratoaluminate ($C_6H_{11}N_6AlO_{12}$). An ionic liquid of the same anion synthesized by Jones, et. al. [76], 1- ethyl-4,5-dimethyltetrazolium tetranitratoaluminate ($C_5H_{11}N_8AlO_{12}$), had a chemical specific impulse of 280 seconds, but at a combustion temperature of 2800 K, well above the sintering temperature of current catalyst bed technology. Furthermore, these are not ideal spacecraft monopropellants as their combustion forms a significant amount of solid products, such as Al_2O_3, which are objectionable in many spacecraft applications, as mentioned previously [10]. It is unknown to this point whether these propellants have the electrochemical properties required for electrospray propulsion. However, based on trends reported for many imidazole-based ionic liquids these can be reasonably inferred qualitatively and commented upon. In general, ionic liquids with large, bulky anions have both lower electrical conductivity and lower surface tension [5, 6]. Additionally, increasing the size of the cation for imidazole-based liquids always decreases the surface tension and electrical conductivity. This is in an almost direct contradiction to what is typically preferred in energetic ionic liquid design. Making use of an increased alkyl chain size in the cation or increased number of N-N bonds in the anion, therefore raising the heat of formation of the liquid combined with the requirement for oxygen balance is actually detrimental to the minimum performance requirements to achieve PIR for electrospray propulsion: high surface tension and high electrical conductivity.

Perhaps the most important consideration to be made in the early stages of dual-mode propellant design is actually the thermal stability of ionic liquids. The high thermal stability of ionic liquids compared to more traditional energetic materials is usually viewed as a benefit rather than a strict requirement. For dual-mode propellants, this will be a requirement. The reason is that larger molecular weight propellants will inevitably require the emitter to be preheated due to their inherently low surface tension and electrical conductivity. As mentioned, in some cases this has been found to be greater than 200°C, which actually is above or near the decomposition temperature of many energetic ionic liquids that have been synthesized [77]. It is therefore likely that with current emitter technology, oxygen-balanced ionic liquids may be limited to emission in a droplet regime rather than PIR. Based on the discussion above, to produce an oxygen-

balanced ionic liquid with improved performance over state-of-the-art will require a higher technology level than is currently available on either chemical monopropellant or electrospray thrusters. The inherently high combustion temperature of currently synthesized oxygen-balanced ionic liquids is far above that of current monopropellants, and the lower thermal stability compared to state-of-the-art electrospray propellants could pose issues in attaining high-specific impulse emissions. As mentioned, with porous metal emitters the latter could be avoided, but at the cost of lower current per emitter. If the emitter preheat temperature is limited due to the thermal stability consideration when spraying an energetic ionic liquid rather than a much more stable fluorinated ionic liquid, then either the extraction voltage or the number of emitters will have to be increased to compensate. Higher power requirements compared to state-of-the-art electrospray propellants may therefore be inevitable for a dual-mode monopropellant/electrospray system if specific impulse near the state-of-the art in each mode individually is desired. Ultimately, considering the lower-specific impulse droplet mode for these types of ionic liquids may be more advantageous given the reduction in thruster hardware, but will depend on the desired mission capabilities.

In this paper, the method of combining a fuel-rich ionic liquid with an ionic oxidizer such as HAN or ADN as means of obtaining a workable dual-mode propellant is presented. This may be a much simpler method than developing a task-specific ionic liquid because the anticipated physical properties are closer to the present state-of-the-art in both modes. It was shown that in order to obtain performance closer to state-of-the-art more power and emitters will be necessary given the low molecular weight of the oxidizer. However, PIR is likely easier to achieve, given that both HAN and an ionic liquid fuel have electrical conductivities near 1 S/m [78], therefore requiring a reduced emitter preheat compared to oxygen-balanced ionic liquids. The main challenge for this method will be the chemical compatibility and also the miscibility of the oxidizer in the ionic liquid fuel. To be even usable in the electrospray mode, it is absolutely paramount that no portion of the mixture be volatile, which departs from conventional 'green' monopropellants which make use of both water and a volatile fuel. While it may be possible that the addition of water to a certain ionic liquid system may show azeotropic behavior, this is difficult to assess and even in the best case scenario will be detrimental

to electrospray performance as a whole. When selecting candidate ionic liquid fuels, liquids that have a higher oxygen balance will be more promising when considering the dual-mode system as a whole. The main reason, as discussed is the fact that a smaller amount of the lower molecular weight oxidizer is required. However, an interesting point can be made when considering the minimum amount of oxidizer required. Although the chemical performance drops, mass can be saved on the electrospray system and therefore the potential for increased flexibility in the design choices exists.

6. CONCLUSIONS

Imidazole based ionic liquids have been examined as potential candidates for dual-mode chemical monopropellant and electrospray propulsion. Physical properties required of ionic liquids for dual-mode spacecraft propulsion are high density, low melting temperature, high electrical conductivity, high surface tension, and high molecular weight. These properties should be comparable to current state-of-the-art propellants hydrazine and [Emim][Im] for the chemical and electrical modes, respectively. Three generic, sample ionic liquids were identified that exceed or are close to meeting the physical property criteria: [Bmim][dca], [Bmim][NO_3], and [Emim][$EtSO_4$].

Theoretical chemical performance was calculated for these ionic liquids using the NASA CEA computer code and performance equations. Considering these ionic liquids as monopropellants shows that they do not perform well compared to hydrazine and will be essentially unusable due to the large amounts of solid carbon predicted in the exhaust species. Considering the ionic liquids as fuel components in a binary monopropellant mixture with 60-70% HAN oxidizer shows performance exceeding that of ADN-based monopropellants. Ionic liquid fuel components with more oxidizing elements in the anion require less additional HAN oxidizer to form gaseous CO, and thus achieve an acceptable level of performance.

Examination of the electrospray performance of these ionic liquids shows that they may compete with current state-of-the-art propellants with improvements in technology. High molecular weight propellants reduce the number of required electrospray emitters, while also requiring higher power. The addition of a lower molecular weight oxidizer to an imidazole-based ionic liquid fuel increases the number of emitters required, but is necessary to obtain good chemical performance. Ionic liquid fuel components with oxidizing components in the anion require less additional oxidizer to achieve similar chemical performance, thereby reducing the number of required emitters for electrospray propulsion. By extension, in terms of pure performance oxygen-balanced ionic liquids may be the ultimate in dual mode propulsion as they have the required oxidizer to combust into complete products, while most likely retaining high molecular weight favorable to electrospray propulsion.

Two methods typical of design of energetic ionic liquids for monopropellant applications were discussed: design of a task-specific, oxygen balanced ionic liquid or design of a mixture of multiple ionic liquids. In terms of performance, a task-specific ionic liquid will likely outperform any mixture in a dual-mode system, but will require advances in both monopropellant and electrospray technology to achieve high performance due to the anticipated high combustion temperature, as well as low thermal stability compared to estimated required heating of a capillary electrospray emitter to achieve high-specific impulse PIR emission. A workable dual-mode propellant utilizing binary mixture of ionic liquids will be easier to achieve given current technology. Utilization of ionic liquid fuels with higher oxygen balance provided by the anion is desired when forming binary mixtures with an oxidizer such as HAN, as comparatively this results in reduction of electrospray hardware, while still achieving equal performance in both modes compared to more fuel-rich ionic liquid fuels. The drawback is an increase in required power to achieve high performance electrospray emission compared to state-of-the-art electrospray-specific propellants due to the low molecular weight of the additional oxidizer.

REFERENCES

[1] Hass, J.M., Holmes, M.R., "Multi-Mode Propulsion System for the Expansion of Small Satellite Capabilities," NATO MP-AVT-171-05, 2010.

[2] Donius, B.R. "Investigation of Dual-Mode Spacecraft Propulsion by Means of Ionic Liquids," Masters Thesis, Department of Mechanical and Aerospace Engineering, Missouri University of Science & Technology, Rolla, MO., May 2010.

[3] Donius, B. R., Rovey, J. L., "Ionic Liquid Dual-Mode Spacecraft Propulsion Assessment," *Journal of Spacecraft and Rockets*, Vol. 48, No. 1, 2011, pp. 110-123. doi:10.2514/1.49959

[4] Donius, B. R., Rovey, J. L., "Analysis and Prediction of Dual-Mode Chemical and Electric Ionic Liquid Propulsion Performance," *48th Aerospace Sciences Meeting*, AIAA Paper 2010-1328, 2010.

[5] Wilkes, J.S., Wasserscheid, P., Welton, T., *Ionic Liquids in Synthesis*, 2nd ed., WILEY-VCH Verlag GmbH &Co., 2008, Ch.1.

[6] Freemantle, M. *An Introduction to Ionic Liquids*, RSC Publishing, 2010.

[7] Plechkova, N. V., Seddon, K. R., "Applications of Ionic Liquids in the Chemical Industry," *Chemical Society Reviews*, Vol. 37, 2008, pp. 132-150. doi: 10.1039/B006677J

[8] Boatz, J., Gordon, M., Voth, G., Hammes-Schiffer, S., "Design of Energetic Ionic Liquids," *DoD HPCMP Users Group Conference*, IEEE Publ., Piscataway, NJ, Pittsburgh, 2008, pp. 196-200.

[9] Smiglak, M., Reichert, M. W., Holbrey, J. D., Wilkes, J. S., Sun, L., Thrasher, J. S., Kirichenko, K., Singh, S., Katritzky, A. R., Rogers, R. D., "Combustible ionic liquids by design: is laboratory safety another ionic liquid myth?," Chemical Communications, Issue 24, 2006, pp. 2554-2556. doi: 10.1039/b602086k

[10] Sutton, G. P., Biblarz, O., *Rocket Propulsion Elements*, 7th ed., John Wiley & Sons, New York, 2001, Ch. 5, 7, 19.

[11] Amariei, D., Courtheoux, L., Rossignol, S., Batonneau, Y., Kappenstein, C., Ford, M., and Pillet, N., "Influence of the Fuel on the Thermal and Catalytic Decompositions of Ionic Liquid Monopropellants," 41st AIAA Joint Propulsion Conference, AIAA, Paper 2005-3980, 2005.

[12] Anflo, K., Grönland, T. A., Bergman, G., Johansson, M., Nedar, R., "Towards Green Propulsion for Spacecraft with ADN-Based Monopropellants," 38th AIAA Joint Propulsion Conference, AIAA Paper 2002-3847, 2002.

[13] Slettenhaar, B., Zevenbergen, J. F., Pasman, H. J., Maree, A. G. M., Moerel, J. L. P. A. "Study on Catalytic Ignition of HNF Based Non Toxic Monopropellants," 39th AIAA Joint Propulsion Conference. AIAA Paper 2003-4920, 2003.[14] Anflo, K., Persson, S., Thormahlen, P., Bergman, G., Hasanof, T., "Flight Demonstration of an ADN-Based Propulsion System on the PRISMA Satellite," 42nd AIAA Joint Propulsion Conference, AIAA Paper 2006-5212, 2006.

[15] Chang, Y. P.,Josten, J. K., Zhang, B. Q., Kuo, K. K., "Combustion Characteristics of Energetic HAN/Methanol Based Monopropellants," 38th AIAA Joint Propulsion Conference, AIAA Paper 2002-4032, 2002.

[16] Chiu, Y., Dressler, A., "Ionic Liquids for Space Propulsion," In *Ionic Liquids IV: Not Just Solvents Anymore*, ACS Symposium Series, Vol. 975, American Chemical Society, Washington, DC, 2007, pp. 138-160.

[17] Romero-Sanz, I., Bocanegra, R., Fernandez De La Mora, J., Gamero-Castano, M., "Source of Heavy Molecular Ions Based on Taylor Cones of Ionic Liquids Operating in the Pure Ion Evaporation Regime," *Journal of Applied Physics*, Vol. 94, 2003, pp. 3599-3605.
doi: 10.1063/1.1598281

[18] Gamero-Castano, M., "Characterization of a Six-Emitter Colloid Thruster Using a Torsional Balance," *Journal of Propulsion and Power*, Vol. 20, No. 4, 2004, pp. 736-741.
doi: 10.2514/1.2470

[19] Larriba, C., Garoz, D., Bueno, C., Romero-Sanz, I., Castro, S., Fernandez de la Mora, J., Yoshida, Y., Saito, G., Hagiwara, R., Masumoto, K., Wilkes, J., "Taylor Cones of Ionic Liquids as Ion Sources: The Role of Electrical Conductivity and Surface Tension," *Ionic Liquids IV: Not Just Solvents Anymore*, ACS Symposium Series, Vol. 975, American Chemical Society, Washington, DC, 2007, Ch. 21.

[20] Legge, R. S., Lozano, P. C., "Electrospray Propulsion Based on Emitters Microfabricated in Porous Metals," *Journal of Propulsion and Power*, Vol. 27, No. 2, 2011, pp. 485-495.

[21] Demmons, N., Hruby, V., Spence, D., Roy, T., Ehrbar, E., Zwahlen, J., Martin, R., Ziemer, J., Randolph, T., "ST7-DRS Mission Colloid Thruster Development," *44th AIAA Joint Propulsion Conference*, AIAA Paper 2008-4823, 2008.

[22] Gamero-Castano, M., Fernandez De La Mora, J., "Direct Measurement of Ion Evaporation Kinetics from Electrified Liquid Surfaces," *Journal of Chemical Physics*, Vol. 113, 2000, pp. 815-832.
doi: 10.1063/1.481857

[23] Fernandez de la Mora, J., Loscertales, I. G., "The Current Emitted by Highly Conducting Taylor Cones," *Journal of Fluid Mechanics*, Vol. 260, 1994, pp. 155-184.
doi: 10.1017/s0022112094003472

[24] De Grys, K. H., Wilson, A. C., "Ionic Liquid Multi-Mode Propulsion System," Aerojet Corporation, International Patent Application No. PCT/US2009/003732. Publication No. WO/2010/036291, Jan 2010.

[25] Seddon, K., Stark, A., Torres, M., "Viscosity and Density of 1-Alkyl-3-methylimidazolium Ionic Liquids", *Clean Solvents*, ACS Symposium Series, Vol. 819, American Chemical Society, 2002, Ch. 4.

[26] Emel'yanenko, V. N., Verevkin, S. P., Heintz, A., Schick, C., "Ionic Liquids. Combination of Combustion Calorimetry with High-Level Quantum Chemical Calculations for Deriving Vaporization Enthalpies", *Journal of Physical Chemistry B*, Vol. 112, 2008, pp. 8095-8098.
doi: 10.1021/jp802112m

[27] Kowsari, M. H., Alavi, S., Ashrafizaadeh, M., Najafi, B., "Molecular Dynamics Simulation of Imidazolium Based Ionic Liquids. II. Transport Coefficients," *Journal of Chemical Physics*, Vol. 130, 2009.

doi: 10.1063/1.3042279

[28] Mokhtarani, M., Sharifi, A., Mortaheb, H. R., Mirzaei, M., Mafi, M., Sadeghian, F., "Density and viscosity of 1-butyl-3-methylimidazolium nitrate with ethanol, 1-propanol, or 1-butanol at several temperatures," *Journal of Chemical Thermodynamics*, Vol. 41, 2009, pp. 1432-1438.

doi: 10.1016/j.jct.2009.06.02

[29] Fredlake, C. P., Crosthwaite, J. M., Hert, D. G., Aki, S. N. V. K., Brennecke, J. F., "Thermophysical Properties of Imidazolium-Based Ionic Liquids," *Journal of Chemical Engineering Data*, Vol. 49, 2004, pp. 954-964.

doi: 10.1021/je034261a

[30] Emel'yanenko, V. N., Verevkin, S. P., Heintz, A., "The Gaseous Enthalpy of Formation of the Ionic Liquid 1-Butyl-3 methylimidazolium Dicayanamide from Combustion Calorimetry, Vapor Pressure Measurements, and Ab Initio Calculations*," Journal of the American Chemical Society*, Vol. 129, 2007, No. 13, pp. 3930-3937.

doi: 10.1021/ja0679174

[31] Zech, O., Stoppa, A., Buchner, R., Kunz, W., "The Conductivity of Imidazolium-Based Ionic Liquids from (248 to 468) K. B. Variation of the Anion," *Journal of Chemical Engineering Data*, Vol. 55, 2010, pp. 1774-1778.

doi: 10.1021/je900793r

[32] Klomfar, J., Souckova, M., Patek, J., "Temperature Dependence of the Surface Tension and Density at 0.1 MPa for 1-Ethyl- and 1-Butyl-3-methylimidazolium Dicyanamide," *Journal of Chemical Engineering Data*, Vol. 56, 2011, pp. 3454-3462.

doi: 10.1021/je200502j

[33] Carvalho, P. J., Regueira, T., Santos, L. M. N. B. F., Fernandez, J., Coutinho, J. A. P., "Effect of Water on the Viscosities and Densities of 1-Butyl-3-methylimidazolium Dicyanamide and 1-Butyl-3-methylimidazolium Tricyanomethane at Atmospheric Pressure," *Journal of Chemical Engineering Data*, Vol. 55, 2010, pp. 645-652.

doi: 10.1021/je900632q

[34] Hofman, T., Goldon, A., Nevines, A., Letcher, T. M., "Densities, excess volumes, isobaric expansivity, and isothermal compressibility of the (1-ethyl-3-methylimidazolium ethylsulfate + methanol) system at temperatures (283.15 to 333.15) K and pressures from (0.1 to 35) MPa," *Journal of Chemical Thermodynamics*, Vol. 40, 2008, pp. 580-591.

doi: :10.1016/j.jct.2007.11.01

[35] Domanska, U., Laskowska, M., "Phase Equilibria and Volumetric Properties of (1-Ethyl-3-Methylimidazolium Ethylsulfate + Alcohol or Water) Binary Systems," *Journal of Solution Chemistry*, Vol. 37, Issue 9, 2008 pp. 1271-1287.

doi: 10.1007/s109530089306y

[36] Zhang, Z. H., Tan, Z. C., Sun, L. X., Jia-Zhen, Y., Lv, X. C., Shi, Q., "Thermodynamic investigation of room temperature ionic liquid: The heat capacity and standard enthalpy of formation of EMIES," *Thermochimica Acta,* Vol. 447, 2006, pp. 141-146.

doi: 10.1016/j/tca.2006.04.022

[37] Vila, J., Gines, P., Rilo, E., Cabeza, O., Varela, L. M , "Great Increase of the Electrical Conductivity of Ionic Liquids in Aqueous Solutions," *Fluid Phase Equilibria*, Vol. 247, 2006, pp. 32-39.

doi: 10.1016/j.fluid.2006.05.028

[38] Gomez, E., Gonzalez, B., Calvar, N., Tojo, E., Dominguez, A., "Physical Properties of Pure 1-Ethyl-3-methylimidazolium Ethylsulfate and Its Binary Mixtures with Ethanol and Water at Several Temperatures," *Journal of Chemical Engineering Data,* Vol. 51, 2006, pp. 2096-2102.

doi: 10.1021/je060228n

[39] Arce, A., Rodil, E., Soto, A., "Volumetric and Viscosity Study for the Mixtures of 2-Ethoxy-2-methylpropane, Ethanol, and 1-Ethyl-3-methylimidazolium Ethyl Sulfate Ionic Liquid," *Journal of Chemical Engineering Data*, Vol. 51, 2006, pp. 1453-1457.

doi: 10.1021/je060126x

[40] Schreiner, C., Zugmann, S., Hartl, R., Gores, H. J., "Fractional Walden Rule for Ionic Liquids: Examples from Recent Measurements and a Critique of the So-Called Ideal KCl Line for the Walden Plot," *Journal of Chemical Engineering Data*, Vol. 55, 2010, pp. 1784-1788.

doi: 10.1021/je900878j

[41] Tokuda, H., Tsuzuki, S., Abu Bin Hasan Susan, M., Hayamizu, K., Watanabe, M., "How Ionic Are Room-Temperature Ionic Liquids? An Indicator of the Physicochemical Properties," *Journal of Physical Chemistry B*, Vol. 110, 2006, pp. 19593-19600.

doi: 10.1021/jp064159v

[42] Widegren, J. A., Saurer, E. M., Marsh, K. N., Magee, J. W., "Electrolytic Conductivity of Four Imidazolium-Based Room-Temperature Ionic Liquids and the Effect of Water Impurity*," Journal of Chemical Thermodynamics*, Vol. 37, 2005, pp. 569-575.

doi: 10.1016/j.jct.2005.04.009

[43] Carvalho, P. J., Freire, M. G., Marrucho, I. M., Queimada, A. J., Coutinho, J. A. P., "Surface Tensions for the 1-Alkyl-3-methylimidazolium Bis(trifluoromethylsulfonyl)imide Ionic Liquids," *Journal of Chemical Engineering Data*, Vol. 53, 2008, pp. 1346-1350.

doi: 10.1021/je800069z

[44] Gordon, S., "Computer Program for the Calculation of Complex Chemical Equilibrium Compositions and Applications," NASA RP-1311-P2, 1996.

[45] Schmidt, E. W., *Hydrazine and Its Derivatives: Preparation, Properties, Applications*, Wiley-Interscience, 2001.

[46] Vila, J., Gines, P., Pico, J. M., Franjo, C., Jimenez, E., Varela, L. M., Cabeza, O., "Temperature dependence of the electrical conductivity in EMIM-based ionic liquids: Evidence of Vogel–Tamman–Fulcher behavior," *Fluid Phase Equilibria*, Vol. 242, 2006, pp. 141-146.

doi: 10.1016/j.fluid.2006.01.02

[47] Sanchez, L. G., Espel, J. R., Onink, F., Meindersma, G. W., De Haan, A. B., "Density, Viscosity, and Surface Tension of Synthesis Grade Imidazolium, Pyridinium, and Pyrrolidinium Based Room Temperature Ionic Liquids," *Journal of Chemical Engineering Data*, Vol. 54, 2009, pp. 2803-2812.

doi: 10.1021/je800710p

[48] Yan, T., Li, S., Jiang, W., Gao, X., Xiang, B., Voth, G., "Structure of the Liquid-Vacuum Interface of Room Temperature Ionic Liquids: A Molecular Dynamics Study," *Journal of Physical Chemistry B*, Vol. 110, 2006, pp. 1800-1806.

doi: 10.1021/jp055890p

[49] Fletcher, S. I., Sillars, F. B., Hudson, N. E., Hall, P. J., "Physical Properties of Selected Ionic Liquids for Use as Electrolytes and Other Industrial Applications," *Journal of Chemical Engineering Data*, Vol. 55, 2010, pp. 778-782.

doi: 10.1021/je900405j

[50] Strechan, A. A., Kabo, A. G., Paulechka, Y. U., Blokhin, A. V., Kabo, G. J., Shaplov, A. S., Lozinskaya, E. I., "Thermochemical Properties of 1-butyl-3-methylimidazolium nitrate", *Thermochimica Acta*, Vol. 47, 2008, pp. 25-31.

doi: 10.1016/j.tca.2008.05.002

[51] Stoppa, A., Hunger, J., Buchner, R., "Conductivities of Binary Mixtures of Ionic Liquids with Polar Solvents," *Journal of Chemical Engineering Data*, Vol. 54, 2009, pp. 472-479.

doi: 10.1021/je800468h

[52] Sanchez, L. G., Espel, J. R., Onink, F., Meindersma, G. W., de Haan, A. B., "Density, Viscosity, and Surface Tension of Synthesis Grade Imidazolium, Pyridinium, and Pyrrolidinium Based Room Temperature Ionic Liquids," *Journal of Chemical Engineering Data*, Vol. 54, 2009, pp. 2803-2812.

doi: 10.1021/je800710p

[53] Yoshida, Y., Baba, O., Larriba, C., Saito, G., "Imidazolium-Based Ionic Liquids Formed with the Dicyanamide Anion: Influence of Cationic Structure on Ionic Conductivity," *Journal of Physical Chemistry B*, Vol. 111, 2007, pp. 12204-12210. doi: 10.1021/jp0745236

[54] Krummen, M., Wasserscheid, P., Gmehling, J., "Measurement of Activity Coefficients at Infinite Dilution in Ionic Liquids Using the Dilutor Technique," *Journal of Chemical Engineering Data*, Vol. 47, 2002, 1411-1417. doi: 10.1021/je0200517

[55] Gomez, E., Gonzalez, B., Calvar, N., Tojo, E., Dominguez, A., "Physical Properties of Pure 1-Ethyl-3-methylimidazolium Ethylsulfate and Its Binary Mixtures with Ethanol and Water at Several Temperatures," *Journal of Chemical Engineering Data*, Vol. 51. 2006, pp. 2096-2102. doi: 10.1021/je060228n

[56] Yang, J., Lu, X., Gui, J., Xu, W., "A new theory for ionic liquids—the Interstice Model
Part 1. The density and surface tension of ionic liquid EMISE," *Green Chemistry*, Vol. 6, 2004, pp. 541-543. doi: 10.1039/B412286K

[57] Wingborg, N., Eldsater, C., Skifs, H., "Formulation and Characterization of ADN-Based Liquid Monopropellants," 2nd International Conference on Green Propellants for Space Exploration, ESA SP-557, 2004.

[58] Garoz, D., Bueno, C., Larriba, C., Castro, S., Fernandez de la Mora, J., "Taylor Cones of Ionic Liquids from Capillary Tubes as Sources of Pure Ions for Electrical Propulsion," 42nd AIAA Joint Propulsion Conference, AIAA Paper 2006-4639.

[59] "CPIA/M5 Liquid Propellant Engine Manual," Johns Hopkins University, Columbia, MD. Chemical Propulsion Information Agency, 1998.

[60] Holbrey, J. D., Rogers, R. D., "Physiochemical Properties of Ionic Liquids: Melting Points and Phase Diagrams," In *Ionic Liquids in Synthesis*, 2nd ed., WILEY-VCH Verlag GmbH &Co., 2008, Ch.3.

[61] Klein, N., "Liquid Propellants for Use in Guns-A Review," BRL-TR-2641, 1985.

[62] Dambach, E., Heister, S., Ismail, I., Schneider, S., Hawkins, T., "An Investigation of Hypergolicity of Dicyanamide-Based Ionic Liquid Fuels with Common Oxidizers," Air Force Research Laboratory, AFRL-RZ-ED-TP-2008-371, 2008.

[63] Chiu, Y., Austin, B. L., Dressler, R. A., Levandier, D., Murray, P. T., Lozano, P., Martinez-Sanchez, M., "Mass Spectrometric Analysis of Colloid Thruster Ion Emission from Selected Propellants," *Journal of Propulsion and Power*, Vol. 21, 2005, pp. 416-423.

[64] Pencil, E. J., "Recent Electric Propulsion Development Activities for NASA Science Missions," *IEEE Aerospace Conference*, IEEE Publ., March 2009.

[65] Chambreau, S. D., Boatz, J. A., Vaghjiani, G. L., Koh, C., Kostko, O., Golan, A., Leone, S. R., "Thermal Decomposition Mechanism of 1-Ethyl-3-methylimidazolium Bromide Ionic Liquid," *Journal of Physical Chemistry A* [online], URL: http://pubs.acs.org/doi/pdf/10.1021/jp209389d [cited 7 March 2012].
doi: 10.1021/jp209389

[66] Frankel, M. B., Burns, E. A., Butler, J. C., Wilson, E. R., "Derivatives of Dicyanamide," *Journal of Organic Chemistry*, Vol. 28, 1963, pp. 2428.

[67] Jurgens, B. A., Hoppe, H. A., Irran, E., Schnick, W., "Transformation of Ammonium Dicyanamide in the Solid," *Inorganic Chemistry*, Vol. 41, 2002, pp. 4849-4851.
doi: 10.1021/ic025800k

[68] Lotsch, B. V., Schnick, W., "Towards Novel C-N Materials: Crystal Structures of Two Polymorphs of Guanidinium Dicyanamide and Their Thermal Conversion into Melamine," *New Journal of Chemistry*, Vol. 28, 2004, pp. 1129-1136.
doi: 10.1039/B403788J

[69] Roemer, J. J., Kaiser, D. W., "Reaction product of sodium dicyanamide and hydroxylamine hydrochloride," American Cyanamid Co., Old Greenwich, CT, U. S. Pat. 2648669 (29 May 1951/11 Aug 1953).

[70] Demmons, N., "20 mN Variable Specific Impulse Colloid Thruster," Busek, Co., NASA SBIR Proposal 10-1 S3.04,-8878, Natick, MA, 2010.

[71] Maslennikov, N. A., "Lifetime of the Stationary Plasma Thruster," 24th International Electric Propulsion Conference, IEPC-1995-75, 1995.

[72] Coffman, C. S., Courtney, D. G., Hicks, F. M., Jamil, S., Li, H., Lozano, P. C., "Progress Toward a Variable Specific Impulse Electrospray Propulsion System," *47th AIAA Joint Propulsion Conference*, AIAA Paper 2011-5591, 2011.

[73] Romero-Sanz, I., de Carcer, I. A., de la Mora, J. F., "Ionic Propulsion Based on Heated Taylor Cones of Ionic Liquids," *Journal of Propulsion and Power*, Vol. 21, 2005, pp. 239-242.
doi: 10.2514/1.5493

[74] Tao, G-H., Huang, Y., Boatz, J. A., Shreeve, J. M., "Energetic Ionic Liquids Based on Lanthanide Nitrate Complex Anions," *Chemical European Journal*, 2008.
doi: 10.1002/chem.200800828

[75] Christe, K. O., Drake, G. W., "Energetic Ionic Liquids," United States Air Force, United States Patent 7771549, Aug 2010.

[76] Jones, C. B., Haiges, R., Schroer, T., Christe, K. O., "Oxygen-Balanced Energetic Ionic Liquid," *Angewandte Chemie International Edition*, Vol. 45, 2006, 4981-4984.
doi: 10.1002/anie.200600735

[77] Zhang, Y., Gao, H., Joo, Y., Shreeve, J. M., "Ionic Liquids as Hypergolic Fuels," *Angewandte Chemie International Edition*, Vol. 50, 2011, 9554-9562.
doi: 10.1002/anie.201101954

[78] Vanderhoff, J. A., Bunte, S. W., "Electrical Conductivity Measurements of Hydroxylammonium Nitrate: Design Considerations," U. S. Army Ballistic Research Laboratory, Rept. BRL-MR-3511, Aberdeen Proving Ground, MD, April 1986.

II. Assessment of Multi-Mode Spacecraft Micropropulsion Systems

Steven P. Berg and Joshua L. Rovey
Missouri University of Science and Technology, Rolla, Missouri, 65409

ABSTRACT

Multi-mode spacecraft micropropulsion systems which include a high-thrust chemical mode and high-specific impulse electric mode are assessed with specific reference to cubesat-sized satellite applications. Both cold gas Freon-14 propellant and ionic liquid chemical monopropellant modes were investigated alongside pulsed plasma, electrospray, and Hall effect electric thruster modes. Systems involving chemical monopropellants have the highest payload mass fractions for a reference mission of a 500 m/s delta-V and 6U sized cubesat for electric propulsion usage below 70% of total delta-V, while for higher electric propulsion usage, cold gas thrusters delivered a higher payload mass fraction due to lower system inert mass. Due to the combination of a common propellant for both propulsive modes, low inert mass, and high electric thrust, the monopropellant/electrospray system has the highest mission capability in terms of delta-V for missions lasting shorter than 150 days.

NOMENCLATURE

A_c = combustion chamber cross sectional area, [m^2]

A_t = throat area, [m^2]

C_F = thrust coefficient

C = effective exhaust velocity, [m/s]

D_c	=	combustion chamber diameter, [m]
D_t	=	throat diameter, [m]
EP	=	electric propulsion usage fraction
F	=	thrust, [N]
F_{tu}	=	ultimate strength of material, [N/m^2]
f_{inert}	=	inert mass fraction
f_{SI}	=	system integration fraction
g_0	=	acceleration of gravity, [m/s^2]
I_{sp}	=	specific impulse, [s]
$I_{sp,chem}$	=	chemical mode specific impulse, [s]
$I_{sp,elec}$	=	electric mode specific impulse, [s]
$I_{sp,mm}$	=	multi-mode effective specific impulse, [s]
L_c	=	combustion chamber length, [m]
L^*	=	characteristic combustion chamber length
m_0	=	initial mass of spacecraft, [kg]
m_c	=	combustion chamber mass, [kg]
m_{chem}	=	mass of chemical propellant, [kg]
m_e	=	propulsion system mass, [kg]
$m_{e,int}$	=	integrated propulsion system mass, [kg]
m_{elec}	=	mass of electric propellant, [kg]
m_f	=	final mass of spacecraft, [kg]
m_{f1}	=	mass of spacecraft after first burn, [kg]
m_{inert}	=	inert mass, [kg]
m_{pay}	=	payload mass, [kg]
m_{PPU}	=	mass of power processing unit, [kg]
m_{prop}	=	propellant mass, [kg]
m_{sa}	=	mass of solar array, [kg]
m_{tank}	=	mass of propellant tank, [kg]
P_b	=	burst pressure, [Pa]
P_c	=	chamber pressure, [psi]
P_e	=	nozzle exit pressure, [Pa]

P_{thr} = electric thruster power, [kW]

r_c = combustion chamber radius, [m]

r_t = throat radius, [m]

t_b = thruster burn time [day]

t_w = wall thickness, [m]

α = nozzle divergence half-cone angle, [degrees]

ΔV = velocity increment, [m/s]

ε = nozzle expansion ratio

η_p = propulsive efficiency

η_t = thrust efficiency

η_v = mission planning efficiency

θ_c = convergent section angle, [degrees]

γ = specific heat ratio

λ = nozzle divergence correction factor

φ_{tank} = empirical tank sizing parameter

ρ_{prop} = propellant density, [kg/m^3]

ρ_w = wall material density, [kg/m^3]

1. INTRODUCTION

Multi-mode spacecraft propulsion is the use of two or more propulsive devices on a spacecraft, specifically making use of a high-thrust, usually chemical, mode and a high-specific impulse, usually electric mode. This can be beneficial in two primary ways. The first is to increase the mission flexibility of a single spacecraft architecture in that both high-thrust and high-specific impulse maneuvers are available to mission designers at will, perhaps even allowing for drastic changes in the mission plan while on-orbit or with a relatively short turnaround from concept to launch. The second way a multi-mode propulsion system can be beneficial is by designing a mission such that the high-thrust and high-specific impulse maneuvers are conducted in such a way that it provides a more

optimum trajectory over a single chemical or single electric maneuver. This study will use methods developed in a previous analyses of high-power electric multi-mode systems,[1] extending them to multi-mode micropropulsion systems.

One of the main drivers for research into multi-mode spacecraft propulsion is the potential for flexible spacecraft.[2, 3] Since either high-thrust or high-specific impulse maneuvers can be performed at-will, this leads to the possibility of launching a spacecraft without a wholly predetermined mission profile, or simply reducing the length of time from development to launch. Propulsion modes can then be selected as mission needs arise in-situ rather than precisely choreographed prior to launch. Additionally, it has been shown that under certain mission scenarios it is beneficial in terms of spacecraft mass savings, or deliverable payload, to utilize separate high-thrust and high-specific impulse propulsion systems even if there is no common hardware or propellant.[4-6] For example, use of a chemical rocket to escape earth gravity avoids a long spiral trajectory characteristic of an electric burn, while a high-specific impulse electric burn in interplanetary space saves propellant mass over a chemical rocket.[7] However, it has been shown that even greater mass savings can potentially be realized through the use of shared propellants or shared hardware.[8, 9] The use of shared propellants is essential in order to realize the full potential of the multi-mode system under the flexible mission scenario since utilizing separate propellants for each mode fixes the possible delta-V from each mode, whereas there is a wider range of possible delta-V if propellants are shared. The only possible deviations under the separate propellants architecture inherently lead to underutilization of propellant.[1]

Recent efforts have placed a greater emphasis on smaller spacecraft, specifically microsatellites (10-100 kg) and nanosatellites (1-10 kg), including the subset of cubesats.[10] Many different types of thrusters have been proposed to meet the stringent mass and volume requirements placed on spacecraft of this type. A few multi-mode systems have been proposed as well. One includes the use of an ionic liquid propellant for chemical combustion or decomposition as well as for electrospray.[8, 9, 11] A specific propellant for this purpose is even under development.[12] This study will examine this type of system, as well as others, specifically to compare these systems in reference to their multi-mode performance in reference to both mission-defined and

flexible-mission scenarios. Analyses will focus on small satellites where, as will be discussed, the propulsion system is a large fraction of the total spacecraft mass. Section II will introduce the systems to be examined in this study. Section III will describe the analysis methods and assumptions made in reference to developing the multi-mode systems comparisons. Section IV will present the results of analysis. Section V will discuss the results and Section VI presents the relevant conclusions from all analyses.

2. MULTI-MODE PROPULSION SYSTEMS

Two chemical thrust modes and three electric thrust modes are selected for this study. The chemical thrusters include cold gas with Freon-14 or Xenon as the working gas [10, 13] and monopropellant with either AF315E or the [Emim][EtSO$_4$]/HAN dual-mode propellant.[9, 12] The three electric thrusters are the pulsed plasma thruster (PPT), the electrospray thruster, and the helicon thruster. Combining these yields six multi-mode systems, shown in Table 1. Teflon is chosen as the electric propellant for the monopropellant system involving PPT thrusters and the PPT thruster in the cold gas system will utilize common Freon-14 propellant. Although Freon-14 has not been investigated as a propellant in gas-fed PPTs, there is no fundamental reason it could not be used and for this study it will provide decent comparison for what might be possible by using a common propellant for both propulsive modes. System CE will be retained for the mission-defined analysis, but will not be included in the flexible-mission analysis since cold gas and electrospray are not compatible with the same propellant.[11] Finally, the hall thruster is used for this study to provide a baseline comparison of the state-of-the-art.

Thrust and specific impulse values for Freon-14 and Xenon cold gas systems are based on typical values from flight heritage thrusters.[10, 14] The performance of the AF315E monopropellant thrusters is based on a commercially available design from Busek, Inc.[15] The performance of the [Emim][EtSO$_4$]/HAN propellant is scaled from

the theoretical specific impulse of 251 seconds from CEA computations to match the same reduction in performance between the theoretical specific impulse of AF315E[16] and the Busek thruster. The PPT performance selected is based on a commercially available thruster from Clyde Space, Inc.[17] For the Freon-14 gas-fed PPT, the same performance values are used. Although this is speculative, again the main purpose for including the gas-fed PPT is to examine what may be accomplished through the use of a common propellant. The [Emim][Im] performance values are taken from a commercially available thruster from Busek, Inc.[18] The performance of the [Emim][EtSO$_4$]\HAN blend in the electrospray device is scaled in a similar manner as described for the chemical monopropellant performance. The performance for the Hall thruster is scaled from larger thrusters as done in a study by Khayms.[19]

Table 1. Performance of Multi-Mode Propulsion Systems.

System Designation	CP	CE	CH	MP	ME	MH
Chemical Mode						
Type	Cold Gas	Cold Gas	Cold Gas	Monopropellant	Monopropellant	Monopropellant
Propellant	Freon-14	Freon-14	Xenon	AF315E	[Emim][EtSO$_4$]/HAN	AF315E
I_{sp} (sec)	45	45	30	230	226	230
Thrust (N)	0.1	0.1	0.1	0.5	0.5	0.5
Electric Mode						
Type	PPT	Electrospray	Hall Thruster	PPT	Electrospray	Hall Thruster
Propellant	Freon-14	[Emim][Im]	Xenon	Teflon	[Emim][EtSO4]/HAN	Xenon
I_{sp} (sec)	600	800	1600	600	1280	1600
Thrust (mN)	0.14	0.7	0.8	0.14	0.43	0.8

3. MULTI-MODE PROPULSION SYSTEMS ANALYSIS METHODS

Multi-mode propulsion systems enable two primary spacecraft mission benefits: more efficient planned trajectories and flexible mission scenarios. In either scenario, the primary goal of the propulsion system design is to accomplish the given objective with as little mass dedicated to the propulsion system as possible so as to maximize payload capacity or reduce cost. For multi-mode systems, analysis of spacecraft performance and mass is complicated by utilizing an additional propulsion system, since it opens a large design space. And, since this enables flexible mission design scenarios with loosely defined mission objectives and as yet undetermined requirements, comparing multi-mode systems for use in such a scenario becomes difficult. Finally, multi-mode systems must also be assessed in terms of the effectiveness of integrating components, such as propellants, in terms of gains in mission capability or reduction of propulsion system mass. The following paragraphs describe the analysis used in this paper to assess and compare the systems defined previously.

3.1. THE MULTI-MODE ROCKET EQUATION

Spacecraft maneuvers are governed by the Tsiolkovsky rocket equation, shown in Eq. (10),

$$\frac{m_f}{m_0} = e^{-\frac{\Delta V}{I_{sp} g_0}} \tag{10}$$

Multi-mode systems utilize two separate thrusters with separate specific impulses. Thus, in order to determine the propellant required for a certain maneuver, the chemical and electric modes must be considered as two separate maneuvers in Eq. (10). If one defines a parameter for the percentage of the total delta-V to be conducted by electric propulsion, EP, Eq. (11), one can write the two separate rocket equations, (12) and (13),

$$EP = \frac{\Delta V_{elec}}{\Delta V} \tag{11}$$

$$\frac{m_{f1}}{m_0} = e^{-\frac{(1-EP)\Delta V}{I_{sp,chem}g_0}} \tag{12}$$

$$\frac{m_f}{m_{f1}} = e^{-\frac{EP\Delta V}{I_{sp,elec}g_0}} \tag{13}$$

where it is assumed that the chemical burn is conducted first. Practically, for electric propulsion maneuvers, the actual delta-V required is higher than that of an impulsive burn. This effect can be accounted for by using a 'mission planning efficiency' parameter,[6, 20] Eq. (14),

$$\eta_v = \frac{\Delta V_{elec,eff}}{\Delta V_{elec}} \tag{14}$$

Substituting Eq. (14) into Eq. (13) and multiplying Eqs. (12) and (13) and simplifying yields Eq. (15),

$$\frac{m_f}{m_0} = e^{-\frac{\Delta V}{g_0}\left[\frac{1-EP}{I_{sp,chem}} + \frac{EP}{\eta_v I_{sp,elec}}\right]} \tag{15}$$

and it can then be easily seen that an effective specific impulse can be defined, which is a function of the chemical and electric mode specific impulse as well as the *EP* usage fraction. The multi-mode specific impulse is then Eq. (16),

$$I_{sp,mm} = \left[\frac{1-EP}{I_{sp,chem}} + \frac{EP}{\eta_v I_{sp,elec}}\right]^{-1} \tag{16}$$

It is also notable that this equation is exactly the same regardless of the order or number of chemical or electric thrust maneuvers. Finally, since the mission planning efficiency has been introduced, the delta-V requirement input for Eq. (15) is the delta-V that would

be required to complete a given mission with impulsive maneuvers. It is important then to analyze the mission planning efficiency for each unique continuous thrust maneuver. This will be discussed further in a later section.

For electric propulsion systems, there exists an optimum specific impulse which maximizes delivered spacecraft mass under power and time constraints. Oh, et. al.[6] have used a similar derivation to that above to derive the optimum electric specific impulse for a combined chemical-electric maneuver, Eq. (17),

$$4Pt\eta_P\left(1-\frac{\eta_v I^*_{sp,elec}}{I_{sp,chem}}\right)+\frac{\eta_v I^*_{sp,elec}}{I_{sp,chem}}\left(2Pt\eta_P+\frac{I^{*2}_{sp,elec}}{g^2}m_f\right)\ln\left(\frac{2Pt\eta_P g^2}{m_f I^{*2}_{sp,elec}}+1\right)=0 \qquad (17)$$

Examination of this equation shows that for a given power and time constraint, the optimum electric specific impulse is a function of the desired final spacecraft mass, the mission planning efficiency, and, interestingly, the chemical specific impulse. It is important to note that this was derived by optimizing the payload mass delivered per time; thus, more payload could be delivered if longer transit times are tolerable, or the mission could be completed in less time at the expense of payload mass. This will be discussed further in the discussion section.

Eqs. (14) and (17) describe the final spacecraft mass after a propulsive maneuver. The final spacecraft mass includes both the desired payload and the mass of the propulsion hardware. Normally, metrics such as specific impulse are sufficient to describe propulsion system performance. This assumes that the inert mass fraction is small compared to the propellant mass fraction and is typically the case with launch vehicles and large spacecraft. However, for microsatellites, the inert mass fraction of the propulsion system may be half of the entire satellite mass or more. For multi-mode systems, this could be an even bigger fraction. Thus, specific impulse is not wholly representative of the propulsion system, but rather a description of how effectively the onboard propellant is being utilized. To account for the performance losses due to large propulsion system hardware penalty, the final spacecraft mass fraction is separated into payload mass fraction and engine mass fraction, Eq. (18),

$$\frac{m_f}{m_0} = \frac{m_l}{m_0} + \frac{m_e}{m_0} \tag{18}$$

The engine mass fraction then includes the mass of all propulsion system associated hardware such as tanks, valves, thrusters, power processing units, and solar arrays. One of the central design goals for multi-mode propulsion systems, in addition to utilizing a common propellant, is to make use of common hardware to reduce the mass of the propulsion system and increase the deliverable payload. In order to gauge this effect, and provide relevant information in propulsion system conceptual design and selection, a system integration factor is introduced, Eq. (19),

$$f_{SI} = 1 - \frac{m_{e,\text{int}}}{m_{e,sep}} \tag{19}$$

Eq. (19) essentially describes the mass by which a multi-mode propulsion system can be reduced by using common components, such as tanks and lines, between the two propulsive modes over a system of the same modes utilizing completely separate components. Inserting Eqs. (18) and (19) into Eq. (15) gives Eq. (20),

$$\frac{m_l}{m_0} = e^{-\frac{\Delta V}{g_0 I_{sp,mm}}} - \frac{m_{e,sep}}{m_0}(1 - f_{SI}) \tag{20}$$

From this equation, the design goals for multi-mode propulsion systems are clearly evident. The first term on the right hand side describes the propellant usage, which may be allocated between two modes, and the second term describes the inert mass penalty, which can be recovered through designs using common hardware between the two modes.

3.2. CHEMICAL THRUSTER SIZING

The two chemical propellants selected for study are Freon-14 for cold gas and either [Emim][EtSO$_4$] or AF315E for monopropellant systems as defined in Table 1. For chemical propellants, relevant parameters for thruster sizing include chamber temperature and specific heat ratio. The [Emim][EtSO$_4$] propellant combusts to a temperature of 1900 K, a specific heat ratio of 1.22, and a characteristic velocity of 1330 m/s. [9] AF315E combusts to a chamber temperature of 2300K.[16] The exact composition of AF315E is not given in the literature, so a specific heat ratio of 1.2 is chosen based on typical values for combustion products of HAN-based ionic liquid propellants.[9, 21] Given the combustion characteristics of the propellant, a chemical thruster at a desired thrust level can be sized by specifying three additional parameters: chamber pressure, nozzle expansion ratio, and divergence half-cone angle. This study will assume a 300 psi chamber pressure and a nozzle expansion ratio of 200, which are typical values for on-orbit thrusters.[14] The nozzle throat area is calculated from Eq. (21),

$$A_t = \frac{F}{C_F P_C},$$
(21)

where the thrust coefficient is given by Eq. (22),

$$C_F = \lambda \sqrt{\frac{2\gamma}{\gamma-1}\left(\frac{2}{\gamma+1}\right)^{\frac{\gamma+1}{\gamma-1}}\left[1-\left(\frac{P_e}{P_c}\right)^{\frac{\gamma-1}{\gamma}}\right]} + \frac{P_e}{P_c}\varepsilon,$$
(22)

and the pressure ratio can be solved iteratively using Eq. (23),

$$\frac{1}{\varepsilon} = \left(\frac{\gamma+1}{2}\right)^{\frac{1}{\gamma-1}}\left(\frac{P_e}{P_c}\right)^{\frac{1}{\gamma}}\sqrt{\left(\frac{\gamma+1}{\gamma-1}\right)\left(1-\frac{P_e}{P_c}\right)^{\frac{\gamma-1}{\gamma}}}.$$
(23)

where the divergence correction factor has been added, shown in Eq. (24),

$$\lambda = \frac{1}{2}\left(1 + \cos(\alpha)\right)$$

(24)

and for all analysis herein a 15° half cone divergence angle is used with a 20% reduction in length to estimate the mass of a bell nozzle.

Given the specified parameters, and calculations from Eqs. (21)-(24), the remaining geometry of the divergence section, namely exit area and length are calculated through simple trigonometric relations. The thrust chamber geometry can be calculated through empirical means by Eqs. (25) and (26),[14]

$$A_c = A_t\left(8D_t^{-0.6} + 1.25\right)$$

(25)

$$L_c = L^* \frac{A_t}{A_c}$$

(26)

where the characteristic length, L^*, historically falls between 0.5 and 2.5, with monopropellant thrusters having characteristic lengths at the high end of this range. Therefore, a characteristic length of 2.5 is chosen for monopropellant thrusters, and a value of 0.5 is chosen for cold gas thrusters since they only require essentially a convergent nozzle section and tubing thick enough to withstand the chamber pressure. Since all of the geometric parameters of the thruster have been calculated, the mass can be estimated by the following equations. The wall thickness is estimated by Eq. (27),

$$t_w = \frac{P_b D_c}{2F_{tu}}$$

(27)

and the mass of the thrust chamber is subsequently calculated using Eq. (28),

$$m_c = \pi \rho_w t_w \left[2 r_c L_c + \frac{r_c^2 - r_t^2}{\tan \theta_c} \right].$$

(28)

For the preliminary calculations, the burst pressure is assumed to be twice the chamber pressure and the material is assumed to be columbium (F_{tu}=310 MPa, ρ_w=8600 kg/m^3), a generic thrust chamber material. Additionally, the angle of the convergence section is assumed to be 45° in all cases, recognizing that it typically comprises only a small percentage of the total thruster mass.

3.3. MULTI-MODE PROPULSION SYSTEM MASS ESTIMATION PARAMETERS

3.3.1. Propellant Tankage. The majority of the propulsion system sizing conducted in this study is based on empirical baseline design estimates outlined in Humble.[14] The mass of propellant required to accelerate a spacecraft through a desired velocity change can be calculated by solving Eq. (20). The inert, or engine, mass is composed of the thruster, propellant feed lines and valves, propellant and pressurant tanks, power processing unit (PPU), and structural mounts for the propulsion system. The mass of the tanks can be estimated empirically by Eq. (29),

$$m_{\tan k} = \frac{P_b m_{prop} \rho_{prop}}{g_0 \phi_{\tan k}}$$

(29)

where the burst pressure is again assumed to be 1.25 times the tank pressure as is standard design practice for spacecraft. For [Emim][Im], [Emim][EtSO$_4$]-HAN, and AF315E propellant tanks the tank pressure is chosen to be 300 psi plus a 20% injector

head loss and 0.35 psi overall line losses for the propellant tanks and 1450 psi is chosen for the helium pressurant tanks. Xenon is typically stored in supercritical state at around 1100 psi.[14] The density of these propellants at the chosen conditions and teflon is shown in Table 2. Also, the empirical tank sizing parameter is chosen to be 6350 m. This value corresponds to typical titanium tank material. Since the volume of the pressurant tank is not known beforehand, the pressurant required must be solved iteratively until the mass of pressurant is sufficient to occupy both pressurant and propellant tanks at the desired propellant tank pressure. The mass of lines and valves is estimated as 50% of the thruster mass, a value typical of spacecraft thrusters historically. Finally, the mass of structural mounts is assumed to be 10% of the total inert mass.

Table 2. Storage Properties of Propellants.

Propellant	Pressure (psi)	State	Density (kg/m^3)
Freon-14	300	Liquid	1603
[Emim][EtSO$_4$]-			
HAN	300	Liquid	1419
AF315E	300	Liquid	1460
[Emim][Im]	15	Liquid	1519
Xenon	1100	Supercritical	1642
Teflon	-	Solid	2200

3.3.2. Power Processing Systems.   In terms of the electric mode of propulsion, the mass of the power processing unit (PPU), associated cables and switches, as well as the powertrain components of the electric thruster itself will have a substantial effect on the overall propulsion system mass. Mass and volume of the power processing unit and cables are taken from the commercially available PPUs manufactured by Clyde Space, Inc.[22] These are shown in Table 3. For the solar panels, a constant value of 15.5 g/W is

used. This is a typical value for current state of the art solar cell technology.[10] Batteries will be used for purposes of monopropellant catalyst bed heating, and the current state-of-the-art for cubesat battery power density is 0.15 W-hr/g.[22]

Table 3. Mass and Volume of Cubesat PPUs.

Power	Volume	Mass
(W)	(U)	(g)
9	0.127	83
12	0.127	85
15	0.127	87
27	0.153	129
39	0.153	133
42	0.153	137
72	0.153	139

4. RESULTS

The results of the analysis methods and system sizing estimates are presented in this section. First, the equations developed or shown in Section III are examined for general trends. Next, the chemical thruster and electric thruster masses for the specific thrusters selected for this study are computed using the equations described in Section III. Then, performance is computed for each multi-mode thruster, and the mass and volume of each multi-mode propulsion system is computed in order to draw comparisons between each system.

4.1. OPTIMUM SPECIFIC IMPULSE

Perhaps the most interesting portion of Eq. (17) is the observation that the optimum electric specific impulse for a chemical-electric combined system is dependant on the chemical mode specific impulse. Oh, et. al.[6] examined the optimum specific impulse for a single chemical specific impulse, assumed to be 310 seconds for typical bipropellant propulsion systems for large commercial satellites. It was found that a higher mission planning efficiency reduces the optimum electric specific impulse. A mission planning efficiency of unity corresponds to a Hohmann transfer, which is obviously impossible for a continuous thrust maneuver. It has been found that the mission planning efficiency does not vary much for earth-orbiting satellites, with values ranging from 0.45 to 0.65, and is typically dependant on the starting and ending orbits and steering profile, and therefore weakly dependant on the propulsion system technology.[6, 20] A value of 0.5 for the mission planning efficiency will be used for all calculations hereafter.

Since there are many chemical micropropulsion concepts, and also many electric micropropulsion concepts, it is useful to examine the general trends for optimum electric specific impulse and the interplay with chemical propulsion system selection in a multi-mode system. Figure 1 shows the optimum electric specific impulse calculated using Eq. (17). Figure 1a shows the optimum electric specific impulse at varied energy, the $Pt\eta_p$ term in Eq. (17), Figure 1b at varied spacecraft mass, and Figure 1c at varied chemical mode specific impulse. For each figure, when two of the parameters are not varied, values of 5 MJ, 10 kg, and 250 seconds are chosen for the energy, spacecraft mass, and chemical specific impulse, respectively. From Figure 1b it is easily seen that the optimum electric specific impulse does not vary significantly with spacecraft mass, by less than 1% over the entire range chosen in this case, which is representative of small satellites. The optimum electric specific impulse does vary somewhat significantly as energy required is increased. However, for a 30 W, 50% efficiency thruster, the range in Fig 1a represents 0-2 years of thrusting time. If propulsion systems are compared for missions at roughly the same, but slightly different duration then the optimum electric specific impulse can also be assumed constant for comparative purposes. Finally, Figure 1c shows the variation with chemical specific impulse. For a system consisting of a chemical mode
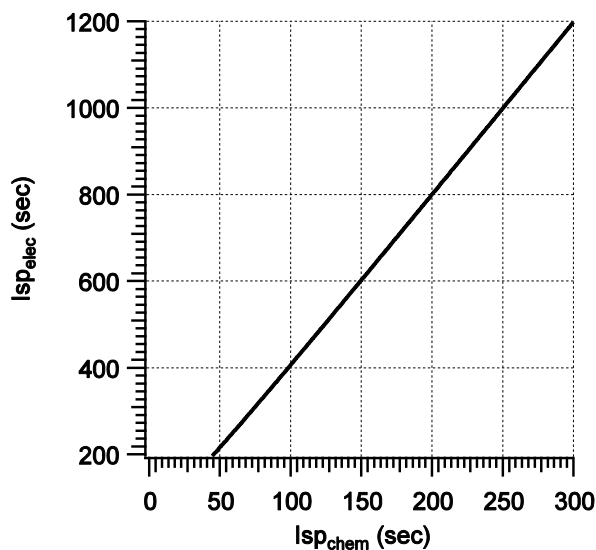
thruster of 50 seconds specific impulse, the optimum electric specific impulse is 220 seconds, and for 250 second chemical mode Isp the optimum electric Isp is 1000 seconds.
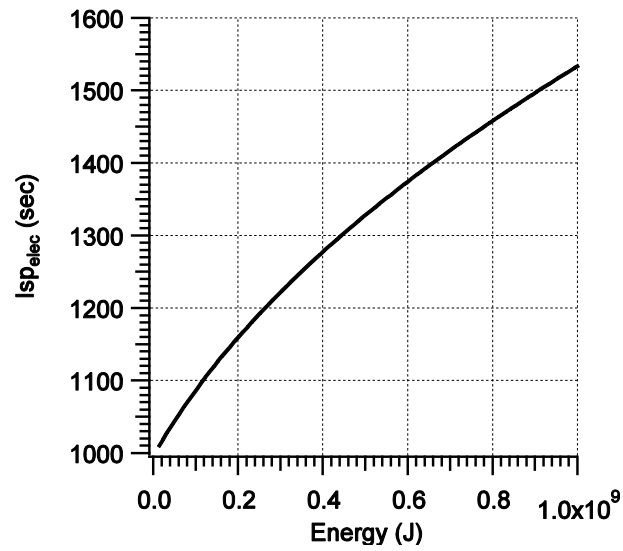
a)
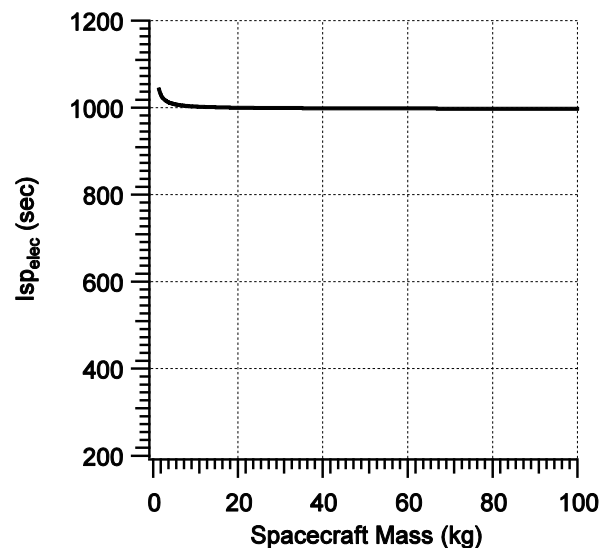
b)

c)

Figure 1. Optimum Electric Specific Impulse as a Function of a) Energy, b) Spacecraft Mass, and c) Chemical Mode Specific Impulse.

4.2 SYSTEM SIZING

Thruster mass of the chemical thrusters was computed using the equations described in Section III. The results are shown in Table 4. Additionally, mass of the PPU is also shown since it depends only on thruster power. The PPT thruster used in Systems CP and MP requires 2 W of power.[17] The electrospray thruster requires 9 W,[18] and the Hall thruster requires 20 W.[19] The mass of the PPU and solar panel mass for each system are sized according to these values. Solar panel mass is included as a penalty, although it is likely the payload would also make use of power from solar panels if the payload were not required to be powered on during electic thrusting. Additionally, the monopropellant thrusters require 20 W to preheat the catalyst bed to high enough temperature to initiate decomposition of the propellant.[15] However, these are typically not powered directly from solar panels, but from batteries since they require short times to achieve heating. The current state-of-the art battery power density will be used for mass estimates assuming a 30 minute preheat time, a typical value for advanced monopropellant thrusters.[23] Although volume is a consideration for cubesats, it has

been shown that for these particular systems, mass is the most stringent constraint except for large delta-V missions with high chemical mode usage and thus a large tank volume requirement.[24]

Table 4. Mass of Propulsion System Components Excluding Tankage.

System Designation	CP	CE	CH	MP	ME	MH
Chemical Thruster Mass (g)	200	200	200	500	500	500
Electric Thruster Mass (g)	190	900	700	190	900	700
PPU Mass (g)	50	83	108	50	83	108
Solar Array Mass (g)	31	139	310	31	139	310
Battery Mass (g)	-	-	-	100	100	100
Lines and Valves (g)	195	550	450	345	700	600
Structural Mounts (g)	67	187	177	122	242	232
Total Mass (g)	733	2059	1945	1338	2664	2550

Table 4 includes the line, valve, and structural mount mass assuming separate chemical and electric propellant tanks. As mentioned, for multi-mode propulsion systems it is desirable to combine components. Utilizing a common propellant allows for valves and lines to be shared since they emanate from a single propellant tank. Systems CP, CH, and ME make use of a common propellant for both modes. Assuming the mass of lines and valves for these systems is that of the heaviest thruster, the mass of lines and valves is reduced by 95 g, 100 g and 250 g for these systems, respectively. Additionally, the mass of structural mounts is reduced, resulting in a system integration factor of 0.14,

0.06, and 0.11 for systems CP, CH, and ME, respectively. This factor will be used for calculations in the next section.

4.3. MULTI-MODE SYSTEM PERFORMANCE

The multi-mode specific impulse for each system as defined by Eq. (16) was computed and is shown in Fig. 2 as a function of EP usage fraction. Obviously, the bounds of the multi-mode specific impulse are the specific impulses of the chemical and electric thrusters chosen for the system, with recognition that the electric specific impulse effectiveness is modified by the mission planning efficiency, chosen to be 0.5 as discussed earlier. However, as seen in Fig. 2, the behavior of the function between these bounds is nonlinear. Furthermore, it is seen that most of the benefit of the high-specific impulse electric thruster is utilized at EP fractions close to unity. For example, system MH increases by 170 seconds in multi-mode specific impulse from EP usage fraction of 0 to 0.6, then increases by a factor of 400 seconds from 0.6 to 1.0. All systems utilizing cold-gas thrusters perform lower than systems utilizing a monopropellant thruster for EP fractions lower than 0.92, where the performance of System CH overtakes that of system MP.
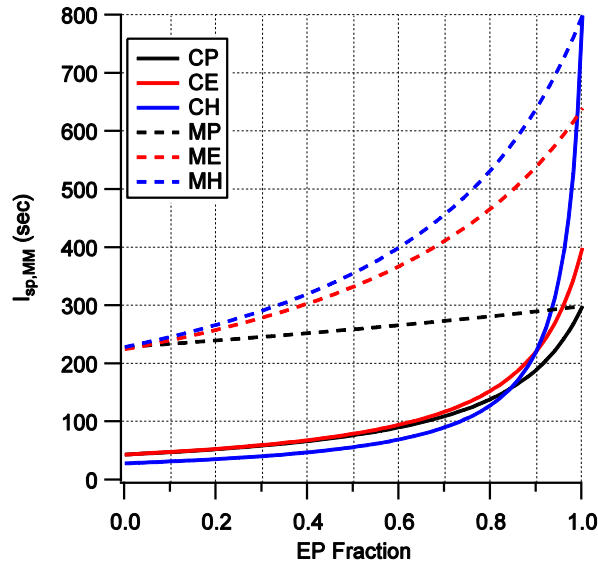
Figure 2. Multi-Mode Specific Impulse as a Function of EP Usage.

4.4. MULTI-MODE SYSTEM CAPABILITIES

As mentioned in the introduction, there are two main approaches to preliminary design and selection for multi-mode propulsion systems. The first approach is more traditional in that maneuvers are planned at an early design state. The propulsion system is then tailored to that set of maneuvers. This is especially true for electric propulsion systems, since the continuous thrust maneuver could be more or less efficient depending on the start and stop points on the trajectory. For a multi-mode system, this is even more complex because conducting an impulsive maneuver via a high-thrust chemical burn could effectively instantaneously change the efficiency of the next planned electric maneuver, as previous research has shown.[6, 20] Thus, simply defining a reference delta-V and payload mass and sizing the propulsion system may not tell the entire story, as other mission needs could dictate propulsion system choice. However, by loosely defining a reference mission one can eliminate obviously poor candidate systems, as well as gain an understanding of the strengths and potential weaknesses of the multi-mode system prior to fully defining the mission scenario. Additionally, as will be discussed,

this can provide insight into the second approach to multi-mode system design, which is where a mission is not defined prior to spacecraft design maturation or even launch itself.

For a design reference mission, a delta-V of 500 m/s and a total satellite mass of 6.9 kg is chosen. The latter corresponds to a 6U cubesat. The payload fraction for each system defined in Table 1 is shown in Fig. 3. Clearly, systems involving the cold gas thruster have a clear disadvantage compared to their corresponding monopropellant systems for low EP usage fractions. Only the cold gas system also utilizing a PPT is able to complete a 500 m/s delta-V without the required propellant pushing the satellite over the limit of 6.9 kg. System CH is unable to complete the defined mission unless at least 32% of the total delta-V is dedicated to electric propulsion. For EP usage below 88%, System MP is able to complete the mission with the highest payload fraction of all systems, while System CP has the highest payload fraction for missions allowing more than 88% of the delta-V to be accomplished via an electric thrust maneuver. System ME has a roughly 4% higher payload mass fraction than system MH for all EP usage fractions.
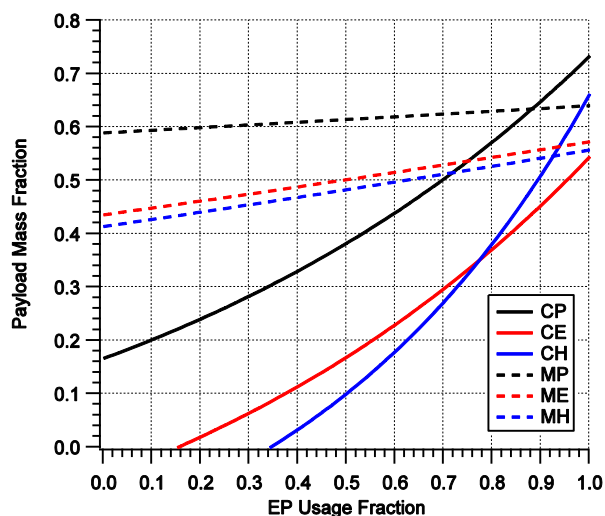

Figure 3. Payload Mass Fraction for Reference Mission as a Function of EP Usage.

An additional consideration important in electric propulsion systems, and thus multi-mode propulsion systems also, is the required time to expel all propellant carried onboard the spacecraft. This can serve as a comparison for how long the mission will take with a given propulsion system. However, this may not describe the entire scenario as the length between burns is not defined. Furthermore, the selection of burn type and duration could play a significant role such that the time of unpowered flight is significantly larger than the burn duration in one case, but not in another. So, while simply comparing burn duration required of a propulsion system does not come close to describing the actual mission scenario, it does at minimum serve as a lower bound. The burn duration for the reference mission described previously is shown in Fig. 4. For all three electric propulsion systems, the burn duration is longer when using a monopropellant thruster compared to a cold gas thruster. Systems using a PPT in the electric mode require the longest burn durations, while the cold gas system involving the Hall thruster has the lowest overall burn times, requiring only about 20% of the total time required to perform the 500 m/s delta-V compared to the PPT systems. Systems ME and MH appear identical in the graph, however closer examination reveals system ME actually requires roughly 1% shorter burn times than System MH.
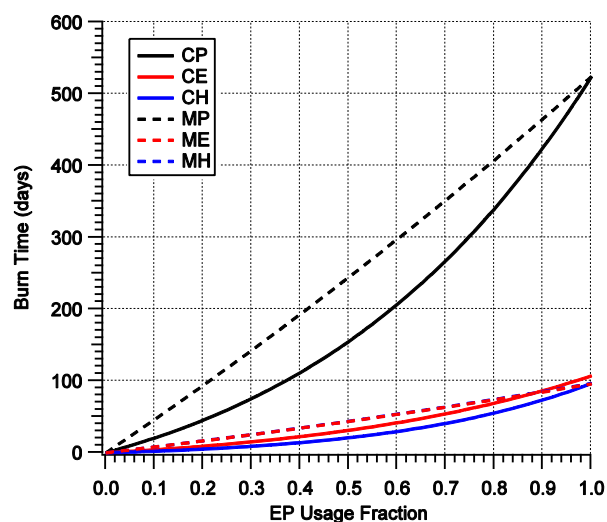
Figure 4. Burn Time for Reference Mission as a Function of EP Usage.

As mentioned, one of the main drivers toward multi-mode propulsion usage is the ability to design a system to meet a large number of mission scenarios. Additionally, multi-mode propulsion systems utilizing a single propellant for both modes offer the highest flexibility since any give EP usage fraction may be chosen as mission needs arise rather than defined to a strict ratio as would be the case if two propellants had to be loaded into two separate tanks. The mission trade space for Systems CP, CH, and ME is shown in Fig. 5 since these systems involve utilization of a common propellant. The burn duration versus delta-V is shown for a 6U (6.9 kg) satellite with a 2 kg payload. This may be viewed as the mission trade space with the same caveats applied to the use of burn duration as a comparison tool as described in the previous paragraph. System CH can achieve the highest delta-V of the three systems, but only achieves less than half of the delta-V of System ME for burn times less than 150 days. System CP requires the longest burn time per delta-V of any system, except for System CH below about 30 days.

Figure 5. Mission Trade Space for Systems Utilizing Common Propellant.

To further illustrate the gains in mission flexibility by using a common propellant in a multi-mode propulsion system, System ME is compared to a system consisting of the same thruster modes, but with separate AF315E and [Emim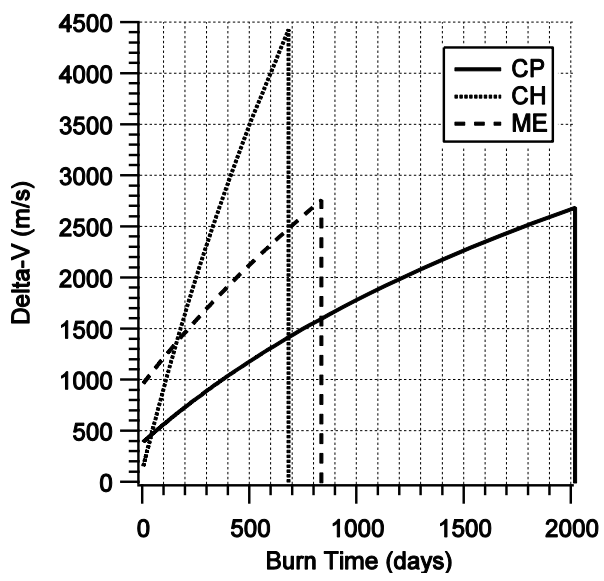][Im] propellants for the chemical mode and electric mode, respectively. The performance and mass estimates for these thrusters are the same as given in Section II and III, except here the specific impulse of the electric mode is scaled up to 1280 seconds. Note that this could be accomplished through addition of accelerator grids with additional mass penalty. For this analysis, however no additional mass penalty is applied. The mission trade space for these two systems is shown in Fig. 6 for a 180 kg satellite with a 65 kg payload. The solid black line represents System ME, which uses a common propellant, and the colored lines represent the system using separate propellants. For the system using separate propellants it is necessary to define the mission trade space by choosing a single allocation of propellant mass. Stated differently, a mission designer may only allocate propellant usage before the mission begins and may only select one of the colored curves. Anything except for the peak of the colored curves is therefore a mission that does not result in 100% propellant utilization. On the other hand, if a common propellant is used, the entire area under the black curve is available for mission applications, even after launch, and 100% propellant utilization is achieved for any mission chosen on the black curve. Also notable is that the combined system has a higher delta-V at a given burn duration for all missions except the 100% chemical and 100% electric missions in which the mass of the opposite mode thruster and associated hardware has been removed. This is due to the use of shared hardware in the common propellant system.
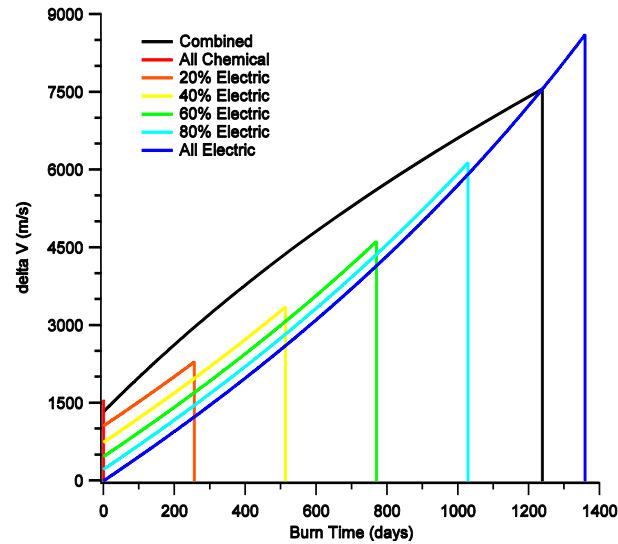
Figure 6. Mission Design Trade Space for Multi-mode Ionic Liquid Propulsion Systems.

5. DISCUSSION

Clearly, from the results, missions requiring a majority of the total delta-V to be performed through quick, impulsive chemical maneuvers, the specific impulse of the chemical mode is the most important consideration, since from Fig. 3 all of the monopropellant systems have a higher payload mass fraction for EP usage below 88% of the total delta-V. Of the monopropellant systems, System MP has the highest payload fraction, but requires a significant burn duration. Despite having a higher thruster and powertrain mass than System MH, System ME has a higher payload mass fraction for the reference mission while still requiring shorter burn times. This is due to both the fact that System ME has a reduced inert mass due to shared lines and vales, but also somewhat due to the electric mode specific impulse being closer to optimum for the chemical monopropellant mode specific impulse, Fig. 1c, than the hall thruster.

In terms of required burn duration to expend all onboard propellant, the PPT systems have the longest burn times. This is due directly to the fact that they have the

lowest electric mode thrust of any propulsion system considered in this study. The thrust of the electric mode effectively dictates the burn duration of the entire multi-mode propulsion system since any low-thrust maneuver utilizing electric propulsion takes significantly longer than a chemical burn even to expel 100% of the propellant. Thus, systems involving the higher-power thrusters could be advantageous for multi-mode systems where spacecraft lifetime or mission lifetime is a critical factor.

For spacecraft designs involving flexible mission scenarios, the system with the cold gas thruster combined with the hall thruster could be the most advantageous since it offers a relatively high delta-V capability in a short amount of time for a given payload mass and total spacecraft mass. However, for most earth-orbiting missions typically lasting shorter than 150 days, the monopropellant/electrospray system is the most advantageous. Furthermore, for flexible mission design, it is crucial to make use of a common propellant between modes as from Fig. 6 the mission design space not only encompasses the design space of all possible propellant budget allocations using separate propellants, but exceeds the performance except for missions involving 100% chemical or 100% electric maneuvers due to the use of shared hardware reducing the propulsion system inert mass.

As mentioned in the results section, the shape of the multi-mode specific impulse function is exponential, with most of the specific impulse benefit of the electric system being realized through high values of EP usage. In a flexible mission design scenario such as that defined in the results section where the only constraints are payload mass and total spacecraft mass, limiting propulsion system inert mass is more important than high specific impulse in either chemical or electric mode. Or stated differently, reducing inert mass of the propulsion system allows for a greater fraction of the onboard mass to be propellant. The fact that specific impulse grows at a rate greater than linear according to the multi-mode specific impulse function means that more available propellant will result in an exponentially growing delta-V availability as propulsion system inert mass is reduced. It is therefore highly advantageous to reduce propulsion system inert mass as much as possible through hardware integration or careful selection of components.

Finally, the concept of the optimum electric mode specific impulse must be revisited. As discussed in the results section the optimum electric specific impulse depends on the chemical mode specific impulse. The optimum occurs because there is a trade-off between the payload mass fraction gain by increased specific impulse and increased time required by decreased power. [6] Under a fixed mission duration, for a large electric specific impulse, the electric propulsion system makes efficient use of the propellant, but would deliver a smaller fraction of the total delta-V. The chemical thruster would then provide the remaining delta-V at a defined ratio in order to meet the mission time requirements. Conversely, if the chemical thruster specific impulse is low, it would be desirable to use less of the chemical thruster. Thus, as the chemical mode specific impulse decreases, it is desirable to increase the electric mode thrust at the expense of specific impulse.

For multi-mode propulsion system design it is desirable to select electric propulsion technology near this optimum. However, this only describes performance from a propellant usage standpoint. If an electric technology is sufficiently low in mass, or it can be integrated partially or fully with the chemical mode, it may result in a higher performance system even if the electric specific impulse is far from optimum.

6. CONCLUSIONS

Multi-mode spacecraft propulsion systems involving separate chemical and electric thrusters were compared and analyzed in terms of mission capability and overall system sizing. Propulsion systems involving chemical monopropellant thrusters generally outperformed their cold-gas counter parts in terms of both payload mass fraction and propulsion system volume required to perform a 500 m/s delta-V with a 6U scale spacecfraft (6.9 kg). The thrust of the electric mode effectively determines minimum burn duration directly, and as such the systems utilizing the PPT had the highest burn durations since they also had the lowest thrust of all electric propulsion systems

considered in this study. For flexible propulsion system design, a multi-mode system utilizing a common propellant is the most important consideration, followed by reduction of propulsion system inert mass through the use of common hardware. There exists an optimum electric specific impulse for a unique chemical specific impulse selection. It is ideal then, to pair electric technology near this optimum specific impulse for a given chemical thruster technology.

REFERENCES

[1] S. P. Berg, and Rovey, J. L., "Assessment of High-Power Electric Multi-Mode Spacecraft Propulsion Concepts," 33rd International Electric Propulsion Conference, IEPC-2013-308, 2013.

[2] J. M. Haas, and Holmes, M. R., "Multi-Mode Propulsion System for the Expansion of Small Satellite Capabilities," NATO, Rept. MP-AVT-171-05, 2010.

[3] T. Rexius, and Holmes, M., "Mission Capability Gains from Multi-Mode Propulsion Thrust Profile Variations for a Plane Change Maneuver," AIAA Modeling and Simulation Technologies Conference, AIAA Paper 2011-6431, 2011.

[4] L. M. Mailhe, Heister, S. D., "Design of a Hybrid Chemical/Electric Propulsion Orbital Transfer Vehicle," Journal of Spacecraft and Rockets, Vol. 39, No. 1, 2002, pp. 131-139.

[5] C. A. Kluever, "Spacecraft Optimization with Combined Chemical-Electric Propulsion," Journal of Spacecraft and Rockets, Vol. 32, No. 2, 1994, pp. 378-380.

[6] D. Y. Oh, Randolph, T., Kimbrel, S., and Martinez-Sanchez, M., "End-toEnd Optimization of Chemical-Electric Orbit Raising Missions," Journal of Spacecraft and Rockets, Vol. 41, No. 5, 2004, pp. 831-839.

[7] J. H. Gilland, "Synergistic Use of High and Low Thrust Propulsion Systems for Piloted Missions to Mars," AIAA Paper 1991-2346, 1991.

[8] B. R. a. R. Donius, J. L., "Ionic Liquid Dual-Mode Spacecraft Propulsion Assessment," Journal of Spacecraft and Rockets, Vol. 48, No. 1, 2011, pp. 110-123.

[9] S. P. Berg, and Rovey, J. L., "Assessment of Imidazole-Based Energetic Ionic Liquids as Dual-Mode Spacecraft Propellants," Journal of Propulsion and Power, Vol. 29, No. 2, 2013, pp. 339-351.

[10] J. R. Wertz, Everett, D. F., and Puschell, J. J., Space Mission Engineering: The New SMAD, Microcosm Press, Hawthorne, CA, 2011.

[11] K. Masuyama, and Lozano, P. C., "Bimodal Propulsion System Using Ionic Liquid Propellant for Pico- and Nano-satellite Applications," 49th AIAA/ASME/SAE/ASEE Joint Propulsion Conference, AIAA Paper 2013-3962, 2013.

[12] S. P. Berg, and Rovey, J. L., "Decomposition of Monopropellant Blends of Hydroxylammonium Nitrate and Imidazole-Based Ionic Liquid Fuels," Journal of Propulsion and Power, Vol. 29, No. 1, 2013, pp. 125-135.

[13] G. P. Sutton, and Biblarz, O., Rocket Propulsion Elements, 7th, Wiley, New York, 2001.

[14] R. W. Humble, Henry, G. N., and Larson, W. J., Space Propulsion Analysis and Design, McGraw-Hill, 1995.

[15] "Green Monopropellant Thrusters." Busek, Inc.

[16] T. Hawkins, Brand, A., McKay, M., Drake, G., and Ismail, I. M. K., "Characterization of Reduced Toxicity, High Performance Monopropellants at the U. S. Air Force Research Laboratory," Air Force Research Laboratory, Rept. AFRL-PR-ED-TP-2001-137, 2001.

[17] "Cubesat uPulse Plasma Thruster." Clyde Space, Inc.

[18] "Busek Electrospray Thrusters." Busek, Inc.

[19] V. Khayms, "Advanced Propulsion for Microsatellites," PhD Thesis, Aeronautics & Astronautics, Massachusetts Institute of Technology, 2000.

[20] C. A. Kluever, "Optimal Geostationary Orbit Transfers Using Onboard Chemical-Electric Propulsion," Journal of Spacecraft and Rockets, Vol. 49, No. 6, 2012, pp. 1174-1182.

[21] D. Zube, Wucherer, E., and Reed, B., "Evaluation of HAN-Based Propellant Blends," 39th AIAA/ASME/SAE/ASEE Joint Propulsion Conference & Exhibit, AIAA Paper 2003-4643, 2003.

[22] "Cubesat Electrical Power Systems." Clyde Space, Inc.

[23] K. Anflo, Persson, S., Thormahlen, P., Bergman, G., and Hasanof, T., "Flight Demonstration of ADN-Based Propulsion System on the PRISMA Satellite," 42nd AIAA/ASME/SAE/ASEE Joint Propulsion Conference & Exhibit, AIAA Paper 2006-5212, 2006.

[24] S. P. Berg, and Rovey, J. L., "Assessment of Multi-Mode Spacecraft Micropropulsion Systems," 50th AIAA/ASME/SAE/ASEE Joint Propulsion Conference, AIAA Paper 2014-3758, 2014.

III. Decomposition of a Double Salt Ionic Liquid Monopropellant on Heated Metallic Surfaces

Steven P. Berg and Joshua L. Rovey

Missouri University of Science and Technology, Rolla, Missouri, 65409

ABSTRACT

A monopropellant consisting of 59% hydroxylammonium nitrate and 41% 1-ethyl-3-methylimidazolium ethyl sulfate is tested for decomposition on heated platinum, rhenium, and titanium surfaces. It was found that the propellant decomposes at 165 ^{o}C on titanium, which is the decomposition temperature of HAN. The onset temperature for decomposition on platinum was 85 ^{o}C and on rhenium it was 125 ^{o}C. This suggests that platinum and rhenium act as catalysts for the decomposition of the monopropellant. From the experimental data, Arrhenius-type reaction rate parameters were calculated. The activation energy for platinum was 3 times less than that of titanium suggesting it could be a prime choice for catalyst material in further thruster development.

NOMECLATURE

A	=	activity coefficient, [1/sec]
$C_{p,i}$	=	specific heat of species i, [J/kg-K]
E	=	activation energy, [J]
k'	=	reaction rate coefficient, [1/sec]
k_B	=	Boltzmann constant, [m^2-kg/sec^2-K]
N_i	=	number of moles of species i, [mol]

$\dot{Q}$ =   heat transfer rate, [W]

$\dot{Q}''$ =   heat flux, [W/mm^2]

$\dot{Q}_E$ =   heat transfer rate due to electrical heating, [W]

r_A =   reaction rate, [mol/m-sec]

T =   temperature, [K]

$\dot{T}_{blank}$ =   heating rate on blank surface, [K/s]

$\dot{T}_E$ =   electrical heating rate, [K/s]

$\dot{T}_s$ =   self heating rate, [K/s]

T_m =   melting temperature, [K]

t =   time, [sec]

V =   volume, [m^3]

ΔH_{Rx} =   heat of reaction, [J/mol]

ρ =   resistivity, [Ω-m]

κ =   thermal conductivity, [W/m-K]

1. INTRODUCTION

Multi-mode spacecraft propulsion is the use of two or more propulsive devices on a spacecraft, specifically making use of a high-thrust, usually chemical, mode and a high-specific impulse, usually electric mode. This can be beneficial in two primary ways. One way a multi-mode propulsion system can be beneficial is by designing a mission such that the high-thrust and high-specific impulse maneuvers are conducted in such a way that it provides a more optimum trajectory over a single chemical or single electric maneuver.[1-4] The second is to increase the mission flexibility of a single spacecraft architechture in that both high-thrust and high-specific impulse maneuvers are available to mission designers at will, perhaps even allowing for drastic changes in the mission

plan while on-orbit or with a relatively short turnaround from concept to launch.[5-9] For the second method, it is extremely beneficial to utilize a common propellant for both modes as this provides the highest flexibility in terms of mission design choices. Two propellants have been developed which may function and theoretically perform well in both a chemical monopropellant and electric electrospray mode.[10] These propellants, based on mixtures of ionic liquids [Emim][EtSO$_4$] and [Bmim][NO$_3$] with ionic liquid oxidizer hydroxylammonium nitrate (HAN), have been previously synthesized and assessed for thermal and catalytic decomposition in a microreactor.[11] This paper presents results of further experiments to characterize the decomposition of the [Emim][EtSO$_4$]-HAN monopropellant, specifically on catalytic surfaces relevant to application in a microtube thruster.[12-14] The electrospray capabilities of the propellants have been investigated previously.[15]

Hydrazine has been the monopropellant of choice for spacecraft and gas generators because it is storable and easily decomposed to give good combustion properties [16]. However, hydrazine is also highly toxic and recent efforts have been aimed at replacing hydrazine with a high-performance, non-toxic monopropellant. Many of these efforts have focused on energetic ionic liquids, which are essentially molten salts capable of rapid decomposition into gaseous products. The energetic salts hydroxylammonium nitrate (HAN), ammonium dinitramide (ADN), and hydrazinium nitroformate (HNF) have received attention for this purpose.[16-20] All of these salts have melting points above room temperature, and it is therefore necessary to use them in an aqueous solution to create a storable liquid propellant. Typically, these are also mixed with a compatible fuel component to provide improved performance. The main limitation to the development of these as monopropellants has been excessive combustion temperatures, but recent efforts in materials and thermal management have mitigated some of these issues and flight tests have been conducted or are scheduled.[20-22] These propellants, while performing well for chemical propulsion, fundamentally will not perform well in an electrospray thruster; therefore, for a proposed multi-mode monopropellant/electrospray system, novel system-specific propellants will be needed and the first generation has been synthesized.[10, 11]

Recent efforts have placed a greater emphasis on smaller spacecraft, specifically microsatellites (10-100 kg) and nanosatellites (1-10 kg), including the subset of cubesats.[23] Many different types of thrusters have been proposed to meet the stringent mass and volume requirements placed on spacecraft of this type. Electrospray, in particular, may be well suited for micropropulsion, and has been selected for these types of applications.[24-26] Many types of thrusters have been proposed for chemical propulsion for small spacecraft. One type is the chemical microtube.[12-14] This type of thruster is simply a heated tube of diameter ~1 mm or less that may or may not consist of a catalytic surface material. Additionally, from a multi-mode system standpoint, there is no fundamental reason why this geometry could not be shared with the electrospray mode as capillary type emitters can be roughly the same diameter tube.[15, 27]

Due to the stringent mass, volume, and power requirements on micropropulsion systems, the required preheat temperature and overall length of the tube to achieve peak performance is important. However, in order to assess these requirements, and in turn design an experimental thruster, basic properties of the propellant decomposition and burning behavior must be determined. This paper presents results on the experimental determination and assessment of the decomposition characteristics of the [Emim][EtSO$_4$]-HAN propellant on various catalytic surfaces through the use of a batch reactor. These measurements, taken together, can be used directly or compared to existing models of HAN propellant decomposition to aid the design of a catalytic microtube thruster. Section II will describe the setup of the experiment, Section III will present the results of the experiments, Section IV will discuss the results including relevant development or selection of decomposition model parameters, and Section V presents the conclusions of this study.

2. EXPERIMENTAL SETUP

The batch reactor used in this study is similar in function to that used in the previous studies with the same propellant or other HAN-based propellants.[11, 17, 28] The previous study on catalytic decomposition with the [Emim][EtSO$_4$] blend used a syringe to inject a droplent of the propellant onto pre-heated catalyst particles. Decomposition rate was determined by measuring the pressure change inside the reactor.[11] This was done with application to a conventional monopropellant thruster in mind. In a chemical microtube, the monopropellant decomposition is initiated through heat and catalytic activity from the chamber walls instead of from many small catalyst particles packed into the chamber as in a conventional thruster. The batch reactor in this study therefore uses heated metallic surfaces to generate decomposition of the monopropellant in order to best provide data for use in the design of a monopropellant microtube.

The batch reactor consists of a large (~1L) chamber with feedthroughs to accommodate heating of the catalyst surface and measurement of the surface temperature. Additionally, a gas feedthrough is used to evacuate the air in the chamber via mechanical vacuum pump, as well as to backfill with argon gas back to atmospheric pressure. The experimental setup in the lab is shown in Fig. 1. The propellant itself is held in place on top of the catalytic surface via the sample holder geometry shown in Fig. 2. The sample holder is a quartz tube with an inner diameter of 5.33 mm. The catalytic surface material is sandwiched between two sheets of Teflon material and the top sheet has a cutout of same diameter to the outside diameter of the sample holder cylinder. Additionally, a single strip of Teflon tape is wrapped around the base of the cylinder for experiments. This, combined with the high viscosity of the propellant, was found to provide an adequate seal to keep propellant from leaking out of the containment region provided by the cylinder. The catalytic material is heated by applying a voltage directly across the metallic material. For each experimental run, 50 µL of propellant is injected into the sample holder. The batch reactor is then closed off, evacuated, and back filled with argon. Finally, power is provided to the catalyst material until propellant decomposition is

initiated. A thin wire type-K thermocouple measures the temperature of the catalyst surface throughout the duration of the experiment.
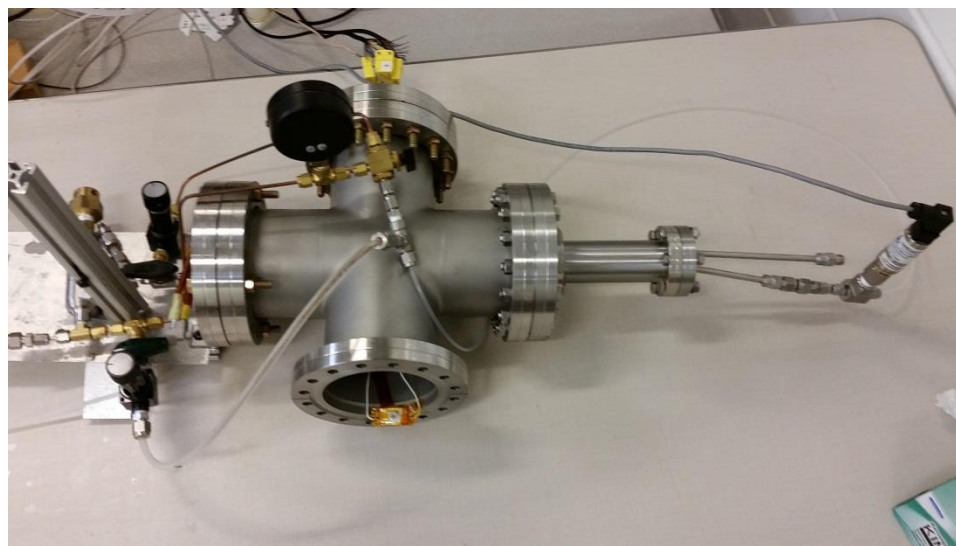

Figure 1. Photograph of the Batch Reactor Experiment in the Lab Showing Atmosphere Control Panel (left), Sample Holder (bottom), Pressure Measurement (right), and Temperature Measurement (top).
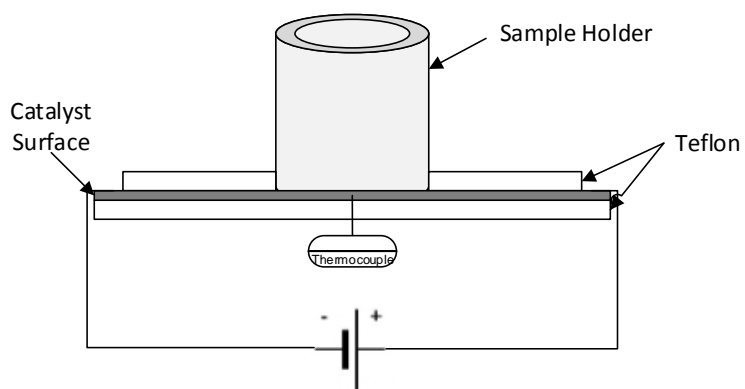

Figure 2. Illustration of the Sample Holder Geometry.

As mentioned, the propellant used in this study is a blend of hydroxylammonium nitrate (HAN) and 1-ethyl-3-methylimidazolium ethyl sulfate ([Emim][EtSO$_4$]) consisting of 59% oxidizer and 41% fuel by mass. The synthesis procedure is described in detail in the previous studies.[11, 15] Three catalyst materials are selected for this investigation: titanium, platinum, and rhenium. Rhenium was found from the previous study to be a good candidate catalyst material.[11] Platinum was the material selected for the previous microtube thruster experiments[12-14] and is also a candidate for HAN propellant catalyst applications.[28] Titanium is selected for this study to provide a measure of thermal decomposition absent catalytic activity since it it known to be compatible with HAN propellants for long term storage.[29] The properties relevant to this study for each material are given in Table 1. For the experiment, a 25 mm x 8 mm strip of 0.025 mm thick material is used for platinum and rhenium. For titanium the dimensions are the same except for the thickness, which is 0.05 mm.

Table 1. Thermal and Electrical Properties of Catalyst Materials Used in This Study.

	ρ [Ω-m] x 10^{-7}	κ [W/m-K]	T_m [K]
Platinum	1.04	71.6	1968
Rhenium	1.85	71.0	3382
Titanium	4.27	20.8	1868

3. RESULTS

Results from the batch reactor experiment described in the previous section are presented here. All decomposition experiments are conducted in a 15 psia argon internal atmosphere and with 50 µL of propellant. For comparison, an 80% HAN/water blend and

pure [Emim][EtSO$_4$] are also tested for decomposition with the same conditions used for the HAN/[Emim][EtSO$_4$] monopropellant blend. Results are displayed in terms of heat flux, which is calculated using the input current, material electrical resistivity and catalyst surface geometry. Due to differences in the material properties, exact heat flux could not be precisely replicated for all materials; however, relevant points will be addressed in the discussion section.

Sample results for the decomposition of the HAN/[Emim][EtSO$_4$] propellant on the catalyst surfaces are shown in Fig. 3. The figure shows the temperature indicated by the thermocouple as a function of time after power is applied through the catalyst surface. The results shown in the figure are for calculated input heat flux of 7.2, 7.9, and 13 mW/mm^2 for platinum, rhenium, and titanium, respectively. For all surface materials, the temperature increase is roughly linear initialy, followed by a transition to another roughly linear region of higher slope, indicating exothermic decomposition of the monopropellant. The temperature at which decomposition of the propellant occurs, which for purposes of this study is taken as the start of the transition from the initial linear temperature slope, is lowest for platinum surface material at 85 ^{o}C, followed by rhenium at 125 ^{o}C and titanium at 165 ^{o}C. Since the rate of temperature increase during decomposition is driven by the exothermic reaction of the monopropellant also of note is that the rate of temperature increase is highest for platinum, which shows a sharp increase in temperature just after decomposition onset. Both rhenium and titanium show a longer transition region and peak at the end of the decomposition event.
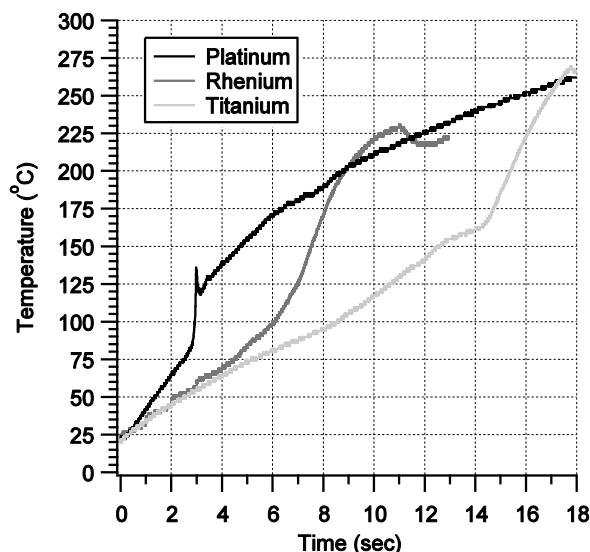
Figure 3. HAN/[Emim][EtSO$_4$] Monopropellant Decomposition on Platinum, Rhenium, and Titanium Surfaces.

The decomposition of the HAN/[Emim][EtSO$_4$] propellant is investigate further by conducting the experiment at various power input levels. Table 2 shows the results for each material at varied heat flux, which is again calculated from the input current and material properties. Results are shown in terms of temperature slope for the region before decomposition onset, during decomposition, and for the same input power with no propellant present. Additionally, for the case with no propellant present, the test is conducted at vacuum ($\sim 10^{-3}$ torr) instead of 15 psia argon. Temperature slope before decomposition and for the blank cases is taken as the line between points at t = 0 and t = 2 seconds. Temperature slope during decomposition is calculated by taking the line between two points as determined by visual inspection of the temperature vs. time results similar to Fig. 3. Cases that do not have a temperature change during decomposition are given a dash-mark in the table. These cases did not show a decomposition event during the test window of 18 seconds. As expected from the results shown in Fig. 3, platinum has the highest rate of temperature change during decomposition at 338-372 $^{\circ}$C/sec. Tests on rhenium show higher rate of temperature change compared to titanium during the decomposition event, 51 $^{\circ}$C/sec vs. 41.5 $^{\circ}$C/sec respectively. Additionally, at similar heat

flux, the platinum cases have a higher temperature slope before decomposition compared to both rhenium and titanium. For example, the temperature slope for heat flux of 3.2 mW/mm^2 is 7.5 ^{o}C/sec for platinum and 6.0 ^{o}C/sec for rhenium; and, the temperature slope is 10 ^{o}C/sec for platinum at 5 mW/mm^2 heat flux and 6.7 ^{o}C/sec at 5.4 mW/mm^2 for titanium. This trend is true for all cases tested. Tests on rhenium also show a slightly higher rate of temperature change prior to decomposition onset compared to titanium, for example 9.3 ^{o}C/sec at 4.3 mW/mm^2 on rhenium versus 8.5 ^{o}C/sec at 7 mW/mm^2 on titanium.

Table 2. Rate of Temperature Change Before and During Decomposition Events for
Each Catalyst Surface at Various Input Power.

$\dot{Q}''$ (mW/mm^2)	$\dot{T}_E$ ($^{\circ}$C/s)	$\dot{T}_S$ ($^{\circ}$C/s)	$\dot{T}_{blank}$ ($^{\circ}$C/s)
Platinum			
3.2	7.5	-	10.0
4.4	9.5	354	17.7
5.0	10.0	363	27.0
6.0	15.0	338	31.7
7.2	21.5	372	37.5
Rhenium			
1.4	3.3	-	6.0
3.2	6.0	-	11.0
4.3	9.3	-	18.5
5.7	11.7	52	34.7
7.9	13.5	50	44.0
Titanium			
5.4	6.7	-	23.3
7.0	8.5	-	35
8.8	9.7	40	47.7
10.9	10.0	41	52.5
13.0	11.0	43	60.3

More information about the propellant decomposition process may be obtained by observing the decomposition of the constituent fuel and oxidizer. As mentioned, an 80% HAN by mass HAN/water solution and pure [Emim][EtSO$_4$] are tested for decomposition. Results on platinum at heat flux of 7.2 mW/mm^2 are shown in Fig. 4.

From the figure, the decomposition of HAN/Water is virtually the same as that of the HAN/[Emim][EtSO$_4$] monopropellant blend. The temperature rate of change is the same value of 21.5 ^{o}C/sec, the onset temperature is 85 ^{o}C, and the temperature slope during decomposition is slightly lower for HAN/Water at 283 ^{o}C/sec. The behavior of temperature data after the decomposition event for HAN/Water is noticeably erratic; this will be discussed in the next section. Pure [Emim][EtSO$_4$] does show an exothermic decomposition peak, which has been observed qualitatively before during spot plate tests.[11] This occurs at roughly 140 ^{o}C on platinum, well above the decomposition onset of 85 ^{o}C for HAN/Water and HAN/[Emim][EtSO$_4$] blend.
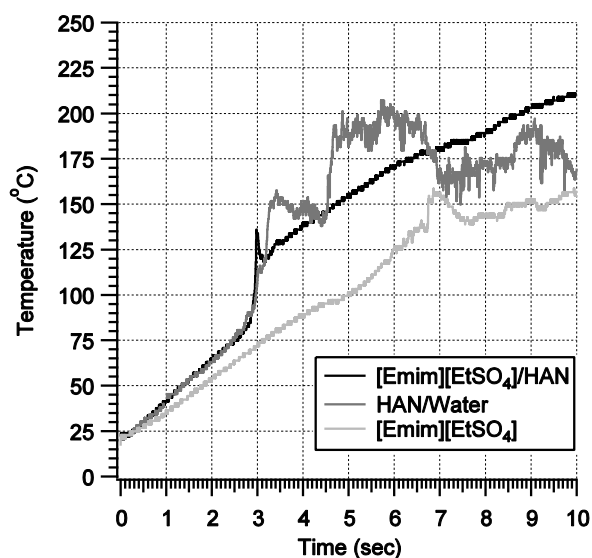

Figure 4. Decomposition of HAN/[Emim][EtSO$_4$] Monopropellant and Constituent Fuel and Oxidizer on Platinum.

4. DISCUSSION

Results from the preceding section are discussed, with particular attention paid to developing insights for the development of a microtube thruster. However, there is no reason why the results could not also be used, at minimum qualitatively, for catalyst development, particularly monolith catalysts. The results and trends seen in the previous section will first be discussed, followed by elucidation of these results into Arrhenius type reaction rate data.

4.1. DISCUSSION OF EXPERIMENTAL RESUTLS

The most significant result of the experiment is the fact that the lowest onset temperature and fastest decomposition rate of the monopropellant is obtained through the use of platinum material. Given that both platinum and rhenium show both lower onset temperature and faster decomposition rate, it is apparent that they do act as a catalyst for the monopropellant decomposition. The fact that the rate of temperature increase prior to the onset temperature is also greater for platinum and rhenium compared to titanium is likely indicative that the monopropellant is undergoing an adsorption process onto the metallic surface, which is exothermic.

Further quantitative assessment of catalytic capability of platinum and rhenium requires the assumption that titanium does not act as a catalyst material for the HAN/[Emim][EtSO$_4$] monopropellant decomposition. The onset temperature for decomposition on titanium material was found in this study to be 165 $^{\circ}$C. This agrees with the literature for the exothermic decomposition temperature for other HAN-based propellants, as well as HAN itself by thermal decomposition initiation means alone.[17, 28, 30] Typically, for HAN-based propellants the initial step in the reaction is assumed to be the initial HAN decomposition step regardless of the fuel choice.[21, 31-33] This is mainly due to the fact that the fuel typically is not decomposed thermally, but through reaction with HAN decomposition intermediate species.[33] Results show that

[Emim][EtSO$_4$] decomposes at much higher onset temperature than HAN for a particular catalyst, although it does appear to be catalyzed by platinum, as evidenced by the exothermic peak at 140 $^{\circ}$C for pure [Emim][EtSO$_4$] on HAN but no such peak at at least 165 $^{\circ}$C on titanium. Additionally, the HAN-water onset temperature is exactly the same as the HAN/[Emim][EtSO$_4$] propellant as seen in Fig. 4. It can therefore be reasonably concluded that titanium does not act as a catalyst for this monopropellant and that the fuel does not decompose thermally prior to the first step in HAN decomposition.

4.2. ELUCIDATION OF ARRHENIUN-TYPE REACTION RATE DATA

Decomposition of HAN-based propellants, even assuming the fuel does not participate in the decomposition initiation, is comprised of many reaction steps.[32, 33] Without knowledge of the intermediate species, or post-reaction species it is not possible to determine a multi-step reaction mechanism from the data garnered in this experiment alone. However, in order to aid preliminary thruster modeling predictions it is useful to develop Arrhenius-type reaction rate equations for the decomposition of this monopropellant on various catalyst surfaces. Using the temperature vs. time data from this study it is possible to determine the activation energy and frequency factor for use in Eq. (1),

$$k' = Ae^{\frac{E}{k_B T}} \tag{1}$$

The energy balance for the system described in the experimental setup is Eq. (2),

$$\frac{dT}{dt} = \frac{\dot{Q} + (-\Delta H_{RX})(-r_A V)}{\sum N_i C_{p,i}} \tag{2}$$

where the contribution to temperature change is heat transfer from the electrical heating and self heating from the exothermic decomposition of the monopropellant, Eqs. (3) and (4), respectively,

$$\dot{T}_E = \frac{\dot{Q}_E}{\sum N_i C_{p,i}} \tag{3}$$

$$\dot{T}_S = \frac{(-\Delta H_{Rx})(-r_A V)}{\sum N_i C_{p,i}} \tag{4}$$

It is clear from the results that prior to the onset temperature the electrical heating rate is much greater than the self heating rate and this region is therefore described fairly accurately by Eq. (3) except perhaps for the cases where catalytic activity is observed. After the onset temperature is achieved the self heating rate described by Eq. (4) clearly dominates the electrical heating rate. This data can therefore be used to determine the targeted reaction rate parameters. Substituting the Arrhenius rate equation into Eq. (4) and taking the natural logarithm of both sides gives Eq. (5),

$$\ln \dot{T}_s = \ln\left(\frac{(-\Delta H_{Rx})V}{\sum N_i C_{p,i}}\right) + \ln A + \ln C_A - \frac{E}{k_B T} \tag{5}$$

Since all parameters are constant aside from the temperature and self heating rate, the activation energy is then the slope of the line of a plot of $\ln \dot{T}_s$ and 1/T. The activity coefficient can then be solved for by substituting the result back into Eq. (5).

The results of these calculations are shown in Table 3. For the calculation of activity coefficient, the propellant specific heat was determined from Eq. (3) from the titanium data only since absorption does not occur and the only heating during the initial phase is due to electrical heating. The value of specific heat for this monopropellant is 95.7 ± 8.6 J/mol-K. Results show what is expected from the assumed catalytic activity described previously, namely that platinum has the lowest activation energy, followed by rhenium.

Table 3. Arrhenius Rate Equation Parameters Calculated from Experimental Data.

Material	E/k_B (K)	A (1/sec)
Platinum	10771 ± 503	$(2.14 \pm 0.23) \times 10^{10}$
Rhenium	16170 ± 107	$(2.23 \pm 0.26) \times 10^{10}$
Titanium	30111 ± 797	$(2.64 \pm 0.26) \times 10^{10}$

5. CONCLUSIONS

A monopropellant blend of hydroxylammonium nitrate and [Emim][EtSO$_4$] was tested on platinum, rhenium, and titanium surfaces in order to garner data for use in microtube thruster or monolith catalyst bed design. When heated on a titanium surface, the monopropellant decomposes at 165 ^{o}C, which agrees with the known decomposition temperature for hydroxylammonium nitrate. Furthermore, the fuel decomposes exothermically at a much higher temperature, which suggests that the reaction mechanism for this monopropellant blend is initiated by HAN decomposition and intermediate species react to decompose the fuel, which agrees with insights from other studies utilizing different fuels.

It was found that platinum and rhenium exhibit catalytic activity for the HAN/[Emim][EtSO$_4$] propellant blend, with platinum initiating decomposition at 85 ^{o}C and rhenium at 125 ^{o}C. Use of these materials will therefore lessen power requirements to start monopropellant rocket engines using this propellant. Platinum initiates the highest rate of reaction, but the material melts at near the flame temperature of the propellant.[10] The flame temperature, however, could be reduced by increasing the fuel mass fraction in the monopropellant bend. Since the decomposition is likely initiated by HAN decomposition and the fuel is then attacked by the reaction intermediates, increasing the fuel ratio of the monopropellant blend could allow use of platinum as a catalyst to start the thruster and thus reduce overall propulsion system power requirements.

REFERENCES

[1] C. A. Kluever, "Spacecraft Optimization with Combined Chemical-Electric Propulsion," Journal of Spacecraft and Rockets, Vol. 32, No. 2, 1994, pp. 378-380.

[2] C. A. Kluever, "Optimal Geostationary Orbit Transfers Using Onboard Chemical-Electric Propulsion," Journal of Spacecraft and Rockets, Vol. 49, No. 6, 2012, pp. 1174-1182.

[3] D. Y. Oh, Randolph, T., Kimbrel, S., and Martinez-Sanchez, M., "End-toEnd Optimization of Chemical-Electric Orbit Raising Missions," Journal of Spacecraft and Rockets, Vol. 41, No. 5, 2004, pp. 831-839.

[4] S. R. Oleson, Myers, R. M., Kluever, C. A., Riehl, J. P., Curran, F. M., "Advanced Propulsion for Geostationary Orbit Insertion and North-South Station Keeping," Journal of Spacecraft and Rockets, Vol. 34, No. 1, 1997, pp. 22-28.

[5] B. R. a. R. Donius, J. L., "Ionic Liquid Dual-Mode Spacecraft Propulsion Assessment," Journal of Spacecraft and Rockets, Vol. 48, No. 1, 2011, pp. 110-123.

[6] T. Rexius, and Holmes, M., "Mission Capability Gains from Multi-Mode Propulsion Thrust Profile Variations for a Plane Change Maneuver," AIAA Modeling and Simulation Technologies Conference, AIAA Paper 2011-6431, 2011.

[7] J. M. Haas, and Holmes, M. R., "Multi-Mode Propulsion System for the Expansion of Small Satellite Capabilities," NATO, Rept. MP-AVT-171-05, 2010.

[8] S. P. Berg, and Rovey, J. L., "Assessment of Multi-Mode Spacecraft Micropropulsion Systems," 50th AIAA/ASME/SAE/ASEE Joint Propulsion Conference, AIAA Paper 2014-3758, 2014.

[9] S. P. Berg, and Rovey, J. L., "Assessment of High-Power Electric Multi-Mode Spacecraft Propulsion Concepts," 33rd International Electric Propulsion Conference, IEPC-2013-308, 2013.

[10] S. P. Berg, and Rovey, J. L., "Assessment of Imidazole-Based Energetic Ionic Liquids as Dual-Mode Spacecraft Propellants," Journal of Propulsion and Power, Vol. 29, No. 2, 2013, pp. 339-351.

[11] S. P. Berg, and Rovey, J. L., "Decomposition of Monopropellant Blends of Hydroxylammonium Nitrate and Imidazole-Based Ionic Liquid Fuels," Journal of Propulsion and Power, Vol. 29, No. 1, 2013, pp. 125-135.

[12] C. A. Mento, Sung, C-J., Ibarreta, A. F., Schneider, S. J.,, "Catalyzed Ignition of Using Methane/Hydrogen Fuel in a Microtube for Microthruster Applications," Journal of Propulsion and Power, Vol. 25, No. 6, 2009, pp. 1203-1210.

[13] G. A. Boyarko, Sung, C-J., Schneider, S. J.,, "Catalyzed Combustion of Hydrogen-Oxygen in Platinum Tubes for Micro-Propulsion Applications," Proceedings of the Combustion Institute, Vol. 30, No. 2005, pp. 2481-2488.

[14] S. J. Volchko, Sung, C-J., Huang, Y., Schneider, S. J.,, "Catalytic Combustion of Rich Methane/Oxygen Mixtures for Micropropulsion Appications," Journal of Propulsion and Power, Vol. 22, No. 3, 2006, pp. 684-693.

[15] S. P. Berg, Rovey, J. L., Prince, B. P., Miller, S. W., and Bemish, R.J., "Electrospray of and Energetic Ionic Liquid Propellant for Multi-Mode Micropropulsion Applications," 51st AIAA/ASME/SAE/ASEE Joint Propulsion Conference, AIAA Paper 2015-4011, 2015.

[16] G. P. Sutton, and Biblarz, O., Rocket Propulsion Elements, 7th, Wiley, New York, 2001.

[17] D. Amariei, Courtheoux, L., Rossignol, S., Batonneau, Y., Kappenstein, C., Ford, M., and Pillet, N., "Influence of the Fuel on Thermal and Catalytic Decompositions of Ionic Liquid Monopropellants," 41st AIAA/ASME/SAE/ASEE Joint Propulsion Conference & Exhibit, AIAA Paper 2005-3980, 2005.

[18] K. Anflo, Gronland, T. A., Bergman, G., Johansson, M., and Nedar, R., "Towards Green Propulsion for Spacecraft with ADN-Based Monopropellants," 38th AIAA/ASME/SAE/ASEE Joint Propulsion Conference & Exhibit, AIAA Paper 2002-3847, 2002.

[19] B. Slettenhaar, Zevenbergen, J. F., Pasman, H. J., Maree, A. G. M., and Morel, J. L. P. A., "Study on Catalytic Ignition of HNF Based Non Toxic Monopropellants," 39th AIAA/ASME/SAE/ASEE Joint Propulsion Conference & Exhibit, AIAA Paper 2003-4920, 2003.

[20] K. Anflo, Persson, S., Thormahlen, P., Bergman, G., and Hasanof, T., "Flight Demonstration of ADN-Based Propulsion System on the PRISMA Satellite," 42nd AIAA/ASME/SAE/ASEE Joint Propulsion Conference & Exhibit, AIAA Paper 2006-5212, 2006.

[21] Y. P. Chang, Josten, J.K., Zhang, B.Q., Kuo, K.K.,, "Combustion Characteristics of Energetic HAN/Methanol Based Monopropellants," 38th AIAA Joint Propulsion Conference, AIAA Paper 2002-4032, 2002.

[22] C. H. McLean, Deininger, W. D., Joniatis, J., Aggarwal, P. K., Spores, R. A., Deans, M., Yim, J. T., Bury, K., Martinez, J., Cardiff, E. H., Bacha, C. E., "Green Propellant Infusion Mission Program Development and Technology Maturation," 50th AIAA/ASME/SAE/ASEE Joint Propulsion Conference, AIAA Paper 2014-3481, 2014.

[23] Green Monopropellant Thrusters, http://www.busek.com/index_htm_files/70008517B.pdf

[24] Busek Electrospray Thrusters, http://www.busek.com/index_htm_files/70008500E.pdf

[25] Chiu, Y., Dressler, A.,, "Ionic Liquids For Space Propulsion", *Ionic Liquids IV: Not Just Solvents Anymore*, Vol. 975, American Chemical Society, Washington, D. C., 2007, Ch.

[26] M. Gamero-Castano, "Characterization of a Six-Emitter Colloid Thruster Using a Torsional Balance," Journal of Propulsion and Power, Vol. 20, No. 4, 2004, pp. 736-741.

[27] M. S. Alexander, Stark, J., Smith, K. L., Stevens, B., Kent, B., "Electrospray Performance of Microfabricated Colloid Thruster Arrays," Journal of Propulsion and Power, Vol. 22, No. 3, 2006, pp. 620-627.

[28] R. Eloirdi, Rossignol, S., Kappenstein, C., Duprez, D., Pillet, N., "Design and Use of a Batch Reactor for Catalytic Decomposition of Propellants," Journal of Propulsion and Power, Vol. 19, No. 2003, pp. 213-219.

[29] E. W. Schmidt, "Hydroxylammonium Nitrate Compatibility Tests with Various Materials-A Liquid Propellant Study," U.S. Army Ballistic Research Laboratory, Rept. BRL-CR-636, 1990.

[30] A. J. Alfano, Mills, J. D., Vaghjiani, G. L., "Resonant Laser Ignition Study of HAN-HEHN Propellant Mixture," Combustion Science and Technology, Vol. 181, No. 6, 2009, pp. 902-913.

[31] S. R. Vosen, "Hydroxylammonium Nitrate-Based Liquid Propellant Combustion-Interpretation of Strand Burner Data and the Laminar Burning Velocity," Combustion and Flame, Vol. 82, No. 1990, pp. 376-388.

[32] H.-S. Lee, Litzinger, T. A.,, "Chemical Kinetic Study of HAN Decomposition," Combustion and Flame, Vol. 135, No. 2003, pp. 151-169.

[33] Y.-P. Chang, "Combustion Behavior of HAN-Based Liquid Propellants," Mechanical Engineering, Pennsylvania State University, 2002.

IV. Electrospray of an Energetic Ionic Liquid Monopropellant for Multi-Mode Micropropulsion Applications

Steven P. Berg and Joshua L. Rovey

Missouri University of Science and Technology, Rolla, Missouri, 65409

Benjamin D. Prince , Shawn W. Miller and Raymond J. Bemish

Air Force Research Laboratory, Kirtland AFB, Albuquerque, New Mexico, 87117

ABSTRACT

The multi-mode chemical-electric propulsion capable energetic ionic liquid propellant [Emim][EtSO$_4$]-HAN is electrosprayed in a 100 µm capillary emitter to test the electric-mode performance of the propellant. The ionic liquid exhibits stable electrospray emission in both cation and anion extraction modes at a nominal extraction voltage of 3400 V. Near field measurements of current and mass flow rate distribution are taken at flow rates from 0.19 nL/s to 3.06 nL/s. Total emission current, as measured by Faraday cup and integrated, increases from 754 nA to 3195 nA for cation emission and from 552 nA to 2012 nA for anion emission. The thrust and specific impulse at 0.19 nL/s flow rate is 1.08 µN and 412 seconds, respectively, with a beam power of 2.22 mW. At 3.06 nL/s, the thrust is 8.71 µN and the specific impulse is 204 seconds with a beam power of 8.85 mW. Extrapolation of the current data shows that specific impulse in excess of 1000 seconds is achievable through optimized feed system and emitter design.

NOMENCLATURE

D_c = transport capillary inner diameter [µm]

D_n	=	emitter inner diameter [μm]
F	=	thrust [μN]
g_0	=	constant to convert specific impulse to units of seconds [m/s^2]
I	=	current [nA]
I_{sp}	=	specific impulse [sec]
K	=	ionic liquid electrical conductivity [S/m]
L_c	=	length of transport capillary [cm]
L_n	=	length of capillary emitter [cm]
$\dot{m}$	=	mass flow rate [ng/s]
m/q	=	mass to charge ratio [amu/e]
P_0	=	reservoir pressure [torr]
P_c	=	pressure in transport capillary [torr]
P_n	=	pressure at capillary emitter [torr]
Q	=	volumetric flow rate [nL/s]
V_{acc}	=	acceleration voltage [V]
V_E	=	extractor voltage [V]
V_N	=	emitter voltage [V]
$γ$	=	ionic liquid surface tension [N/m]
$ε$	=	ionic liquid dielectric constant
$ε_0$	=	permittivity of free space [F/m]
$μ_l$	=	viscosity of propellant [cP]
$ρ$	=	ionic liquid density [g/cm^3]

1. INTRODUCTION

Multi-mode spacecraft propulsion is the use of two or more types of propulsive devices on a spacecraft that share some commonality in terms of either hardware or propellant. An example is the Mars Global Surveyor, which made use of hydrazine as

both a monopropellant for attitude control and a bipropellant for primary maneuvering.[1] Specific to this study is a multi-mode system making use of a high-thrust, usually chemical, mode and a high-specific impulse, electric mode. Using these two modes can be beneficial in two primary ways. One way is by designing a mission such that the high-thrust and high-specific impulse maneuvers are conducted in such a way that it provides a more optimum trajectory over a single chemical or single electric maneuver.[2-5] The second is to increase the mission flexibility of a single spacecraft architechture in that both high-thrust and high-specific impulse maneuvers are available to mission designers at will, perhaps even allowing for drastic changes in the mission plan while on-orbit or with a relatively short turnaround from concept to launch.[6-10] For the second method, it is extremely beneficial to utilize a common propellant for both modes as this provides the highest flexibility in terms of mission design choices.[9] Previous research has investigated a multi-mode system utilizing a single ionic liquid propellant for chemical monopropellant and electrospray modes.[6, 11] Two propellants were developed that may not only function, but theoretically perform well in both a modes.[11] These propellants, based on binary mixtures of ionic liquid fuels [Emim][EtSO4] and [Bmim][NO3] with ionic liquid oxidizer hydroxylammonium nitrate (HAN), have been previously synthesized and tested for thermal and catalytic decomposition in a microreactor.[12] This paper presents results of experiments measuring the performance of the electrospray emitter and beam composition of the [Emim][EtSO4]-HAN propellant. In a separate paper, the decomposition and performance of this propellant in the chemical, high-thrust mode thruster has been investigated.[13]

Recent efforts have placed a greater emphasis on smaller spacecraft, specifically microsatellites (10-100 kg) and nanosatellites (1-10 kg), including the subset of cubesats.[14] Many different types of thrusters have been proposed to meet the stringent mass and volume requirements placed on spacecraft of this type. Electrospray, in particular, may be well suited for micropropulsion, and has been selected for these types of applications.[15-17] Several types of thrusters have been proposed for chemical propulsion for small spacecraft. One type is the chemical microtube.[18-20] This type of thruster is simply a heated tube of diameter ~1 mm or less that may or may not consist of a catalytic surface material. Additionally, and ideally from a multi-mode system

standpoint, there is no fundamental reason why this geometry could not be shared with the electrospray mode as capillary type emitters can be roughly the same diameter tube.[21] This would reduce the overall propulsion system mass, which is desirable particularly in micropropulsion systems for small spacecraft.

Electrospray is a propulsion technology in which charged liquid droplets or ions are extracted from an emitter via an applied electric field. This produces a high exhaust velocity (high specific impulse) but low flow rate and thrust.[16] Ionic liquids are candidates for electrospray propulsion not only due to their ionic nature, but also their negligible vapor pressure and high electrical conductivity.[22] Charged species emitted from the ionic liquid can range from large m/q charged droplets to a purely ionic regime (PIR), with small m/q values, similar to that of field emission electric propulsion with specific impulses in the range of 200-4000 seconds for current propellants.[16] The ionic liquid 1-ethyl-3-methylimidazolium bis(trifluoromethylsulfonyl)imide ([Emim][Im], or [Emim][Tf2N]) was selected as the propellant for the ST7 Disturbance Reduction System mission, and represents the only planned flight application of electrospray, or colloid, thrusters to date.[17] Several other imidazole-based ionic liquids have been suggested for research in electrospray propulsion due to their favorable physical properties, however, none of these have energetic properties sufficient for chemical propulsion.[17]

Electrospray liquids with relatively high vapor pressure boil off the propellant and produce an uncontrolled, low performance emission. This virtually eliminates most of the advanced monopropellants from multi-mode propulsion consideration since although their main component is an ionic liquid oxidizer, they typically contain water and perhaps a volatile fuel component.[23-25] Mixing electrosprayable, fuel-rich ionic liquids with an ionic liquid oxidizer such as HAN shows theoretical promise in terms of achieving high performance in both chemical and electrospray modes.[11] However, it is difficult to theoretically predict electrospray performance precisely due to relative immaturity of the technology. Additionally, the double salt nature of the ionic liquid propellants to be investigated here could lead to additional difficulties in predicting the electrospray performance.[26] This will be discussed in further detail in a later section, but this illustrates the need for experimental measurements in order to best estimate electrospray performance. This paper describes experimental measurements of the performance and

beam properties of the electrospray emission of the double salt ionic liquid propellant [Emim][EtSO4]-HAN. Section II describes the experimental setup and propellant synthesis. Section III presents the results of the electrospray experiments. Section IV discusses the results and performance of the propellant in a capillary electrospray system. Section V summarizes the relevant conclusions.

2. EXPERIMENTAL SETUP

The electrospray thruster experiment utilized to characterize electrospray performance is a well-characterized experiment that is currently in use at AFRL Kirtland [27, 28]. The experiment consists of a capillary emitter electrospray source, which is effectively the same geometry as the chemical thruster microtube, Figure 1a,[13] but with a voltage applied between the needle tip and an extractor grid, Figure 1b. In order to characterize the performance of the electrospray emission mode, knowledge of the beam current and mass flow rate is required. These measurements are accomplished using the angle-resolved method described by Chiu, et. al.[28] and also conducted by Miller, et.al.[27] to study the capillary electrospray of the ionic liquid [Bmim][dca].
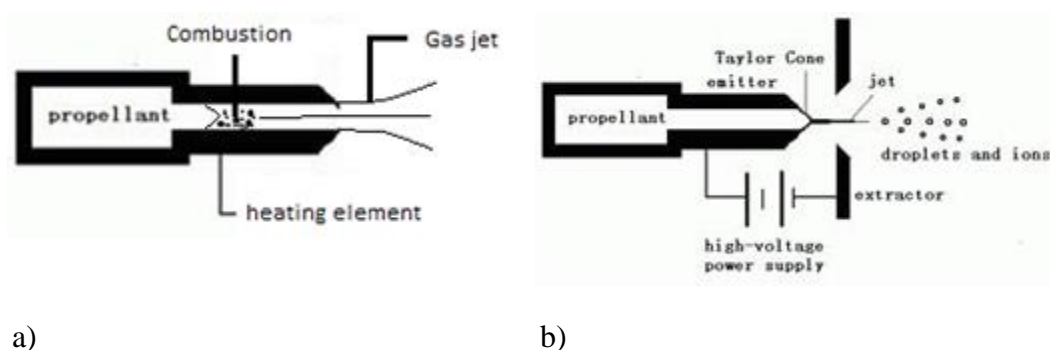

a)   b)

Figure 1. Multi-mode thruster operated in a) chemical microtube and b) electrospray emission modes.

2.1. APPARATUS

A schematic of the instrumentation to diagnose the electrospray emission in the near-field is shown in Figure 2. The electrospray source, as in Figure 1b, consists of a capillary and extractor plate. The capillary is 100 μm internal diameter, 5.0 cm long, and has a tapered tip. The capillary is fed from a propellant reservoir via a 100 μm internal diameter fused silica transport capillary 82.5 cm in length. The feed system is a pressure-fed system similar to that used by Lozano[29] and is shown in Figure 3. Notable differences include direct feed pressure monitoring via a pressure transducer and the fact the reservoir, after achieving nominal pressure, is isolated by closing both shut-off valves and operates in blow-down mode. Since the volume change of the propellant in the reservoir is negligible during normal test opertions (~nL/s flow rate from a ~10 mL reservoir), reservoir pressure, and thus flow rate, can safely be assumed to be constant during the experiment under steady flow conditions. The extractor plate consists of a metal plate with a 1.5 mm orifice to allow for passage of the electrospray beam.

The electrospray source is attached to a rotation stage, which allows the beam to be rotated in order to capture species in the full width of the beam divergence. These measurements allow for computation of the thrust, specific impulse, and efficiency of the electrospray thruster. A Faraday cup and quartz crystal microbalance (QCM) measure the current and mass flow rate of the electrospray beam. Appatures of 0.8 mm are used on both targets located 18 mm downstream of the emission source, and the measurement interval is at minimum 2.5 degrees for all angle-resolved measurements described in this paper.
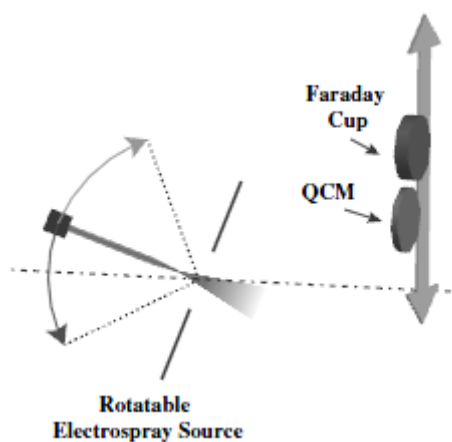
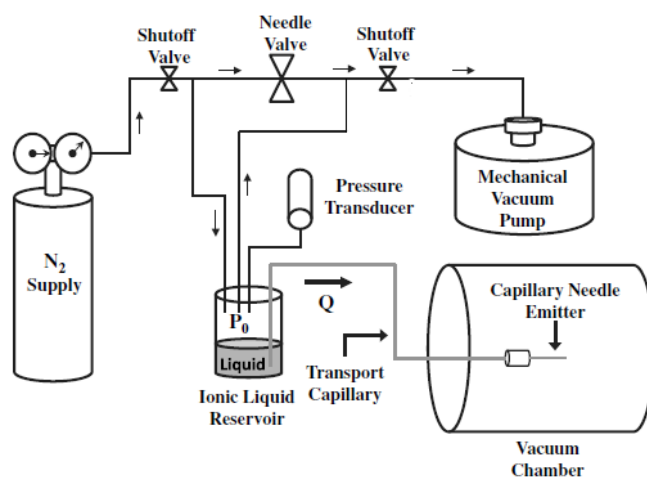Figure 2. Electrospray experiment near-field diagnostics. [27, 28]

Figure 3. Plumbing and instrumentation diagram of the electrospray apparatus.[27]

While the experiment itself is well characterized with various ionic liquids, there are notable differences between ionic liquids previously investigated with the setup and the ionic liquid propellants proposed in this study. The major difference is that previously only single ionic liquids have been used. The multi-mode propellants proposed here are

mixtures of two ionic liquids. Furthermore, the term mixture is actually a misnomer and these may in fact be more accurately referred to as double salt ionic liquids [26]. The reason is in the fundamental nature of ionic liquids, in that they are essentially dissociated pairs of cations and anions in solution. Therefore mixing two ionic liquids could result in not only pairs of the original constituents, but also pairs of the swapped ions. For example, a mixture of two ionic liquids $[A]^+[B]^-$ and $[C]^+[D]^-$ could consist of a mixture of $[A]^+[B]^-$, $[C]^+[D]^-$, $[A]^+[D]^-$, $[C]^+[B]^-$ in some ratio. While trends in the literature predict that the physical properties for double salt ionic liquids in general follow typical mixing laws [26], this could fundamentally alter the species emitted in the electrospray beam, and thus have an effect on the electrospray thruster performance of the ionic liquid propellants.

2.2. PROPELLANT SYNTHESIS

The propellant synthesis method for the binary mixture of $[Emim][EtSO_4]$-HAN was developed in a previous study,[12] however it is repeated here making particular note of the considerations made to ensure successful electrospray operation. Pure 1-ethyl-3-methylimidazolium ethyl sulfate, $[Emim][EtSO_4]$ (95% purity), and hydroxylammonium nitrate, HAN, (24% in water) were purchased from Sigma Aldrich. Pure crystalline HAN was obtained by removing water in high-vacuum ($\sim 10^{-6}$ torr) for ~ 8 h. Additionally, $[Emim][EtSO_4]$ was placed in high vacuum for ~ 8h to remove any volatile impurities. Crystalline HAN was then added to the $[Emim][EtSO_4]$ in a sealable container in the desired ratio; for this study the ratio is 59% HAN, 41% $[Emim][EtSO_4]$ by weight. This ratio was chosen mostly to avoid sooting and burn through in the chemical mode and is described more in the previous studies with this propellant.[11,12] This mixture was allowed to settle overnight at which point solid HAN was no longer visible in the mixture. This process likely could be sped up by mechanically agitating the mixture to allow for faster dissolving. However, due to safety concerns involved with creating the potentially explosive monopropellant, this was avoided, and is not recommended. The propellant reservoir in the electrospray experiment described in this paper was kept under rough vacuum (< 100 mTorr) when not in operation to prevent water absorption.

3. RESULTS

The following section presents results from the near field experiment which measures current and flow rate distribution as a function of angle of the electrospray beam in the region of ±60 degrees in reference to the center of the beam. These measurements will be used to calculate emitter performance in the next section. All measurements in this section are taken with an extraction voltage of 3400 V for both cation (V_N =+900 V, V_E =-2500 V) and anion (V_N = -900 V, V_E = +2500 V) emission. This was found to be the nominal extraction voltage through trial and error, providing a stable beam.

3.1. FLOW RATE CALIBRATION-BUBBLE METHOD

Flow rate is primarily calibrated using the bubble method, and flow rates in the remainder of this paper, except where noted, refer to the values determined through this method. For this method, a bubble is introduced to the transport capillary at its termination in the reservoir. Since the capillary is made of transparent material, the bubble movement can be tracked visually via the use of a magnifying glass. Flow rate as a function of reservoir pressure can then be determined by measuring the distance the bubble travels as a function of time, as measured by a stop watch. The total duration of each test was kept longer than ~15 sec to minimize error from a slow trigger finger. Results are shown in Figure 4. Additionally, the experimental results can be compared to analytical calculations given by the Hagan-Pouiseulle equation, Eq. (1),

$$Q = \frac{\pi D_c^4}{128\mu_l} \frac{(P_0 - P_n)}{L_c} = \frac{\pi D_n^4}{128\mu_l} \frac{(P_n - P_c)}{L_n} \tag{1}$$

where the length and diameter of the capillary and transport capillary are given in the previous section and the viscosity of the liquid propellant is 130 cP as found in a previous experiment.[13] The flow rate range achieved by the feed system is similar to that

conducted for electrospray [Bmim][dca] in a capillary emitter.[27] However, the emitter diameter for the [Bmim][dca] experiments was half that of the current experiments. The flow rate similarity is due to the fact that the viscosity of the [Emim][EtSO$_4$]-HAN propellant is roughly four times that of [Bmim][dca].
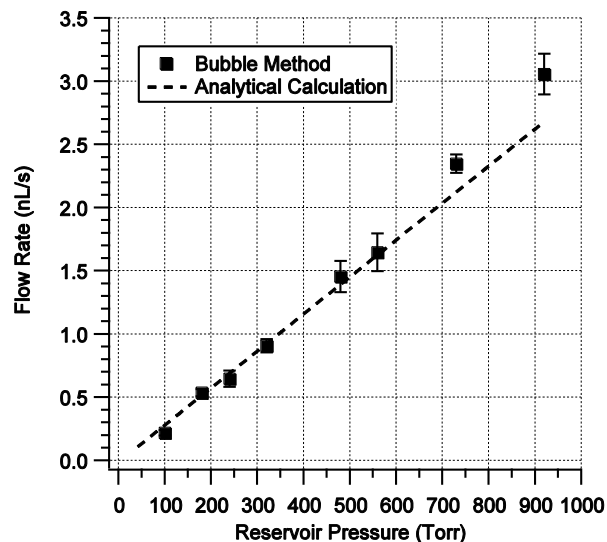

Figure 4. Flow rate as a function of reservoir pressure obtained via the bubble method.

3.2. ANGLE-RESOLVED CURRENT MEASUREMENTS

Beam current measurements as a function of emitter angle to the Faraday cup are taken for both cation and anion emission at the aforementioned extraction conditions and for the range of flow rates illustrated in Figure 4. Total current is calculated by integrating the associated current density profile over a hemisphere, similar to the analysis for a Hall thruster plume conducted by Manzella and Sankovic[30] and the same analysis conducted by Miller, et. al.[27]   Additionally, total emission current on the needle and loss to the extractor is monitored by measuring the potential across a 4.93 MΩ resistor on the associated voltage line for comparison to and verification of the integrated results.

Current density profiles for various flow rates are shown for the electrospray emission in Figure 5. Figure 5a shows the cation emission profile. The highest current densities are obtained near the centerline for each flow rate and decrease as flow rate is increased, peaking at 3.1 nA/mm^2 for 0.19 nL/s and 2.4 nA/mm^2 for 3.06 nL/s. The beam width grows as flow rate is increased, from a 70 degrees at 0.19 nL/s to nearly 90 degrees at 3.09 nL/s, and is roughly 5 degrees asymmetric toward the positive angles. Profiles for anion emission are similar, and are shown in Figure 5b. Peak current is slightly higher for the anion emission compared to the cation emission, with the current density reaching 3.3 nA/mm^2 for 0.19 nL/s flow rate and decreasing to 2.8 nA/mm^2 for 3.06 nL/s flow rate. The beam is slightly narrower compared to the cation case. The beam has a width of 60 degrees for 0.19 nL/s flow rate and increases to 75 degrees for 3.06 nL/s flow rate.
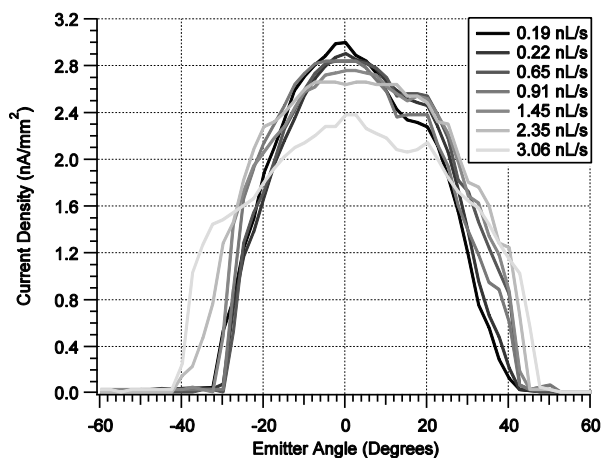

a)
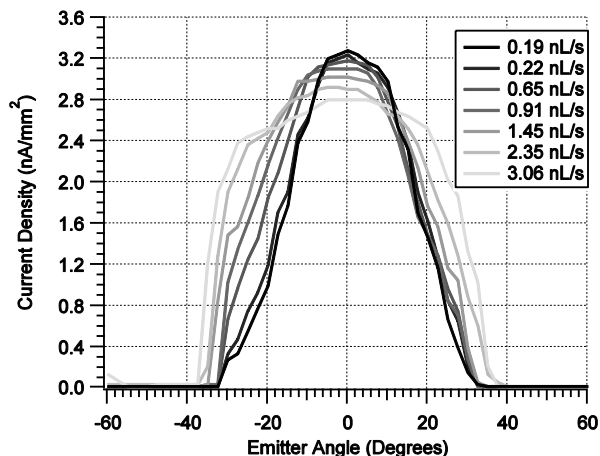
b)

Figure 5. Current density profiles for a) cation and b) anion emission of the electrospray of [Emim][EtSO$_4$]-HAN propellant.

Total emission current obtained by integrating the beam current profiles, along with the measurements from the 4.93 MΩ resistor are shown in Figure 6. The integrated current is the total current obtained by integrating the current profiles in Figure 5 via the method described previously. The emitter current is measured on the needle and is a measure of the overall total current of the electrospray emission. The extractor current is the current lost to the extractor. Figure 6a shows the results from cation emission. At the lowest flow rate conducted in the experiment, 0.19 nL/s, the total current is 680 nA. Both the integrated and emitter current agree at low flow rates. However, due to loss to the extractor at higher flow rates, the current measured via integration of the Faraday cup measurements does not increase markedly although the emitter current does. At the highest flow rate at which experiments were conducted, 3.1 nL/s, the loss to the extractor represents nearly 2/3 of the total emission current. Current measured for anion emission is shown in Figure 6b. The trends in total current are similar to the cation case; however, the current at each flow rate is roughly 70% that of the cation case. The current integrated from the angle-resolved profiles added to the current measured on the extractor agrees well with the emitter current, within 15% for all flow rate cases.
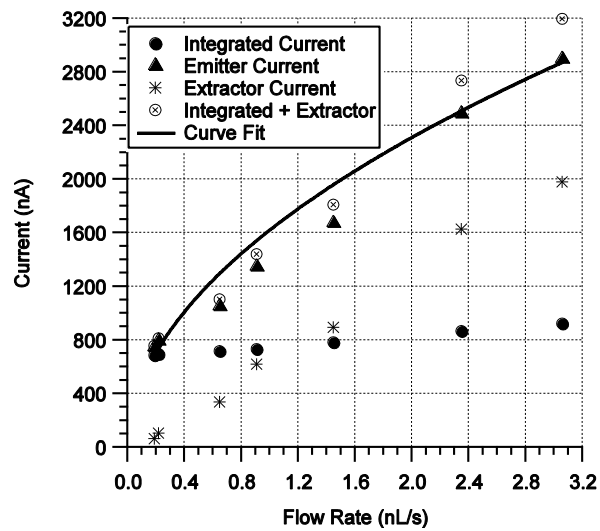
a)
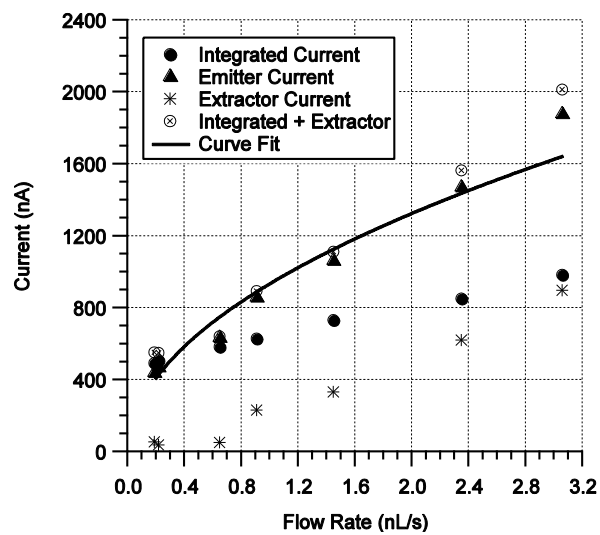
b)

Figure 6. Total emission current as a function of propellant flow rate for a) cation and b) anion emission.

3.3. ANGLE-RESOLVED MASS FLOW MEASUREMENTS

Mass flux as a function of emitter angle is measured in a similar manner to the current profiles with the QCM, but for flow rates from 0.19 nL/s to 1.45 nL/s. Higher flow rates are omitted since the nature of the QCM prevents reliable measurements at higher flow rates. The situation is described in more detail in the work by Miller, et. al.,[27] but is essentially due to violation of the thin film assumption resulting from accumulation of the ionic liquid on the QCM, which does not boil off due to the negligible vapor pressure of the ionic liquid. Raw output of the QCM is converted to mass flux by using the measured density of the ionic liquid propellant (1.42 g/cm^3)[12, 13] and includes small aperture and area ratio corrections.[31]

The mass flux profile for both cation and anion emission as a function of angle is shown in Figure 7. Cation emission is shown in Figure 7a. Peak mass flux, as with current density, occurs at or near the centerline. The peak mass flux for the 0.19 nL/s case is 1.3 ng/s-mm^2 and for the 1.45 nL/s case is 4.5 ng/s-mm^2. The first instance of non-zero mass flux is seen at -25 degrees emitter angle for all flow rates. This is somewhat notable as non-zero current is seen at -30 degrees, as presented in Figure 5. The same trends are seen for anion emission, as shown in Figure 7b, and in fact the profiles are virtually identical numerically by visual inspection.
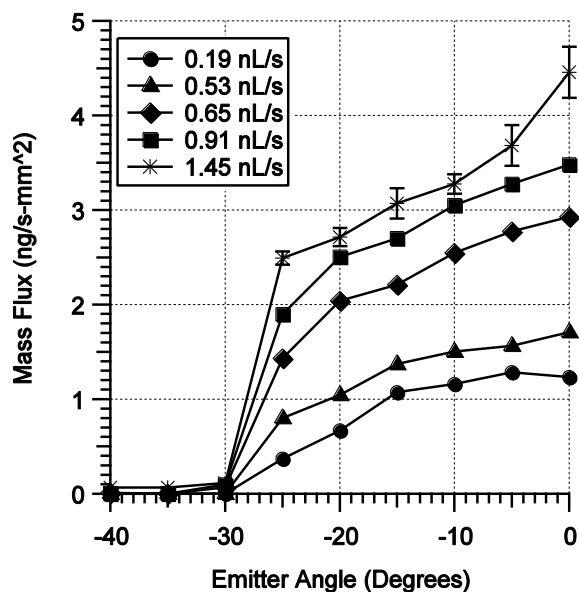
a)
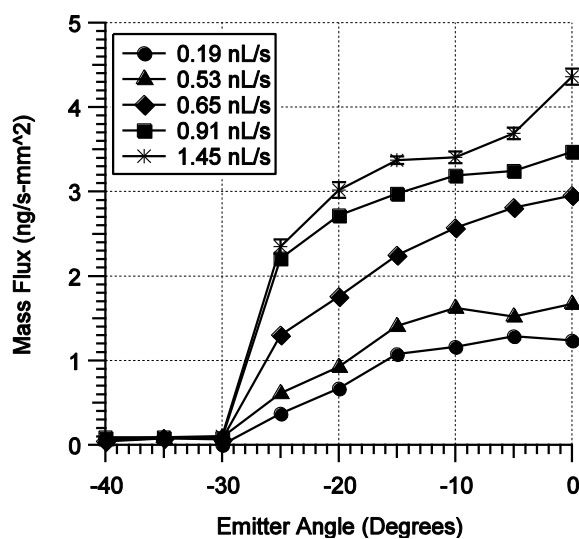
b)

Figure 7. Mass flux profiles for emission of a) cations and b) anions.

The mass flux profiles are integrated over a hemisphere in the same manner as described in the total current integration. Results of the integration are shown in Table 1 and compared to the nominal mass flow rate measured by the bubble method. As with the current measurements, the integrated mass flow rate agrees with the nominal mass flow rate at low flow rates. However, this quickly diverges as flow rate is increased. At the highest flow rate, 1.45 nL/s, integration of measurements taken via the QCM results in a roughly 50% reduced flow rate value. Also notable is that, except for the 0.22 nL/s case, the mass flow rate obtained via integration of the QCM data is smaller than that of the mass flow rate measured by the bubble method.

Table 1. Mass flow rate integrated from QCM data compared to bubble method.

Flow Rate (nL/s)	Integrated Mass Flow (ng/s)	Nominal Mass Flow (ng/s)	% Difference
Cation Emission			
0.19	268	269	0.51
0.22	334	312	-7.27
0.65	720	922	21.89
0.91	890	1291	31.08
1.45	1012	2057	50.82
Anion Emission			
0.19	265	269	1.39
0.22	394	312	26.34
0.65	679	922	26.33
0.91	967	1291	25.10
1.45	1065	2057	48.24

4. DISCUSSION

The near-field measurements described in the previous section provide information on the current and mass distribution of the electrospray emission of the double-salt ionic liquid propellant. Integration of the results from these measurements can be used to predict the performance characteristics of the ionic liquid propellant in an electrospray thruster. While the experiments conducted in this study do not represent the entirety of the possible performance envelope of the propellant, results can be extrapolated to determine the likely bounds of performance for this propellant.

4.1. CURRENT AND MASS DISTRIBUTION

The current and mass distributions of the electrospray of the [Emim][[EtSO$_4$]-HAN double-salt ionic liquid propellant follow trends seen in the literature.[27] Namely, the peak current falls as flow rate is increased and the profile becomes wider, resulting in a higher total integrated current. As noted in the previous section, the QCM data shows a non-zero flow rate at roughly 5 degrees closer to centerline than does the current. This supports the conclusion that much of the species comprising the outer portions of the beam are ions, whereas the center contains higher mass droplets. The mass flow of the ions is so small that it would not read a significant amount on the QCM.

Integrating the current data from the Faraday cup measurements and comparing to the current obtained from measuring the voltage across a resistor on the emitter and extractor lines shows that losses to the extractor become large as flow rate is increased. As mentioned, at the highest flow rates conducted in this study the loss is as much as 66% of the total emission current. This can likely be mitigated with an extractor designed and optimized for this propellant specifically; however, as will be shown in the next sub-section, these flow rates do not represent conditions in which a thruster would likely be operated. Adding the current obtained from the extractor resistor to the integrated current shows good agreement with the current obtained from the emitter resistor measurements, with most values falling within roughly 15% of each other. Though not shown in Figure

6, the measurement error for the resistor currents was also roughly 15%. This represented the average of the highest and lowest values observed on a digital readout, since these values were not instantaneously averaged via computer software but rather recorded by hand. Thus, the error also likely represents higher than one standard deviation.

As in the study of capillary electrospray emission of [Bmim][dca], [27] total mass flow rate calculated by integration of QCM data results agrees well with that obtained by the bubble method at low flow rates, but diverges as flow rate is increased. Curiously, in this study the mass flow calculated by QCM integration is lower than that of the bubble method, whereas in the [Bmim][dca] study it was higher. During the unfortunate situation in which a large amount of liquid was unintentionally deposited on the outer surface of the capillary, the propellant was actually observed to boil in the high vacuum conditions ($\sim10^{-6}$ torr). This is likely the HAN component of the propellant. As a result, liquid deposited on the QCM in any significant amount would contribute a negative component to the mass flow rate during testing operations and would explain why the integrated mass flow rate is lower than the mass flow obtained by the bubble method.

4.2. PERFORMANCE

The primary goal of this study is to predict thruster performance of the [Emim][EtSO$_4$]-HAN propellant operating in the electrospray mode of the proposed multi-mode system. The current and mass flow measurments obtained experimentally are directly used to compute performance. Thrust is calculated by Eq. (2),

$$F = \sqrt{2V_{acc}\dot{m}I} \tag{2}$$

where the current used is the integrated current profile plus extractor current shown in Figure 6. Although the extractor current does not contribute to actual thrust in this experiment, it still represents thrust that could be achieved through optimized extractor design. The specific impulse is then, Eq. (3),

$$I_{sp} = \frac{F}{\dot{m}g_0} \tag{3}$$

Current and calculated thrust values are shown in Table 2 for both cation and anion emission separately. Thrust for both cases is on the order of μN for this single emitter case. The thrust at the lowest flow rate is ~1 μN and increases to 9.71 μN and 7.71 μN for the cation and anion cases, respectively, at the highest tested flow rate of 3.06 nL/s. Thrust is roughly 17% lower for anion emission compared to cation emission, a direct result of the lower current generated by the anion beam.

Table 2. Current, thrust, and mass to charge ratio for cation and anion emission.

Flow Rate (nL/s)	Mass Flow (ng/s)	Current (nA)	Thrust (μN)	m/q (amu)
Cation Emission				
0.19	269	754	1.18	34508
0.22	312	811	1.31	37137
0.65	922	1101	2.63	80815
0.91	1291	1439	3.56	86579
1.45	2057	1807	5.03	109860
2.35	3334	2733	7.87	117722
3.06	4342	3194	9.71	131170
Anion Emission				
0.19	269	551	1.01	47170
0.22	312	547	1.08	55022
0.65	922	640	2.00	139028
0.91	1291	891	2.80	139769
1.45	2057	1110	3.94	178742
2.35	3334	1562	5.95	206000
3.06	4342	2011	7.71	208281

An actual thruster would likely not operate in solely cation or anion emission mode, but rather in AC mode to prevent charge build up and eventual fouling of the emitter. Thus, in order to gauge performance, both the cation and anion emission must be taken into account. Table 3 shows the average thrust of the cation and anion emission at the tested flow rates, along with the beam power and specific impulse. Power ranges from 2.22 mW at the 0.19 nL/s flow rate to 8.85 mW for the 3.06 nL/s flow rate. Thrust per power (in μN/mW) , however, at low flow rate is roughly 0.5 and improves to roughly 1.0 at high flow rate. Specific impulse decreases as flow rate increases, with a calculated value of 412.37 seconds at 0.19 nL/s flow rate and 204.47 seconds at 3.06 nL/s. These values are higher than the specific impulse predicted for the chemical propulsion mode (~180 seconds).[13]

Table 3. Thrust, power, and specific impulse for electrospray emission.

Flow Rate (nL/s)	Mass Flow (ng/s)	Average Thrust (μN)	Power (mW)	Isp (sec)
0.19	269	1.09	2.22	412
0.22	312	1.20	2.31	390
0.65	922	2.32	2.96	255
0.91	1291	3.18	3.96	250
1.45	2057	4.49	4.96	222
2.35	3334	6.91	7.30	211
3.06	4342	8.71	8.85	204

Although the highest specific impulse measured in this study is 412 seconds, this number could likely be improved through optimized thruster and feed system design. In order to gauge what might be possible, scaling laws can be used to extrapolate the data garnered in this study to possible specific impulse and thrust values. Current in the mixed

ion-droplet regime typically scales with flow rate as a power function according to Eq. (4),

$$I(Q) = f(\varepsilon) * \left[\frac{\gamma K Q}{\varepsilon}\right]^{0.5}$$ (4)

Applying a curve fit to the beam current, shown in Figure 6, yields an exponent of approximately 0.5 (0.5092 for cation emission and 0.5019 for anion emission.), with coefficients of 1629.7 and 939.41 for cation and anion emission, respectively. The average of these two values, along with Eqs. (2) and (3) is used to calculate the thrust and specific impulse as a function of flow rate for a range of flows from 0.001 nL/s to 1 nL/s, shown in Figure 8. Achieving a lower flow rate results in a large increase in specific impulse. For the range in the figure, a specific impulse of 1000 seconds is possible if the flow rate could be reduced to 0.001 nL/s. For stable electrospray emission, the flow rate cannot be arbitrarily small and can be predicted through knowledge of the physical properties of the ionic liquid, Eq. (5),

$$Q_{min} = \frac{\gamma \varepsilon \varepsilon_0}{\rho K}$$ (5)

Although the surface tension, electrical conductivity, and dielectric constant of this propellant are not currently known, the value calculated for minimum flow of [Bmim][dca] was 0.09 pL/sec,[27] much lower than the 1 pL/sec shown in Figure 8. Thus, it is likely that performance is not limited by electrospray physics, but rather feed system performance in relation to the thruster geometry. Improvements in the feed system and optimization of emitter geometry for this propellant are likely to result in much improved performance in terms of specific impulse.
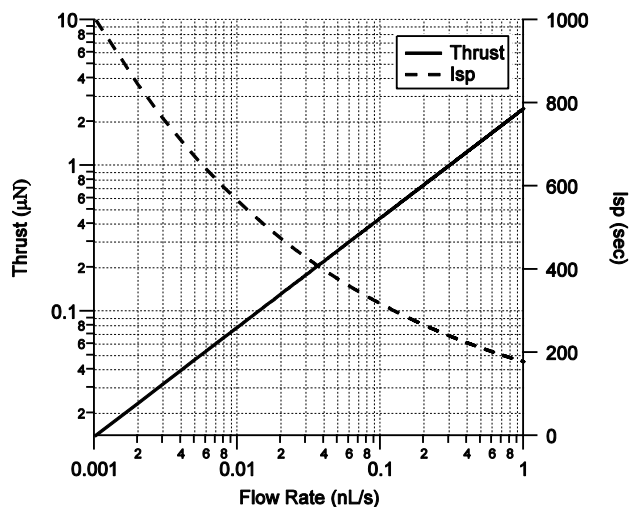
Figure 8. Thrust and specific impulse of IL propellant in a capillary emitter extrapolated from experimental data.

5. CONCLUSIONS

The double-salt, energetic ionic liquid propellant [Emim][EtSO$_4$]-HAN exhibits stable electrospray emission of both cations and anions in a capillary emitter of 100 μm inner diameter with a nominal extraction voltage of 3400 V. Near-field measurements of current and mass flow rate distribution exhibit trends similar to those of other propellants in the literature. The peak current, in the center of the beam, decreases with increase in mass flow rate, however the beam becomes wider and thus total integrated current increases. Current loss to the extractor increases with increasing flow rate, but could be mitigated with an extractor design optimized specifically for this propellant.

The lowest flow rate achieved in this experiment was 0.19 nL/s. This corresponds to the highest specific impulse achieved in this experiment, 412.37 seconds. The thrust at this specific impulse was calculated to be 1.09 μN, and higher thrust is possible with higher flow rates. At the highest flow rate tested, the thrust was 8.71 μN, which also corresponds to the highest thrust per unit power achieved in these experiments. Extrapolation of the data obtained from the electrospray emission currents shows that

higher performance, in terms of specific impulse is possible. For example, if 1 pL/s flow rate could be achieved, the specific impulse would be 1000 seconds. Examination of the scaling laws for minimum flow rate reveals that the electrospray physics likely do not prohibit this performance from being achieved. It is therefore likely that improvements to the feed system and optimization of the emitter hardware in reference to this propellant specifically can realize higher performance than achieved in these experiments.

REFERENCES

[1] S. Dominick, "Design, Development, and Flight Performance of the Mars Global Surveyor Propulsion System," 35th AIAA Joint Propulsion Conference, AIAA Paper 1999-2176, 1999.

[2] C. A. Kluever, "Spacecraft Optimization with Combined Chemical-Electric Propulsion," Journal of Spacecraft and Rockets, Vol. 32, No. 2, 1994, pp. 378-380.

[3] C. A. Kluever, "Optimal Geostationary Orbit Transfers Using Onboard Chemical-Electric Propulsion," Journal of Spacecraft and Rockets, Vol. 49, No. 6, 2012, pp. 1174-1182.

[4] D. Y. Oh, Randolph, T., Kimbrel, S., and Martinez-Sanchez, M., "End-toEnd Optimization of Chemical-Electric Orbit Raising Missions," Journal of Spacecraft and Rockets, Vol. 41, No. 5, 2004, pp. 831-839.

[5] S. R. Oleson, Myers, R. M., Kluever, C. A., Riehl, J. P., Curran, F. M., "Advanced Propulsion for Geostationary Orbit Insertion and North-South Station Keeping," Journal of Spacecraft and Rockets, Vol. 34, No. 1, 1997, pp. 22-28.

[6] B. R. a. R. Donius, J. L., "Ionic Liquid Dual-Mode Spacecraft Propulsion Assessment," Journal of Spacecraft and Rockets, Vol. 48, No. 1, 2011, pp. 110-123.

[7] T. Rexius, and Holmes, M., "Mission Capability Gains from Multi-Mode Propulsion Thrust Profile Variations for a Plane Change Maneuver," AIAA Modeling and Simulation Technologies Conference, AIAA Paper 2011-6431, 2011.

[8] J. M. Haas, and Holmes, M. R., "Multi-Mode Propulsion System for the Expansion of Small Satellite Capabilities," NATO, Rept. MP-AVT-171-05, 2010.

[9] S. P. Berg, and Rovey, J. L., "Assessment of Multi-Mode Spacecraft Micropropulsion Systems," 50th AIAA/ASME/SAE/ASEE Joint Propulsion Conference, AIAA Paper 2014-3758, 2014.

[10] S. P. Berg, and Rovey, J. L., "Assessment of High-Power Electric Multi-Mode Spacecraft Propulsion Concepts," 33rd International Electric Propulsion Conference, IEPC-2013-308, 2013.

[11] S. P. Berg, and Rovey, J. L., "Assessment of Imidazole-Based Energetic Ionic Liquids as Dual-Mode Spacecraft Propellants," Journal of Propulsion and Power, Vol. 29, No. 2, 2013, pp. 339-351.

[12] S. P. Berg, and Rovey, J. L., "Decomposition of Monopropellant Blends of Hydroxylammonium Nitrate and Imidazole-Based Ionic Liquid Fuels," Journal of Propulsion and Power, Vol. 29, No. 1, 2013, pp. 125-135.

[13] S. P. Berg, and Rovey, J. L., "Ignition and Performance of Ionic Liquid Propellants in a Microtube for Multi-Mode Micropropulsion Applications," 51st AIAA/ASME/SAE/ASEE Joint Propulsion Conference, to be presented, 2015.

[14] Green Monopropellant Thrusters,
http://www.busek.com/index_htm_files/70008517B.pdf

[15] Busek Electrospray Thrusters,
http://www.busek.com/index_htm_files/70008500E.pdf

[16] Chiu, Y., Dressler, A.,, "Ionic Liquids For Space Propulsion", *Ionic Liquids IV: Not Just Solvents Anymore*, Vol. 975, American Chemical Society, Washington, D. C., 2007, Ch.

[17] M. Gamero-Castano, "Characterization of a Six-Emitter Colloid Thruster Using a Torsional Balance," Journal of Propulsion and Power, Vol. 20, No. 4, 2004, pp. 736-741.

[18] C. A. Mento, Sung, C-J., Ibarreta, A. F., Schneider, S. J.,, "Catalyzed Ignition of Using Methane/Hydrogen Fuel in a Microtube for Microthruster Applications," Journal of Propulsion and Power, Vol. 25, No. 6, 2009, pp. 1203-1210.

[19] G. A. Boyarko, Sung, C-J., Schneider, S. J.,, "Catalyzed Combustion of Hydrogen-Oxygen in Platinum Tubes for Micro-Propulsion Applications," Proceedings of the Combustion Institute, Vol. 30, No. 2005, pp. 2481-2488.

[20] S. J. Volchko, Sung, C-J., Huang, Y., Schneider, S. J.,, "Catalytic Combustion of Rich Methane/Oxygen Mixtures for Micropropulsion Appications," Journal of Propulsion and Power, Vol. 22, No. 3, 2006, pp. 684-693.

[21] M. S. Alexander, Stark, J., Smith, K. L., Stevens, B., Kent, B., "Electrospray Performance of Microfabricated Colloid Thruster Arrays," Journal of Propulsion and Power, Vol. 22, No. 3, 2006, pp. 620-627.

[22] I. Romero-Sanz, Bocanegra, R., Fernandez De La Mora, J., Gamero-Castano, M.,, "Source of Heavy Molecular Ions Based on Taylor Cones of Ionic Liquids Operating in the Pure Ion Evaporation Regime," Journal of Applied Physics, Vol. 94, No. 2003, pp. 3599-3605.

[23] D. Amariei, Courtheoux, L., Rossignol, S., Batonneau, Y., Kappenstein, C., Ford, M., and Pillet, N., "Influence of the Fuel on Thermal and Catalytic Decompositions of Ionic Liquid Monopropellants," 41st AIAA/ASME/SAE/ASEE Joint Propulsion Conference & Exhibit, AIAA Paper 2005-3980, 2005.

[24] K. Anflo, Gronland, T. A., Bergman, G., Johansson, M., and Nedar, R., "Towards Green Propulsion for Spacecraft with ADN-Based Monopropellants," 38th AIAA/ASME/SAE/ASEE Joint Propulsion Conference & Exhibit, AIAA Paper 2002-3847, 2002.

[25] C. H. McLean, Deininger, W. D., Joniatis, J., Aggarwal, P. K., Spores, R. A., Deans, M., Yim, J. T., Bury, K., Martinez, J., Cardiff, E. H., Bacha, C. E., "Green Propellant Infusion Mission Program Development and Technology Maturation," 50th AIAA/ASME/SAE/ASEE Joint Propulsion Conference, AIAA Paper 2014-3481, 2014.

[26] G. Chatel, Pereira, J.F.B., Debbeti, V., Wang, H., Rogers, R.D.,, "Mixing Ionic Liquids-"Simple Mixtures" or "Double Salts"?," Green Chemistry, Vol. 16, No. 2014, pp. 2051-2083.

[27] S. W. Miller, Prince, B.D., Bemish, R.J., Rovey, J.L.,, "Electrospray of 1-Butyl-3-Methylimidazolium Dicyanamide Under Variable Flow Rate Operations," Journal of Propulsion and Power, Vol. 30, No. 6, 2014, pp. 1701-1710.

[28] Y. Chiu, Gaeta, G., Levandier, D.J., Dressler, R.A., Boatz, J.A.,, "Vacuum Electrospray Ionization Study of the Ionic Liquid, [Emim][Im]," International Journal of Mass Spectrometry, Vol. 265, No. 2-3, 2007, pp. 146-158.

[29] P. C. Lozano, "Studies on the Ion-Droplet Mixed Regime in Colloid Thrusters," 2003.

[30] D. H. Manzella, and Sankovic, J. M., "Hall Thruster Ion Beam Characterization," 31st AIAA/ASME/ASEE Joint Propulsion Conference and Exhibit, AIAA Paper 1995-2927, 1995.

[31] B. A. Martin, and Hager, H. E. , "Velocity Profile on Quartz Crystals Oscillating in Liquids," Journal of Applied Physics, Vol. 65, No. 7, 1989, pp. 2630-2635.

SECTION

2. CONCEPTUAL DESIGN OF A MULTI-MODE INTEGRATED MONOPROPELLANT ELECTROSPRAY PROPULSION SYSTEM

2.1. INTRODUCTION

Results from Papers I-IV of this thesis are used to develop, conceptually, a design for a fully integrated multi-mode propulsion system. This section is not intended to be a fully developed, optimized, and complete design, since there are many possible options, particularly for the thruster architecture and feed system. The intention is then to use the methods and insights developed in the previous sections of this thesis to illustrate the multi-mode propulsion system design process and the considerations that should be made in approaching design of these systems.

The propulsive modes chosen for this study are chemical monopropellant and electrospray thrusters. Specifically, as described in Paper III and IV introduction sections, the chemical mode will be a microtube thruster, and the electric mode will be a capillary electrospray emitter. As described, since these typically have inner diameters on the order of tenths of a millimeter, there is no reason these could not be combined into a single thruster head. Thus, the propulsion system described herein will be a system utilizing a single propellant, the blend of [Emim][EtSO$_4$] and HAN developed in Paper I and tested in Papers III and IV, as well as a single thruster for both modes. Thus, the system is a fully integrated propulsion system, utilizing all common components.

2.2. FEED SYSTEM ARCHITECHTURE

The largest driver for multi-mode propulsion system concepts has been the use of a common propellant. As mentioned, using a common propellant provides the highest level of mission flexibility. However, particularly for micropropulsion systems it is also desirable to limit the inert mass fraction of the propulsion system as much as possible. This particular system will utilize common thruster geometry for both modes. The feed

system, then, will have to accommodate the required flow rates for each mode. Since these are high-thrust and low-thrust modes, this requires flow modulation over roughly three orders of magnitude. However, since this is not continuous, provisions are made to effectively switch between either mode.

A schematic of the multi-mode propulsion system concept is shown in Fig. 2.1. The propulsion system consists of a single propellant tank, which is pressurized by an inert gas source, nitrogen in the figure but could also be helium. In order to accommodate both propulsive modes, pressurant gas is fed through either flow restriction ORCHEM or flow restriction ORELEC, which will be sized to meet flow rate requirements for the chemical mode and electric mode, respectively. When switching between chemical and electric modes, it will be necessary to vent the propulsion tank, since the flow rate required for chemical propulsion is much higher. This is accomplished via a bypass line, activated by valve SV02. Careful maneuver design could even include this as a cold-gas thruster mode, thus making the system a triple-mode propulsion system. For purposes of this study, however, this mode is not included in analysis. Overall, due to the need for flow modulation between the two modes, one might say that this system is more complex and would therefore have a higher mass than a traditional system. However, a traditional monopropellant system is a hydrazine monopropellant system.[20] In these systems, it is necessary to have three valve seats between tank and thruster and two in the propellant loading lines. HAN-based systems only require two and one seat for these systems, respectively, due to the fact that HAN does not pose a respiratory hazard. [21] Because of this fact, this propulsion system actually has less valves than a traditional monopropellant system, but perhaps more line length depending on packaging requirements. For purposes of conceptual design then the mass of lines and valves is assumed to be 50% of the thruster mass, which is the mass for a traditional monopropellant system as described in Paper II.
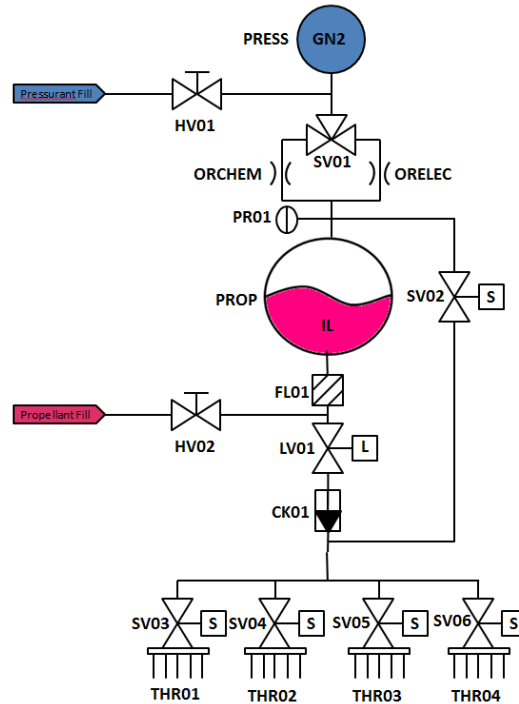
Figure 2.1. Schematic of the Multi-Mode Integrated Monopropellant/Electrospray Propulsion System.

2.3. THRUSTER MODELING

To develop propulsion feed system requirements and then determine propulsion system mission capabilities, it is necessary to develop and use performance models for each mode of the thruster, with consideration that the same geometry will be used for both monopropellant and electrospray modes. For the electric propulsion mode, performance for the [Emim][EtSO$_4$] propellant was obtained from experimental results, as described in Paper IV. The thrust and specific impulse for the electric mode are given by Eqs. (1)-(3)

$$F = \sqrt{2V_{acc}\dot{m}I} \tag{1}$$

$$I_{sp} = \frac{F}{\dot{m}g_0} \tag{2}$$

$$I(Q) = 1284.55 * [Q]^{0.5} \tag{3}$$

Eq. (3) was obtained using a specific emitter and extractor plate geometry. Although it may be possible to alter the performance somewhat by modifying the emitter and extractor geometry, this has not been investigated in detail. However, typically, for droplet-ion mixed regime emission, the emission current is mainly a function of the ionic liquid physical properties and the volumetric flow rate. [22] It is therefore assumed that the performance calculated using Eq. (3) will be the same provided the geometry does not change significantly from that of the experiment which was a 100 μm inner diameter capillary.

The chemical mode chosen for this propulsion system is the catalytic microtube primarily because it is fundamentally the same geometry as a capillary electrospray emitter. The microtube can be modeled as a plug flow reactor [23], and the basic diagram is shown in Fig. 2.2.
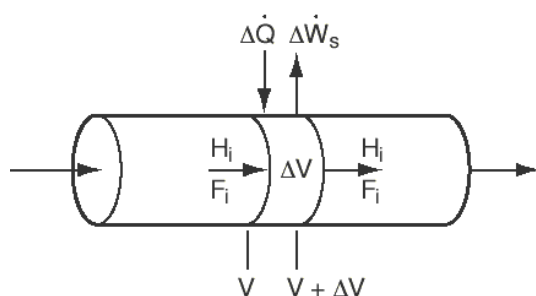

Figure 2.2. Model of plug flow reactor with heat effects.

Applying the mass balance to the PFR model gives Eq. (4),

$$\frac{dX}{dV} = \frac{-r_A}{F_{A0}} \tag{4}$$

where the reaction rate for the monopropellant decomposition as found in Section IV is given by Eq. (5),

$$-r_A = 2.14x10^{10} \exp\left(\frac{-10771}{T}\right)C_A \tag{5}$$

Here, platinum is chosen because it allows the lowest energy input to decompose the monopropellant, which is desired for spacecraft applications. Applying the energy balance to Figure 2 assuming no work interaction, gives the following, Eq. (6),

$$\frac{dT}{dV} = \frac{\dot{Q} + (-r_A)(-\Delta H_{Rx})}{F_{A0}(C_{PA} + \Delta C_P X)} \tag{6}$$

where the heat of reaction is -920.1 kJ/mol and the molar flow rate is related to the mass flow rate by Eq. (7),

$$F_{A0} = \frac{\dot{m}_A}{MW_A} \tag{7}$$

The preceding paragraph describes the power and reactor volume required to initiate decomposition of the monopropellant. However, chemical performance is determined from the results of the decomposition. The specific impulse is calculated from the Chemical Equilibrium with Applications (CEA) computer program assuming equilibrium composition as was done in Section II. Since there is no nozzle, the exhaust gases will be frictionally choked in the microtube and thus the specific impulse is calculated at the throat area and is 170 seconds. The thrust as a function of flow rate can then be calculated, Eq. (8)

$$F = \dot{m}I_{sp}g_0 \tag{8}$$

and the thrust as a function of volumetric flow rate for the monopropellant is shown in Fig. 2.3.
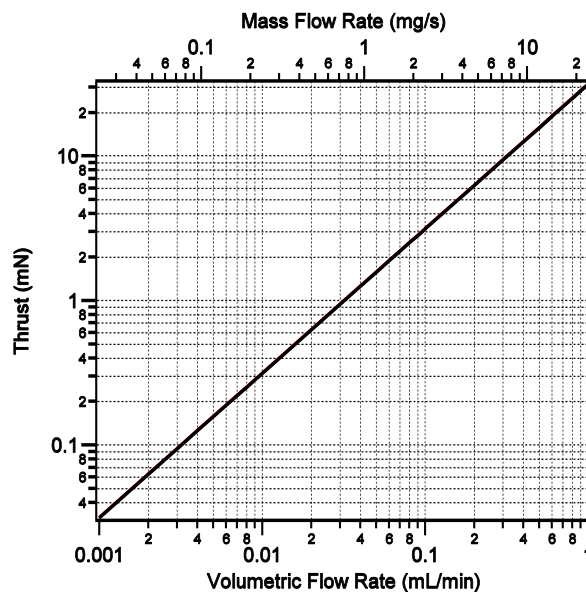

Figure 2.3. Thrust as a Function of Flow Rate for the Chemical Microtube Propulsion Mode.

For the chemical microtube, the flow rate cannot be arbitrarily selected. It is limited by the flashback behavior of the propellant. HAN-based propellant burning behavior has been investigated previously, and in general it has been found to behave similarly to solid propellants in that a distinct linear burning rate as a function of pressure can be determined. [24, 25] Since after ignition occurs, the reaction front will propagate at this rate back into the chamber, it is necessary to maintain sufficient flow rate to keep the reaction front in the microtube. Thus, the minimum flow rate necessary is governed by the burn rate of the monopropellant. The linear burning rate for this monopropellant was not determined as part of this study, however, for other HAN-based monopropellant formulations is typically on the order of ~1-2 mm/s at 300 psi pressure. [25] Since this includes a variety of different fuels combined with HAN, a value of 2 mm/s is selected as sufficient for conceptual design. The minimum mass flow rate as a function of tube inner

diameter is shown in Fig. 2.4. The mass flow rate required grows as the square root of diameter since the burn rate is linear. It is desirable, then, from a system perspective to use lower diameter tubes since as was found in Paper II multi-mode system performance is not significantly dependent on chemical mode thrust and limiting inert mass of the chemical propulsion system is more important. For this study, then, a microtube inner diameter of 0.1 mm is chosen. This is the same diameter as the capillary in the electrospray experiment and corresponds to a chemical thrust of 0.037 mN per emitter, at minimum.
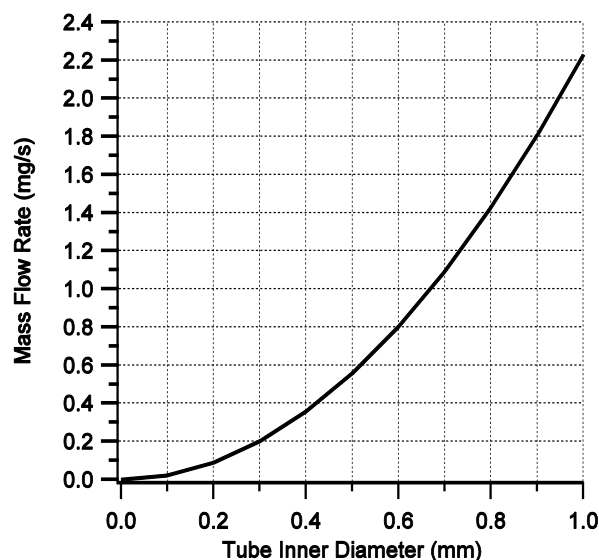
Figure 2.4. Minimum Mass Flow Rate Required as a Function of Microtube Inner Diameter.

With the minimum mass flow rate information and the plug flow reactor model described previously, the required reactor length as a function of input power can be determined. This is shown in Fig. 2.5. The figure depicts the expected trends, namely that the required microtube length to initiate decomposition is reduced either by reducing mass flow rate or increasing input power. Only contours that would yield 100 mm, or the length of a 1U cubesat dimension are shown. However, there is no reason longer

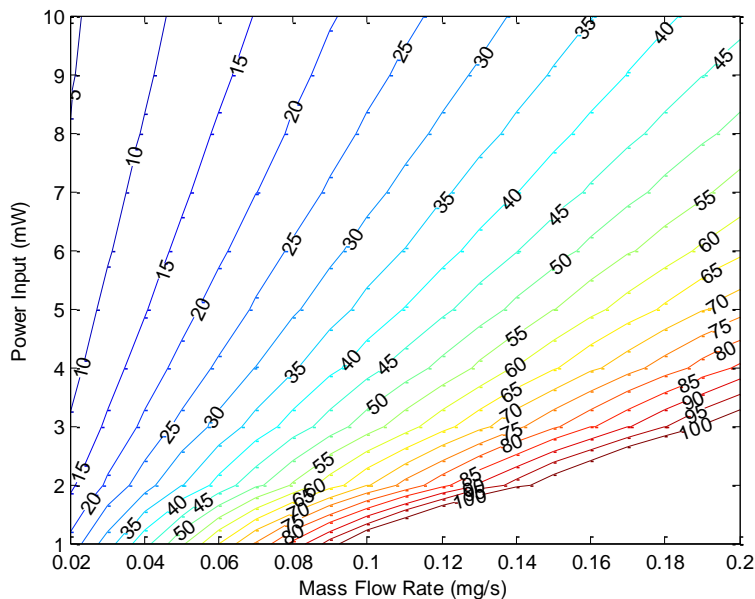microtubes could not be tolerated, particularly if the tubes can be bent and packaged more efficiently.

Figure 2.5. Contours of Reactor Length (mm) Required to Initiate Decomposition of Monopropellant.

Since increased power input reduces microtube length and thus thruster mass, but requires more mass in terms of batteries, there exists an optimum microtube length at a given mass flow rate. Choosing a tube wall thickness of 0.15 mm for the platinum tube material gives a mass per length of 0.00125 g/mm, and from Paper II the mass of batteries is 0.15 W-hr/g. Assuming the batteries need to operate for roughly 15 minutes to operate the thruster, half that assumed in Paper II, gives a mass of 1.67 g/W. This is a reasonable assumption given that the microtube is heated directly rather than providing heat to a large catalyst bed via a thermal blanket. Additionally, a mass flow rate of 0.08 mg/s is selected somewhat arbitrarily. Thus, this design is likely not optimum, but does provide a baseline for methodology development and design trade insights. The mass of the microtube plus battery requirements as a function of microtube length is shown in

Fig. 2.6. The figure shows that for these conditions the optimum mass is reached at around 50 mm. This length is chosen for the thruster geometry. Using the microtube plug flow reactor model results of Fig. 2.5 and thrust calculations of Fig. 2.3, this provides a thrust of 0.13 mN per emitter at 2.3 mW input power.
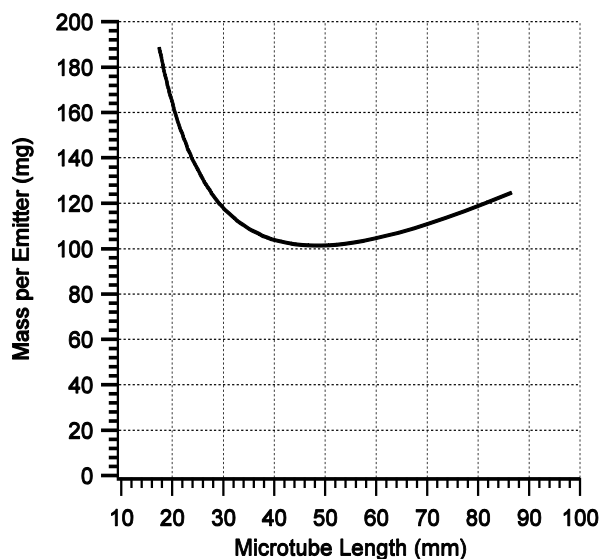

Figure 2.6. Mass of Microtube Plus Battery Power as a Function of Length.

Now that the microtube geometry has been chosen, and its performance is known, the electrospray performance can be computed. Results from Paper II showed that it is desirable to choose an electric propulsion technology that is close to the optimum specific impulse at a given chemical mode specific impulse. For the 170 second chemical mode specific impulse, the optimum electric mode specific impulse is 780 seconds. Although this specific impulse was higher than the 412 second specific impulse attained in the electrospray experiments of Paper IV, it can be achieved with a slight reduction in flow rate; specifically a flow rate of 0.003 nL/sec can achieve this specific impulse with a thrust of 0.03 μN/emitter.

The final consideration is the number of emitters to include in the thruster design. Since multi-mode propulsion system performance is highly dependent on electric thrust, scaling the thrust in the electric mode should be a prime consideration. Achieving 0.3 mN of thrust, in the same range as the systems investigated in Paper II, requires 10000 emitters. This requires 6 W of power, assuming 50% powertrain efficiency. The chemical mode thrust with this number of emitters is 1.3 N and the required power input is 23 W. The thruster mass is 625 grams.

2.4. PROPULSION SYSTEM CAPABILITIES

As mentioned, the main motivation for using the combined thruster geometry is reduction in propulsion system inert mass. Table 2.1 shows the propulsion system dry mass, excluding tankage for the combined propulsion system versus a separate system consisting of state-of-the-art thrusters in chemical and electric modes. These masses were computed using the same methodologies as developed in Paper II, but with the relevant design considerations from this section. It is seen that the total effect of using a combined system, which includes reducing thruster mass by half, results in a total system mass reduction of nearly half since the lines and valves and associated structural mounts mass penalty is also reduced due to the reduction in thruster mass.

Table 2.1. System Mass Comparison for Integrated System Versus Separate System.

System Designation	Separate	Integrated
Chemical Thruster Mass (g)	500	625
Electric Thruster Mass (g)	900	0
PPU Mass (g)	83	70
Solar Array Mass (g)	139	112
Battery Mass (g)	100	110
Lines and Valves (g)	700	313
Structural Mounts (g)	242	123
Total Mass (g)	2664	1353

The mission design space for a 6U cubesat and 2 kg payload utilizing the integrated thruster described in this section is shown in Fig. 2.7. The integrated thruster designed in this section is compared to the monopropellant/electrospray system described in Paper II, which uses the same propellant, but does not utilize a common thruster. The integrated propulsion system outperforms the common propellant only system, having more delta-V capability at every burn duration up to its maximum of 390 days. For an all-chemical burn, the integrated system attains 21% higher delta-V and for an all-electric burn, it attains 41% higher delta-V than the compared to the common propellant system at the same burn duration.
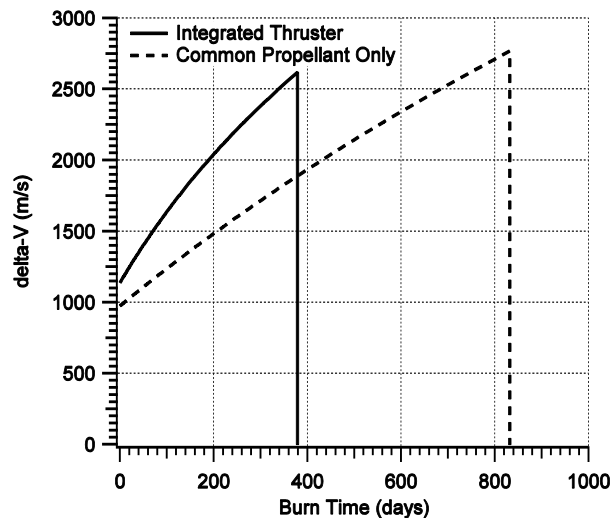
Figure 2.7. Mission Design Space for Fully Integrated System versus Common Propellant Only System.

REFERENCES

[1]   Hass, J.M., Holmes, M.R., "Multi-Mode Propulsion System for the Expansion of Small Satellite Capabilities," NATO MP-AVT-171-05, 2010.

[2]   Donius, B.R. "Investigation of Dual-Mode Spacecraft Propulsion by Means of Ionic Liquids," Masters Thesis, Department of Mechanical and Aerospace Engineering, Missouri University of Science & Technology, Rolla, MO., May 2010.

[3]   Donius, B. R., Rovey, J. L., "Ionic Liquid Dual-Mode Spacecraft Propulsion Assessment," *Journal of Spacecraft and Rockets*, Vol. 48, No. 1, 2011, pp. 110-123.

[4]   Donius, B. R., Rovey, J. L., "Analysis and Prediction of Dual-Mode Chemical and Electric Ionic Liquid Propulsion Performance," *48th Aerospace Sciences Meeting*, AIAA Paper 2010-1328, 2010.

[5]   Sutton, G. P., Biblarz, O., *Rocket Propulsion Elements*, 7th ed., John Wiley & Sons, New York, 2001, Ch. 5, 7, 19.

[6]   Zube, D., Wucherer, E., Reed, B., "Evaluation of HAN-Based Propellant Blends," 39th AIAA Joint Propulsion Conference, AIAA Paper 2003-4643, 2003.

[7]   Amariei, D., Courtheoux, L., Rossignol, S., Batonneau, Y., Kappenstein, C., Ford, M., and Pillet, N., "Influence of the Fuel on the Thermal and Catalytic Decompositions of Ionic Liquid Monopropellants," 41st AIAA Joint Propulsion Conference, AIAA, Paper 2005-3980, 2005.

[8]   Anflo, K., Grönland, T. A., Bergman, G., Johansson, M., Nedar, R., "Towards Green Propulsion for Spacecraft with ADN-Based Monopropellants," 38th AIAA Joint Propulsion Conference, AIAA Paper 2002-3847, 2002.

[9]   Slettenhaar, B., Zevenbergen, J. F., Pasman, H. J., Maree, A. G. M., Moerel, J. L. P. A. "Study on Catalytic Ignition of HNF Based Non Toxic Monopropellants," 39th AIAA Joint Propulsion Conference. AIAA Paper 2003-4920, 2003.

[10]   Anflo, K., Persson, S., Thormahlen, P., Bergman, G., Hasanof, T., "Flight Demonstration of an ADN-Based Propulsion System on the PRISMA Satellite," 42nd AIAA Joint Propulsion Conference, AIAA Paper 2006-5212, 2006.

[11]   Meng, H., Khare, P., Risha, G. A., Yetter, R. A., Yang, V., "Decomposition and Ignition of HAN-Based Monopropellants by Electrolysis," 47th AIAA Aerospace Sciences Meeting, AIAA Paper 2009-451, 2009.

[12]   Wingborg, N., Larsson, A., Elfsberg, M., Appelgren, P., "Characterization and Ignition of ADN-based Liquid Monopropellants," 41st AIAA Joint Propulsion Conference, AIAA Paper 2005-4468, 2005.

[13]   Wilkes, J.S., Wasserscheid, P., Welton, T., *Ionic Liquids in Synthesis*, 2nd ed., WILEY-VCH Verlag GmbH &Co., 2008, Ch.1.

[14]   Boatz, J., Gordon, M., Voth, G., Hammes-Schiffer, S., "Design of Energetic Ionic Liquids," *DoD HPCMP Users Group Conference*, IEEE Publ., Piscataway, NJ, Pittsburgh, 2008, pp. 196-200.

[15]   Smiglak, M., Reichert, M. W., Holbrey, J. D., Wilkes, J. S., Sun, L., Thrasher, J. S., Kirichenko, K., Singh, S., Katritzky, A. R., Rogers, R. D., "Combustible ionic liquids by design: is laboratory safety another ionic liquid myth?" Chemical Communications, Issue 24, 2006, pp. 2554-2556.

[16]   Romero-Sanz, I., Bocanegra, R., Fernandez De La Mora, J., Gamero-Castano, M., "Source of Heavy Molecular Ions Based on Taylor Cones of Ionic Liquids Operating in the Pure Ion Evaporation Regime," *Journal of Applied Physics*, Vol. 94, 2003, pp. 3599-3605.

[17]   Chiu, Y., Dressler,A., "Ionic Liquids for Space Propulsion," In *Ionic Liquids IV: Not Just Solvents Anymore*, ACS Symposium Series, Vol. 975, American Chemical Society, Washington, DC, 2007, pp. 138-160.

[18]   Gamero-Castano, M., "Characterization of a Six-Emitter Colloid Thruster Using a Torsional Balance," *Journal of Propulsion and Power*, Vol. 20, No. 4, 2004, pp. 736-741.

[19]   Larriba, C., Garoz, D., Bueno, C., Romero-Sanz, I., Castro, S., Fernandez de la Mora, J., Yoshida, Y., Saito, G., Hagiwara, R., Masumoto, K., Wilkes, J., "Taylor Cones of Ionic Liquids as Ion Sources: The Role of Electrical Conductivity and Surface Tension," *Ionic Liquids IV: Not Just Solvents Anymore*, ACS Symposium Series, Vol. 975, American Chemical Society, Washington, DC, 2007, Ch. 21.

[20]   R. W. Humble, Henry, G. N., and Larson, W. J., Space Propulsion Analysis and Design, McGraw-Hill, 1995.

[21]   C. H. McLean, Deininger, W. D., Joniatis, J., Aggarwal, P. K., Spores, R. A., Deans, M., Yim, J. T., Bury, K., Martinez, J., Cardiff, E. H., Bacha, C. E., "Green Propellant Infusion Mission Program Development and Technology Maturation," 50th AIAA/ASME/SAE/ASEE Joint Propulsion Conference, AIAA Paper 2014-3481, 2014.

[22]   P. C. Lozano, "Studies on the Ion-Droplet Mixed Regime in Colloid Thrusters," 2003.

[23]   C. A. Mento, Sung, C-J., Ibarreta, A. F., Schneider, S. J.,, "Catalyzed Ignition of Using Methane/Hydrogen Fuel in a Microtube for Microthruster Applications," Journal of Propulsion and Power, Vol. 25, No. 6, 2009, pp. 1203-1210.

[24]   H.-S. Lee, Litzinger, T. A.,, "Chemical Kinetic Study of HAN Decomposition," Combustion and Flame, Vol. 135, No. 2003, pp. 151-169.

[25]   Y.-P. Chang, "Combustion Behavior of HAN-Based Liquid Propellants," Mechanical Engineering, Pennsylvania State University, 2002.

VITA

Steven Paul Berg was born in 1988 in Kansas City, KS. In 1991, he moved to Wentzville, MO and attended St. Dominic High School, graduating in 2006. In August 2006 he began his collegiate career at University of Missouri-Rolla, which changed its name to Missouri University of Science and Technology in January 2008. He graduated Summa Cum Laude with a Bachelors of Science in Aerospace Engineering in May 2010. In August 2010 he began graduate school at the Missouri University of Science and Technology. He was awarded a Master of Science in Aerospace Engineering in May 2012.

Upon completion of his Master of Science degree he decided to pursue a Ph.D. degree in Aerospace Engineering, continuing the research developed in the M.S. phase of his education. He completed his dissertation in the Fall of 2015 and received his Ph.D in December of 2015. Post-graduation, he will continue to further this work through a post-doctoral position alongside developing a small satellite business around the multi-mode propulsion capability.